THE CATHOLIC UNIVERSITY OF AMERICA
DEPARTMENT OF ELECTRICAL ENGINEERING

SEMIANNUAL PROGRESS REPORT

on

TESTING OF ROMPS ROBOT MECHANICAL INTERFACES AND COMPLIANT DEVICE

Research Grant NAG 5-1415

Dr. Charles C. Nguyen
Principal Investigator and Professor

and

Sami S. Antrazi
Graduate Research Assistant

submitted to
Mr. Lloyd Purves
Mr. George Voellmer
Code 714
Goddard Space Flight Center (NASA)
Greenbelt, Maryland

March 1993

Contents

REPORT SUMMARY

This is a semiannual report presenting research results obtained through a research grant with grant number, NAG 5-1415 from August 1, 1992 to February 1, 1993. It deals with testing the mechanical interfaces and compliant device to be used in the robot of the Robot Operated Material Processing System (ROMPS) which has been developed at Goddard Space Flight Center to study in-space material processing using a robotic system. First it describes the main components of the ROMPS robot and its operations . It then presents the objectives of the test and outlines the test plan. After that, the report describes the testbed to be employed in the test plan and then presents the experimental results. The conclusion of the report includes some observations and recommendations made based on the test results.

1 INTRODUCTION

The Robot Operated Materials Processing System (ROMPS) has been developed at Goddard Space Flight Center (GSFC) under a flight project to investigate commercially promising in-space material processes and to design reflyable robot automated systems to be used in the above processes for low-cost operations [1]. The ROMPS is currently scheduled for flight in 1994 as a Hitchhiker payload in a Get Away Special (GAS) can. An important component of the ROMPS is a three degree-of-freedom (DOF) robot which will be responsible for carrying out the required tasks of in-space processing of selected materials.

This report deals with testing of the mating capability of the ROMPS robot fingers with its various mechanical interfaces. In particular, the test plan will focus on studying the capability of a compliance mechanism mounted on the robot fingers in accommodating misalignments between the robot fingers and the interfaces during the mating. The report is organized as follows. Section 2 presents the main components of the ROMPS robot and briefly describes its operations. Section 3 presents the objectives of the test and outlines the test plan. The testbed comprising a Stewart Platform-based high precision manipulator and associated data acquisition and control systems is described in Section 4. Section 5 presents results of numerous experiments conducted to study the mating capability of the robot fingers with its various interfaces under misalignments. The report is concluded with observations and recommendations based on the test results.

2 THE ROMPS ROBOT

Figure 1 gives a sketch of the ROMPS designed to fit within a full-size GAS can. As seen from the figure, the ROMPS basically consists of a robot possessing three DOFs located in the center of the ROMPS, 148 pallets located around the robot on six racks and two ovens located at the top. A simplified version of Figure 1 is presented in Figure 2 which illustrates the ROMPS robot, a rack containing several pallets and the two ovens. Using Figure 2, the steps required in the operation of the ROMPS robot are described as follows:

1. The robot moves to a rack and use its fingers to acquire a pallet containing a sample of material
2. The robot moves to an oven and places the pallet under it
3. The oven heats up the sample while the robot is holding it
4. The robot moves a storage rack and replaces the sample in the rack
5. The robot repeats Steps 1-4 until all samples are processed or a stop command is issued

Based on the description of the above steps, we identify the following tasks the robot must carry out in each particular step:

1. Step 1 requires a successful mating between the robot fingers and the pallet interface
2. Step 2 requires a successful insertion of two pins of the oven into the two holes of the pallet
3. Step 3 requires a successful insertion of the pallet into the rack and a successful demating between the robot fingers and the pallet interface

In the tasks described above, misalignments between the fingers and the pallet interface (Step 1), between the pallet holes and the oven pins (Step 2) and between the pallet interface and the rack (Step 3) may exist because of imperfectness in manufacturing of the parts or errors in the robot position controllers and sensors. A passive compliant device which is composed of two orthogonal nested double blade flexures as shown in Figure 4 is mounted between the robot wrist and robot fingers to provide compliance in the radial and elevation (vertical) directions and thereby to help the fingers to accommodate the misalignments. Under unforeseen misalignments, a task (mating, insertion or demating) is called *successful* if it can be completed within the working range of the passive compliant device in terms of allowable travel and forces and without any damages to the parts involved.

3 STUDY OBJECTIVE AND TEST PLAN

3.1 Study Objective

The main objective of this study is to experimentally evaluate the effectiveness of the passive compliant device in accommodating misalignments and to evaluate the design of the robot fingers, the pallet interface, the oven holes and the rack based on their mating and/or insertion capability.

3.2 Test Plan

In order to achieve the study objective, a test plan is prepared to aim at three different scenarios:

- **Scenario 1: The Pallet/Finger Test**
- **Scenario 2: The Pallet/Oven Test**
- **Scenario 3: The Pallet/Rack Test**

In each of the above scenarios, the following tasks will be carried out:

1. **Operation Under Perfect Alignment:** Check for operation under perfect alignment
2. **Determination of Capture Ranges:** Using visual inspection, determine the capture ranges
3. **Operation under Misalignments:** Perform mating (insertion)/demating under carefully introduced misalignments, measure and record applied forces/torques in six DOFs

4 THE TESTBED AND TEST SETUP

The testbed employed in this study is depicted in Figure 3. The desired misalignments are produced by a Stewart Platform-based (SPB) manipulator possessing six DOF's [2]. The manipulator mainly consists of a lower base platform, an upper payload platform, and six linear actuators. The movable payload platform is supported above the stationary base platform by the linear actuators which are composed of ballnuts and ballscrews providing the extensibility. Stepper motors were selected to drive the ballscrews to extend or shorten the actuator lengths whose variations will in turn produce the motion of the payload platform. The manipulator specifications are given below:

- Tracking accuracy of 1/1000 inch

- Maximum endpoint velocity of 3.2 inches per second
- A six DOF working envelope of one cubic foot
- Payload capacity of 2000 lbs

The test setup is illustrated in Figure 4 and Figure 5. The robot finger assembly is mounted to a stationary location using a vice and the pallet is mounted to the upper payload platform of the SPB manipulator via the passive compliant device as shown in Figure 4. Forces/torques exerted during the mating between the fingers and the pallet interface are measured by a six DOF JR3 force/torque sensor mounted between the compliant device and the upper manipulator platform. Coordinate transformation is used to transform measured forces/torques to forces/torques at the center of the passive compliant device.

We now refer to Figure 5 (test setup for Scenario 1) and Figure 6 to explain the coordinate systems. Assuming that the pallet has been brought to a pose aligned with the ROMPS robot fingers as seen in Figure 5, relationship between the coordinate system used by the SPB manipulator and the ROMPS coordinate system is illustrated in Figure 6. We observe that the elevation axis of the ROMPS robot (indicated by z_{ROMPS}) lies in the opposite direction of the y-axis of the SPB manipulator (indicated by y_M) and the radial axis of the ROMPS robot lies in the opposite direction of the x-axis of the SPB manipulator (indicated by x_M). The ROMPS robot azimuth axis coincides with the negative rotation around the y_M-axis of the SPB manipulator. Thus a desired misalignment between the pallet interface and the fingers can be produced by rotating and/or translating the upper manipulator platform using the coordinate systems shown in Figure 6. In particular, in order to produce a misalignment of +0.5 inch in the ROMPS elevation direction, the upper manipulator platform should move -0.5 inch in the y_M axis. As shown in Figure 5, although the test setup is intended for Scenario 1, the oven pins or the rack can be mounted in the same position of the finger assembly for Scenarios 2 or Scenario 3, respectively, as illustrated in Figure 7.

5 TEST PROCEDURES AND RESULTS

5.1 Scenario 1: The Pallet/Finger Test

- **Perfect Alignment Operation:** Referring to Figure 5, we now describe the testing procedures for Scenario 1. First the perfect alignment between the ROMPS robot fingers and the pallet was established by controlling the SPB manipulator to move the pallet into a position which is roughly aligned with the fingers. The fingers were then commanded to grasp on the pallet interface. After that, the SPB manipulator was controlled to slowly and carefully modify its pose until the reading of forces/torques measured by the JR3 sensor was zero. The pose of the pallet relative to the fingers at which no forces/torques are applied is the perfect alignment pose. Finally the fingers were commanded to open (demating) and then close (mating) under the perfect alignment. According to force reading, the forces/torques exerted to the compliant device were negligble during the mating and mating of the fingers with the pallet interface.

- **Capture Range Determination:** The capture ranges for the Finger/Pallet grasping were not visually determined. However they will be determined in Section 6 (to be presented later) using the results obtained from the test for operation under misalignments presented below.

- **Operation under Misalignments:** From the above-established perfect alignment pose, the SPB manipulator was controlled to translate and/or rotate to produce the amount of desired misalignment (in inches or degrees) in a selected axis. Then the fingers were controlled to grasp the pallet interface. The force/torques in the misalignment axes were measured and are now tabulated in Tables 1 and 2 given below. Table 1 shows results for translational misalignments in x_M-axis and y_M-axis while Table 2 the results for rotational misalignments about the x_M-axis y_M-axis and z_M-axis.

x_M-axis[in.]	Fx_M[lb.]	y_M-axis[in.]	Fy_M[lb.]
-0.1	2.3	-0.1	2.0
-0.15	4.1	-0.15	3.2
-0.2	5.2	-0.2	3.7
-0.25	7.4	-0.25	5.3
-0.3	19.7	-0.3	5.7
0.1	-2.8	0.1	-2.4
0.15	-4.0	0.15	-3.5
0.2	-5.5	0.2	-4.1
0.25	-7.6	0.25	-5.2
0.3	-18.8	0.3	-5.9

Table 1 Translation misalignments in x_M and y_M axes

x_M-axis[deg]	Tx_M[lb-in]	y_M-axis[deg]	Ty_M[lb-in]	z_M-axis[deg]	Tz_M[lb-in]
-0.5	28	-0.5	153	-0.5	4
-1.0	60	-1.0	298	-1.0	7
-1.5	100	0.5	-170	-1.5	15
-2.0	138	1.0	-324	-2.0	25
0.5	-20			0.5	-8.5
1.0	-39			1.0	-12
1.5	-70			1.5	-21
2.0	-103			2.0	-32

Table 2 Rotational misalignments about x_M, y_M and z_M axes

5.2 Scenario 2: The Pallet/Oven Test

The Pallet/Oven test was performed with the oven assembly containing the two pins mounted to a stationary position using a vice and the pallet assembly mounted to the upper platform of the SPB manipulator via the JR3 force/torque sensor.

- **Perfect Alignment Operation:** First the perfect alignment between the oven pins and the pallet was established by controlling the SPB manipulator to move the pallet into a position above the open pins so that the holes on the pallet roughly aligned with the pins. Then the SPB manipulator was controlled to push the pallet onto the pins. After that, the SPB manipulator was controlled to slowly and carefully modify its pose until the reading of forces/torques measured by the JR3 sensor was zero. The resulting pose at which no forces/torques were read was the perfect alignment pose. At the end, the SPB manipulator was controlled to move out from the perfect alignment pose. From the resulting pose, to evaluate the operation under perfect alignment, the SPB manipulator was controlled to move the pallet holes onto the oven pins then demate the pallet from the oven. According to force reading, there were no noticeable forces/torques exerted to the compliant device during the mating and demating.

- **Capture Range Determination:** The capture ranges for the oven/pallet were determined using the following procedures. First the SPB manipulator was controlled to move out from the perfect alignment about 1 in. Then from the resulting pose, the SPB manipulator was used to introduce single-axis misalignments, one axis at a time. After the misalignment was introduced, the pallet was controlled to move onto the oven pins and the gap between the oven surface and the pallet surface was inspected. The misalignments were increased in small increments and after each increase, the above process was repeated. The capture range for each axis was determined as the misalignment amount just before the surfaces of the oven and the pallet failed to completely flush. In other words, any misalignment which is smaller or equal to the capture range ensures the complete flushedness of the surfaces. In each of the misalignment cases, an 0.15 in. overtravel was commanded in the involved axis to help the passive compliant device to make the two surfaces to flush. The capture ranges for the oven/pallet test are tabulated in Table 3 given below. As shown in Table 3, the capture range for translation in x_M-axis was found to be ± 0.15 in. However, the oven pins and pallet holes were designed so that the oven surface and the pallet surface flush completely under a misalignment of ± 0.25 in. along the x_M-axis. As a result, the pallet holes and the oven pins were re-designed and manufactured. Testing of the new setup showed that the capture range for the x_M-axis is ± 0.20 in.

translation along x_M-axis	rotation about x_M-axis	rotation about y_M-axis	rotation about z_M-axis
± 0.150 *inches*	± 0.5 *degrees*	± 6.0 *degrees*	± 1.0 *degrees*

Table 3 Capture ranges for Scenario 2, Pallet/Oven

- **Operation under Misalignments:** Using the same procedure as discussed above, mating between the oven pins and the pallet holes under single-axis misalignments was investigated. In particular, for each of the misalignments to be studied, after the misalignment was introduced, the oven pins were mated and then demated with the pallet holes. During the mating and demating, forces/torques in six DOFs at the center of the passive compliant device were measured and recorded.

  For the old Pallet/Oven, the following work was carried out:

  1. **Translational Misalignment along x_M-axis:** Forces (torques) along (about) x_M-axis, y_M-axis and z_M-axis were measured for mating under perfect alignment, and under misalignments of 0.05 in., 0.1 in., 0.15 in., 0.2 in., -0.05 in, -0.1 in., -0.15 in., and -0.2 in. along x_M-axis.
  2. **Rotational Misalignment about x_M-axis:** Forces (torques) along (about) x_M-axis, y_M-axis and z_M-axis were measured for mating under misalignments of 0.5 deg., 1.0 deg., 1.5 deg., 2.0 deg., -0.5 deg., -1.0 deg., -1.5 deg., and -2.0 deg. about x_M-axis.
  3. **Rotational Misalignment about y_M-axis:** Forces (torques) along (about) x_M-axis, y_M-axis and z_M-axis were measured for mating under misalignments of 0.5 deg., 1.0 deg., -0.5 deg., and -1.0 deg. about y_M-axis.

4. **Rotational Misalignment about z_M-axis:** Forces (torques) along (about) x_M-axis, y_M-axis and z_M-axis were measured for mating under misalignments of 0.5 deg., 1.0 deg., 1.5 deg., 2.0 deg., -0.5 deg., -1.0 deg., -1.5 deg., and -2.0 deg. about z_M-axis.

Although the time responses of forces/torques in six DOFs of the compliant device are available, because of page limitation of this report, we present here in Figures OLDPIN1-OLDPIN18, only those for the case of translational misalignment along the x_M-axis which is the radial axis of the compliant device. The transitions from zero force to high force and from high force to zero force indicate the mating and demating of the oven pins with the pallet holes, respectively.

For the new Pallet/Oven, the following work was completed:

1. **Translational Misalignment along x_M-axis:** Forces (torques) along (about) x_M-axis, y_M-axis and z_M-axis were measured for mating under perfect alignment, and under misalignments of 0.05 in., 0.1 in., 0.15 in., 0.2 in., -0.05 in, -0.1 in., -0.15 in., and -0.2 in. along x_M-axis.

Similar to the case of the old Pallet/Oven, although the time responses of forces/torques in six DOFs of the compliant device are available, we select Figures NEWPIN1-NEWPIN18 to present the time responses of the case of translational misalignment along the x_M-axis which is the radial axis of the compliant device.

5.3 Scenario 3: The Pallet/Rack Test

The Pallet/Rack test was conducted with the rack mounted to a stationary position using a vice and the pallet assembly mounted to the upper platform of the SPB manipulator via the JR3 force/torque sensor. Two different racks were considered, a rack marked with a letter on it *S*, which is referred hereto as the *S Rack* and a rack with high tolerance, which is referred hereto as the *High Tolerance Rack*.

- **Perfect Alignment Operation:** The perfect alignment pose was established using the same procedures of the other scenarios. First the SPB manipulator was controlled to move the pallet into a position roughly aligned with the rack. Then the pallet was carefully pushed into the rack. After that, the SPB manipulator was controlled to slowly and carefully modify its pose until the it reached a pose at which the reading of forces/torques measured by the JR3 sensor was zero. This pose was the perfect alignment pose. Finally from the perfect alignment pose, the pallet was moved out of the rack. To evaluate the operation under perfect alignment, from the above resulting pose, the SPB manipulator was controlled to insert the pallet into the rack and again demate the pallet from the rack. Six DOF forces/torques exerted during the insertion and demating were measured and recorded. The above process was done for both the S Rack and the High Tolerance

Rack. According to force reading, there were no noticeable forces/torques exerted during the insertion and demating for both racks.

- **Capture Range Determination:** The capture ranges for the rack/pallet were visually determined and presented in Table 4 given below:

	translation along y_M-axis [in.]	rotation about x_M-axis [deg.]	rotation about y_M-axis [deg.]	rotation about z_M-axis [deg.]
S Rack	-0.3	±7.0	±8.0	±8.0
High Tolerance Rack	-0.3	±7.0	±8.0	±8.0

Table 4 Capture ranges for Scenario 3, Pallet/Rack

- **Operation under Misalignments:** Using the same procedure employed in other scenarios, insertion of the pallet into the rack under single-axis misalignments was investigated.

  For the S Rack, the following tests were performed:

  1. **Translational Misalignment along y_M-axis:** Forces (torques) along (about) x_M-axis, y_M-axis and z_M-axis were measured for insertion under perfect alignment, and under misalignments of 0.05 in., 0.1 in., 0.15 in., 0.2 in., 0.25 in., 0.30 in., -0.05 in, -0.1 in., -0.15 in., -0.2 in., -0.25 in, and -0.30 in. along y_M-axis.
  2. **Rotational Misalignment about x_M-axis:** Forces (torques) along (about) x_M-axis, y_M-axis and z_M-axis were measured for mating under misalignments of 0.5 deg., 1.0 deg., 1.5 deg., 2.0 deg., -0.5 deg., -1.0 deg., -1.5 deg., and -2.0 deg. about x_M-axis.
  3. **Rotational Misalignment about y_M-axis:** Forces (torques) along (about) x_M-axis, y_M-axis and z_M-axis were measured for mating under misalignments of 0.5 deg., 1.0 deg., 1.5 deg., 2.0 deg., -0.5 deg., -1.0 deg., -1.5 deg., and -2.0 deg. about y_M-axis.
  4. **Rotational Misalignment about z_M-axis:** Forces (torques) along (about) x_M-axis, y_M-axis and z_M-axis were measured for mating under misalignments of 0.5 deg., 1.0 deg., 1.5 deg., 2.0 deg., -0.5 deg., -1.0 deg., -1.5 deg., and -2.0 deg. about z_M-axis.

Although the time responses of forces/torques in six DOFs are available for all above cases, we only select the case of translational misalignment along the elevation axis (which is -y_M) to present here in Figures SRACK1-SRACK26 because of space limitation.

For the High Tolerance Rack, the following tests were finished:

1. **Translational Misalignment along y_M-axis:** Forces (torques) along (about) x_M-axis, y_M-axis and z_M-axis were measured for insertion under perfect alignment, and under misalignments of 0.05 in., 0.1 in., 0.15 in., 0.2 in., 0.25 in., 0.30 in., -0.05 in, -0.1 in., -0.15 in., -0.2 in., -0.25 in, and -0.30 in. along y_M-axis.
2. **Rotational Misalignment about x_M-axis:** Forces (torques) along (about) x_M-axis, y_M-axis and z_M-axis were measured for mating under misalignments of 0.5 deg., 1.0 deg., 1.5 deg., 2.0 deg., -0.5 deg., -1.0 deg., -1.5 deg., and -2.0 deg. about x_M-axis.
3. **Rotational Misalignment about y_M-axis:** Forces (torques) along (about) x_M-axis, y_M-axis and z_M-axis were measured for mating under misalignments of 0.5 deg., 1.0 deg., -0.5 deg., and -1.0 deg. about y_M-axis.
4. **Rotational Misalignment about z_M-axis:** Forces (torques) along (about) x_M-axis, y_M-axis and z_M-axis were measured for mating under misalignments of 0.5 deg., 1.0 deg., 1.5 deg., 2.0 deg., -0.5 deg., -1.0 deg., -1.5 deg., and -2.0 deg. about z_M-axis.

Time responses of forces/torques in six DOFs are available for all above cases. However, because of space limitation, we present here only those for the case of translational misalignment along the elevation axis (which is -y_M) of the compliant device in Figures HRACK1-HRACK26.

6 COMMENTS AND EVALUATIONS

This section gives comments, observations and evaluations which are based upon the experimental results obtained from the tests.

1. **Operation under Perfect Alignment:** Based upon obtained test results, we found that operation under perfect alignment including mating (grasping, insertion) and demating for all three scenarios, Pallet/Finger, Pallet/Oven and Pallet/Rack has been successful. This has been derived from the fact that no noticeable forces/torques were exerted to the compliant device during the mating and demating under perfect alignment for all scenarios.

2. **Operation under Misalignment:** From experimental results, we find, as expected, that the magnitudes of forces/torques exerted in an axis are proportional to the amount of misalignment in this axis. The proportionality is however non-linear.

3. **Capture Ranges for Pallet/Finger:** The capture ranges were not determined for the Finger/Pallet test. However using Table 1, from the fact that the maximum force that the compliant device can yield in the radial and elevation axes is 10 lb., we can safely state that the capture ranges for x_M-axis and y_M-axis are ± 0.25 in. and ± 0.30 in., respectively since the forces in the respective axis did not exceed 10 lb.

4. **Improvement of Pallet/Oven:**

   - After finding out that the old Pallet/Oven does not meet the specification, the old oven pins were re-manufactured (based on George Veollmer's suggestions) to have longer taper, larger diameter and longer length. In addition, the pallet holes were re-manufactured to accommodate the new oven pins.
   - As stated earlier, the capture range of the Pallet/Oven in the radial-axis of the compliant device was increased from ± 0.15 in. (old Pallet/Oven) to ± 0.20 in. (new Pallet/Oven).
   - Observing Figure OLDPIN1-OLDPIN18 and NEWPIN1-NEWPIN18, we find that the new Pallet/Oven has substantial improvement in force time responses. For example, in Figure OLDPIN9 and Figure NEWPIN9 which illustrate the force time histories for 0.20 misalignment, we note the force (after the mating and before the mating) in the x_M-axis was decreased from -9.8 lb. (old Pallet/Oven) to -5.75 lb. (new Pallet/Oven). Inspection of other cases of misalignment shows that the forces are generally decreased if the new Pallet/Oven was used.

5. **Compliant Device Performance:**

   - After conducting the tests presented in this report, we found that the compliant mechanism performed according to its specifications. Based upon the test results, the compliant device provided large compliance in the radial and elevation axes and small compliance in other axes. In addition, it has been able to accommodate misalignments up to $\pm$ 0.2 in. in all the compliance axes (radial and elevation) without exceeding the maximum allowed force of 10 lb. and without hitting the mechanical stops in all three scenarios.
   - Inspecting the time histories of forces/torques for the Pallet/Oven and Pallet/Rack scenarios, we note that the compliant device has good damping which is manifested by generally smooth transitions from mating (insertion) to demating or vice versa without any significant surges in forces/torques.

- From Table 1, we conclude that the compliant device possesses symmetry in the compliance axes, namely the radial and elevation axes and non-symmetry in other axes.

References

[1] **Purves, L.**, "Robot Operated Materials Processing System (ROMPS), Critical Design Review (CDR)," *Goddard Space Flight Center*, 1992.

[2] **Nguyen, C.C., Antrazi, S., Zhou, Z-L, and Campbell, Jr., C.E.**, "Analysis and Implementation of a 6 DOF Stewart-Platform-Based Robotic Wrist," *Computers and Electrical Engineering: An International Journal*, Vol. 17, Number 3, pp. 191-204, 1991.

[3] **Nguyen, C.C.**, "Testing of Robot Fingers and Dedicated Interfaces," *Final Report*, NASA/Goddard Space Flight Center, April 1991

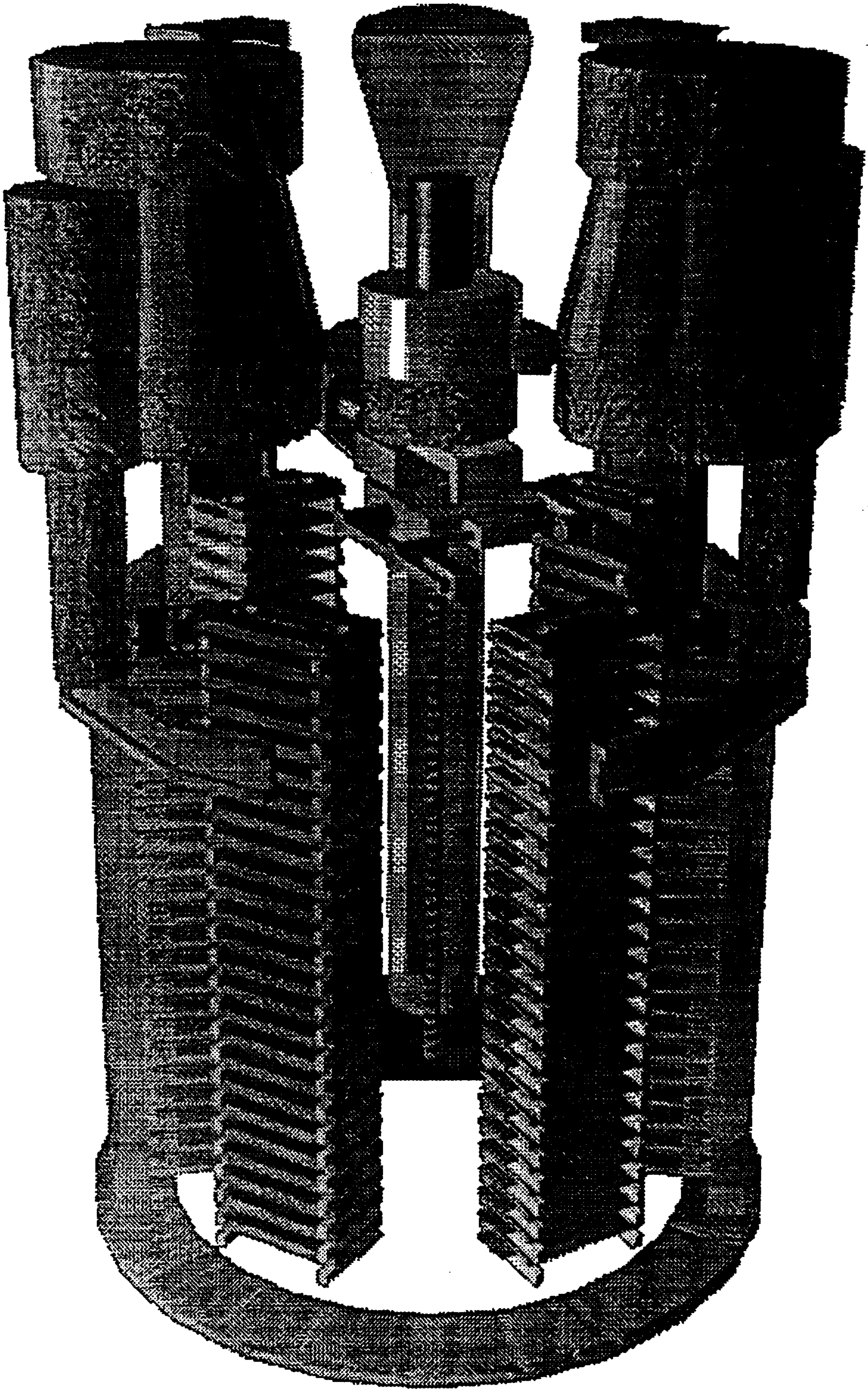

Figure 1 The Robot Operated Materials Processing System (ROMPS)

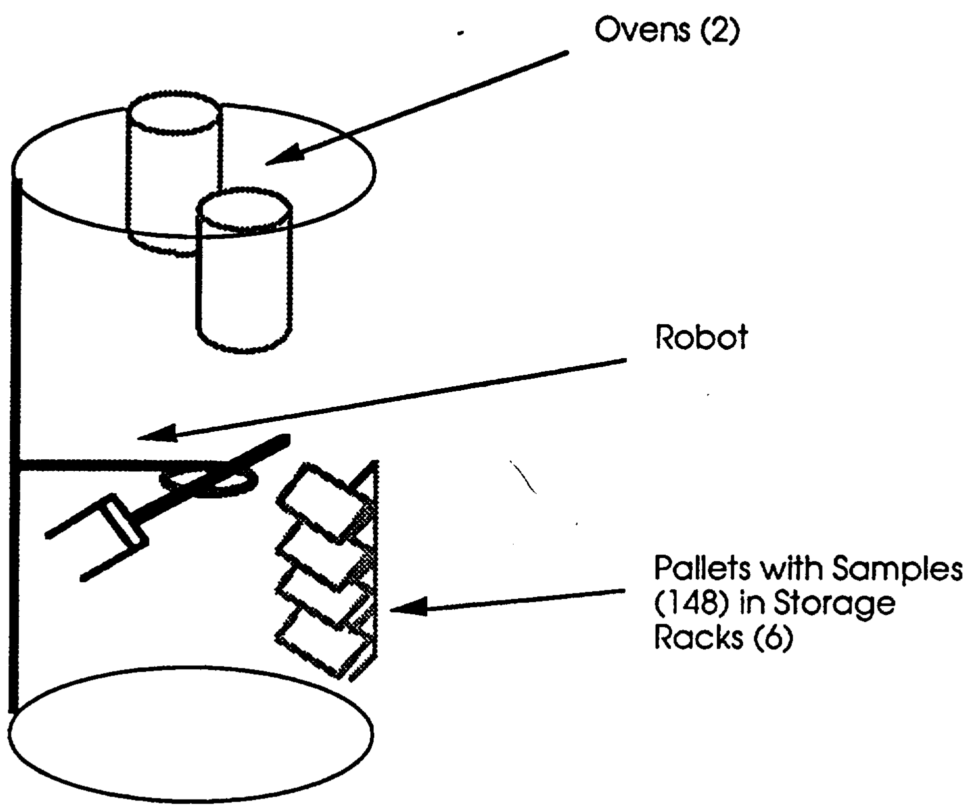

Figure 2 The ROMPS robot

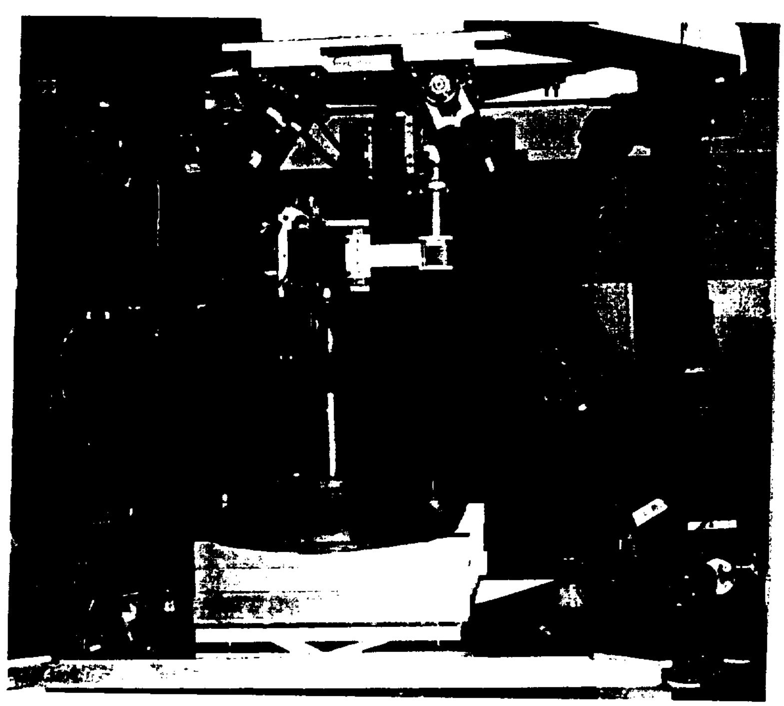

Figure 3 The testbed

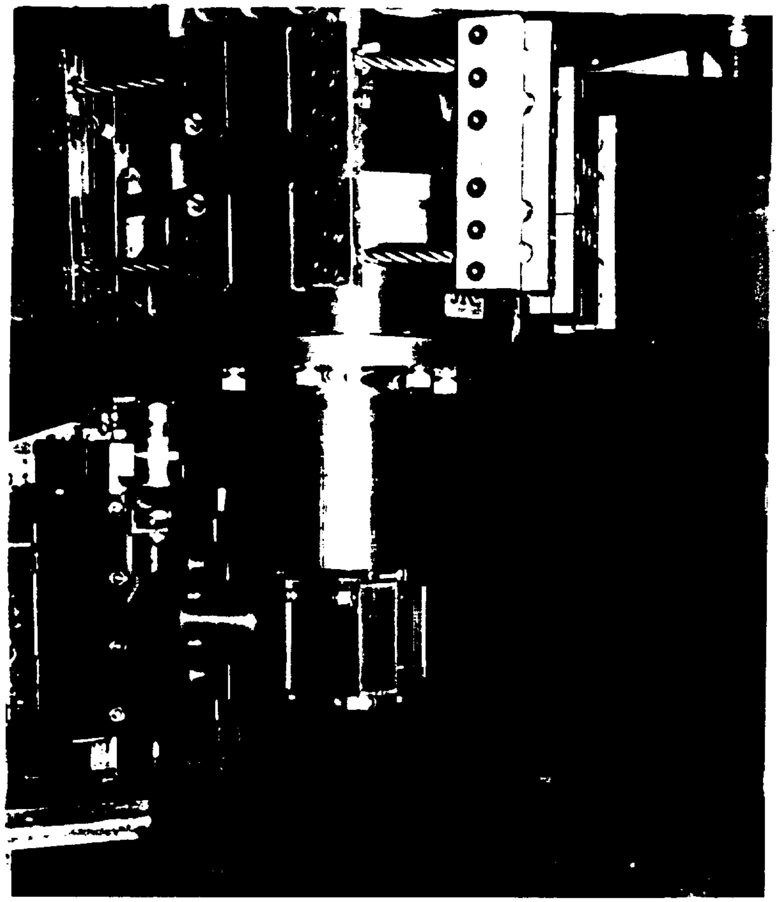

Figure 4 The wrist passive compliant device

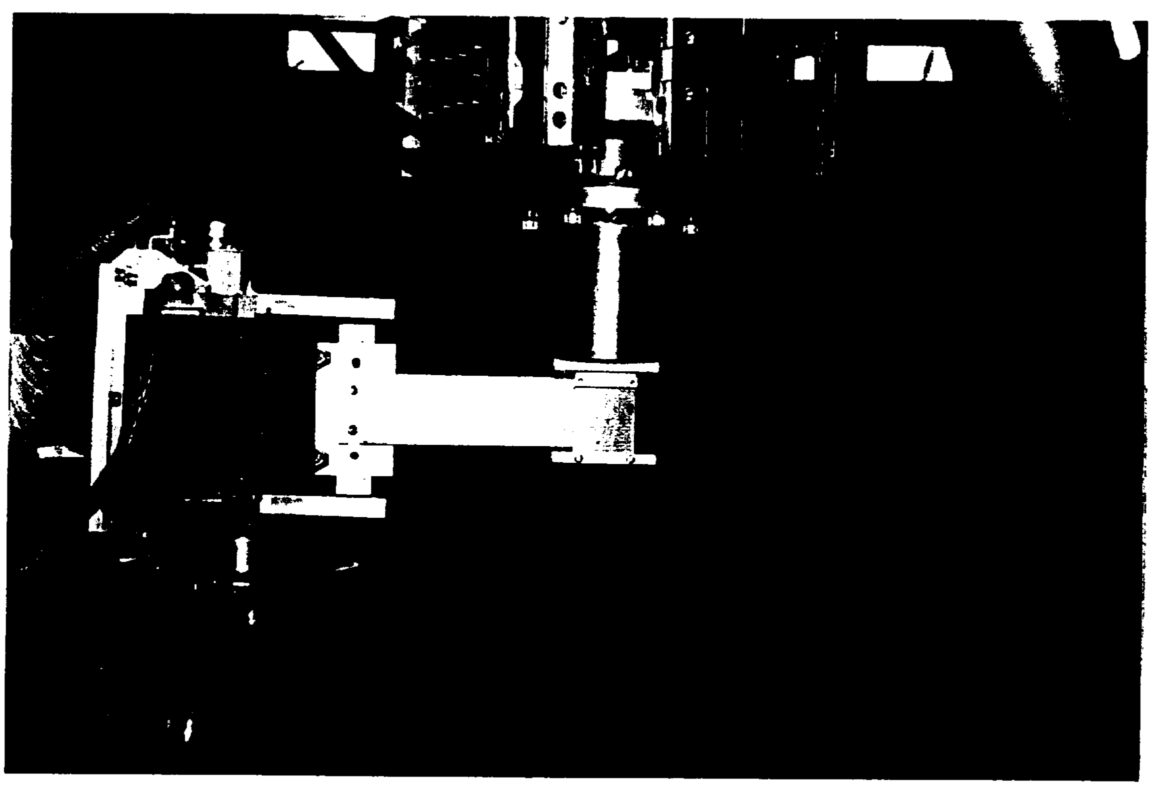

Figure 5 Mating test between the pallet and the robot fingers

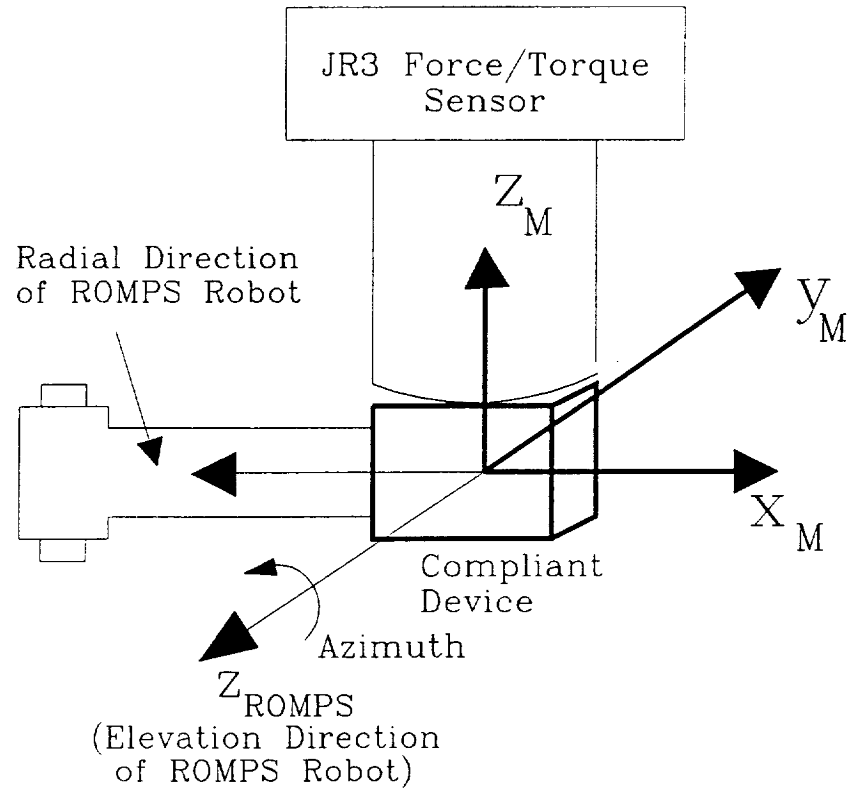

Figure 6 Assignment of coordinate systems

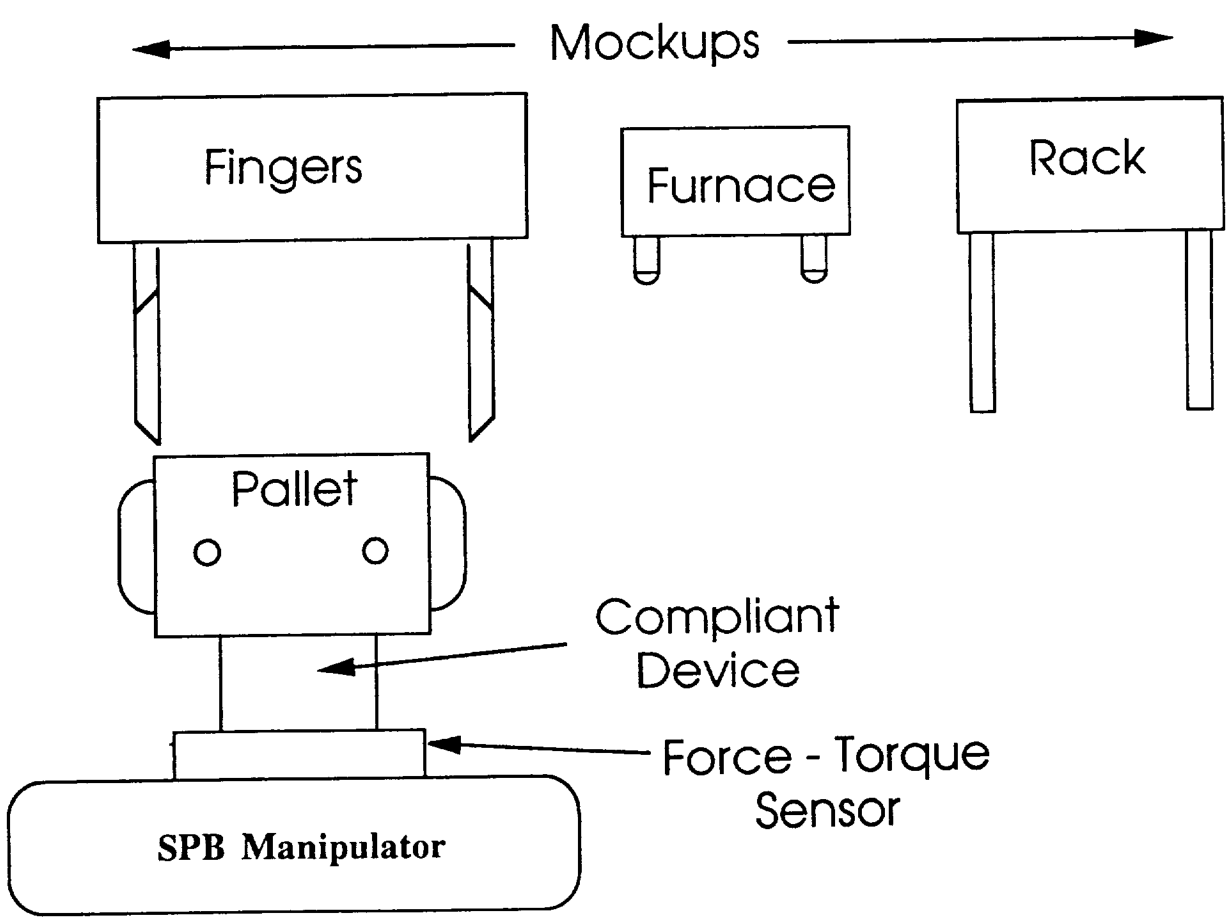

Figure 7 The test setup for the three scenarios

Figure OLDPIN1 Time histories of forces under perfect alignment
dashed: F_x; *dashed-dotted:* F_y; *solid:* F_z

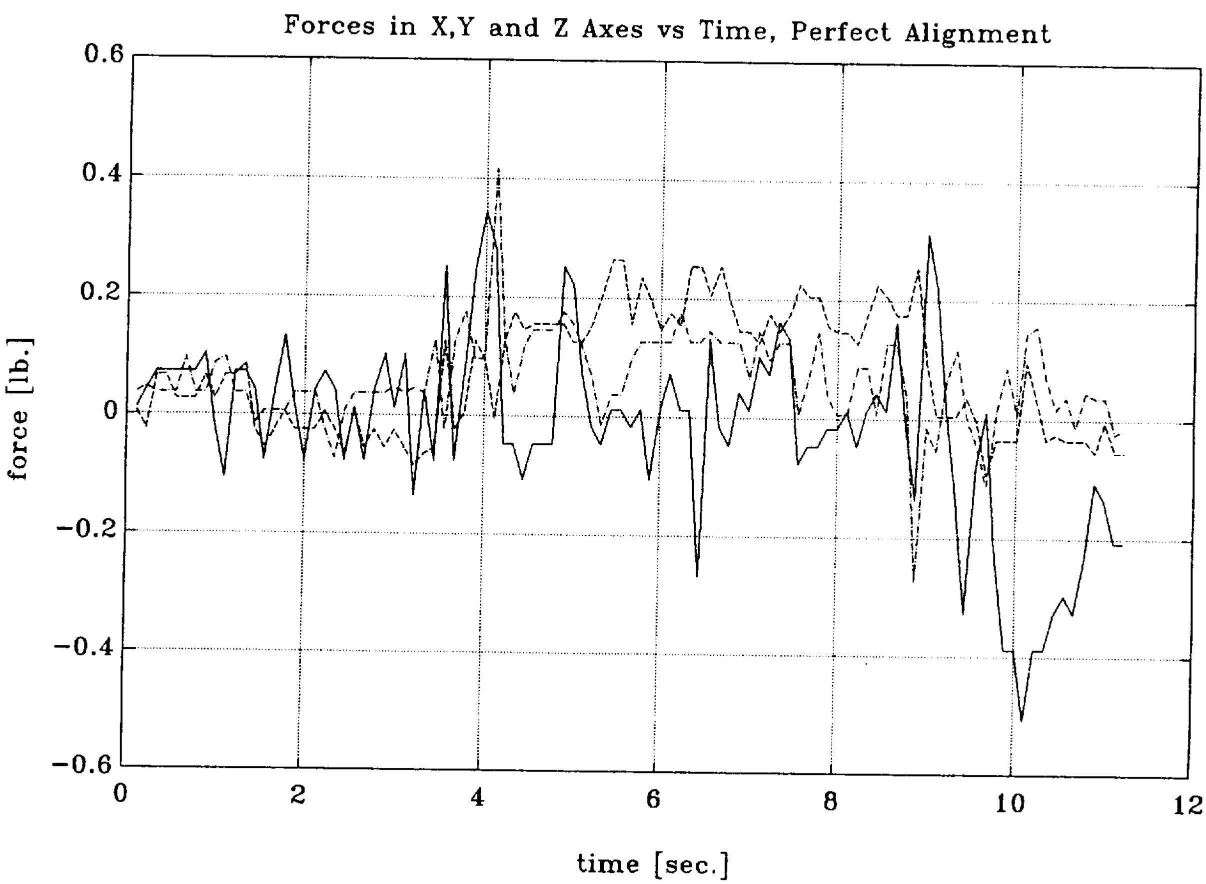

Figure OLDPIN2 Time histories of torques under perfect alignment
dashed: T_x; *dashed-dotted:* T_y; *solid:* T_z

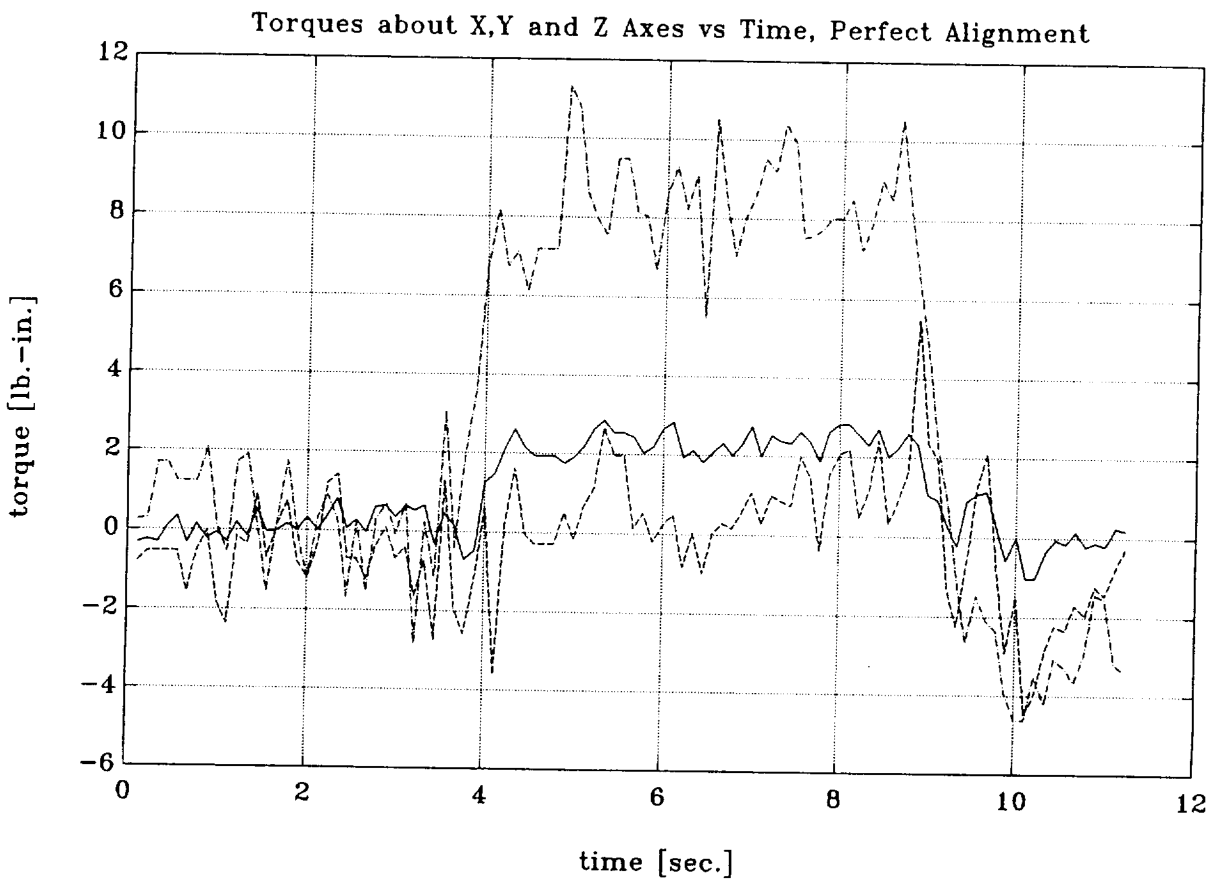

Figure OLDPIN3 Time histories of forces under 0.05 in. misalignment
dashed: F_x*; dashed-dotted:* F_y*; solid:* F_z

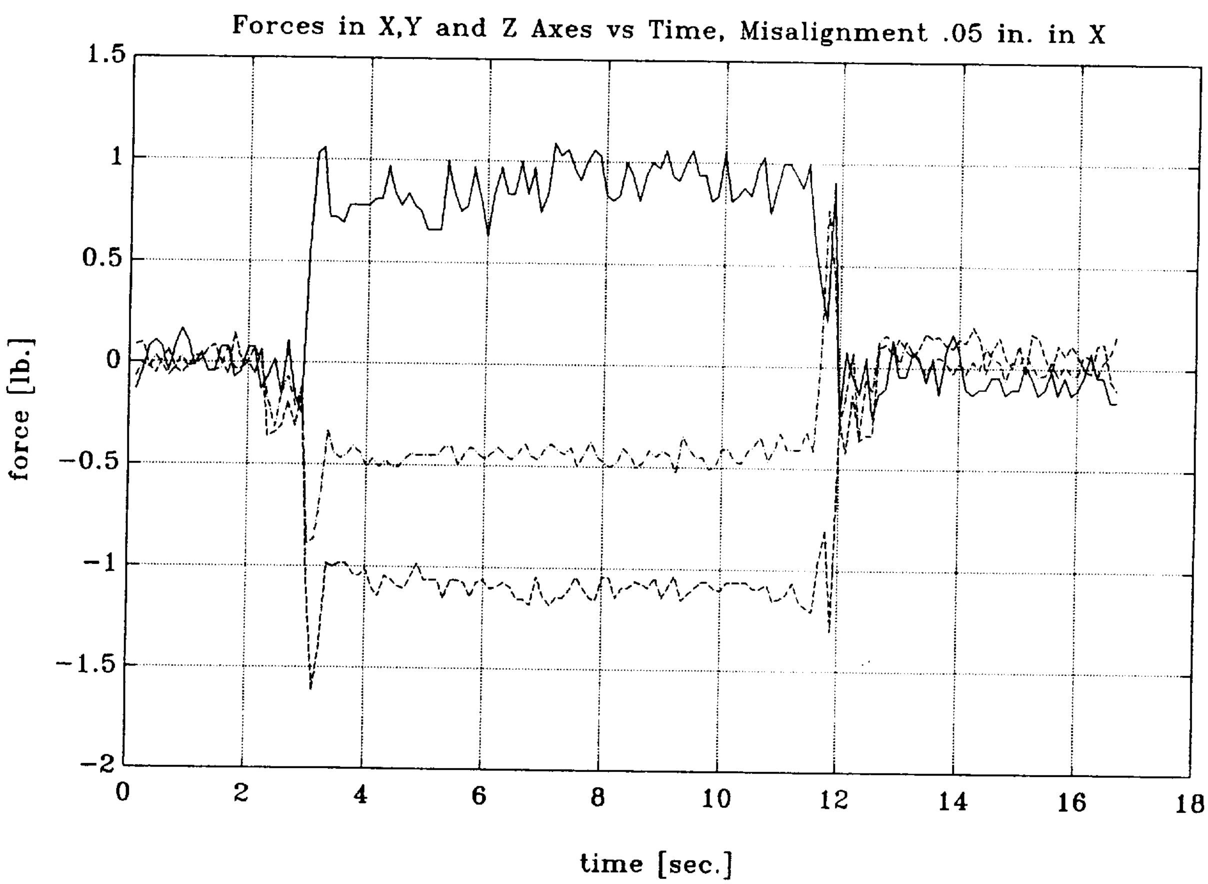

Figure OLDPIN4 Time histories of torques under 0.05 in. misalignment
dashed: T_x; *dashed-dotted:* T_y; *solid:* T_z

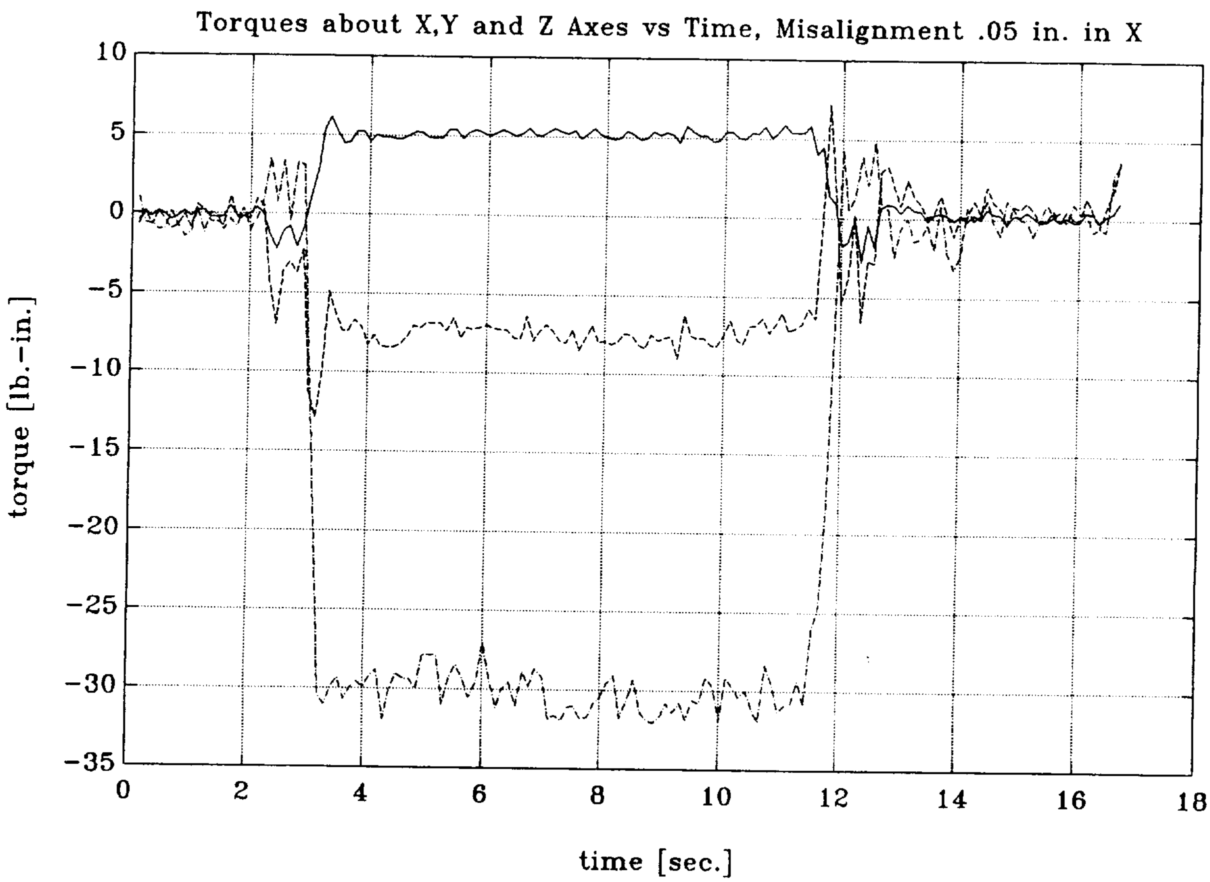

Figure OLDPIN5 Time histories of forces under 0.1 in. misalignment
dashed: F_x; *dashed-dotted:* F_y; *solid:* F_z

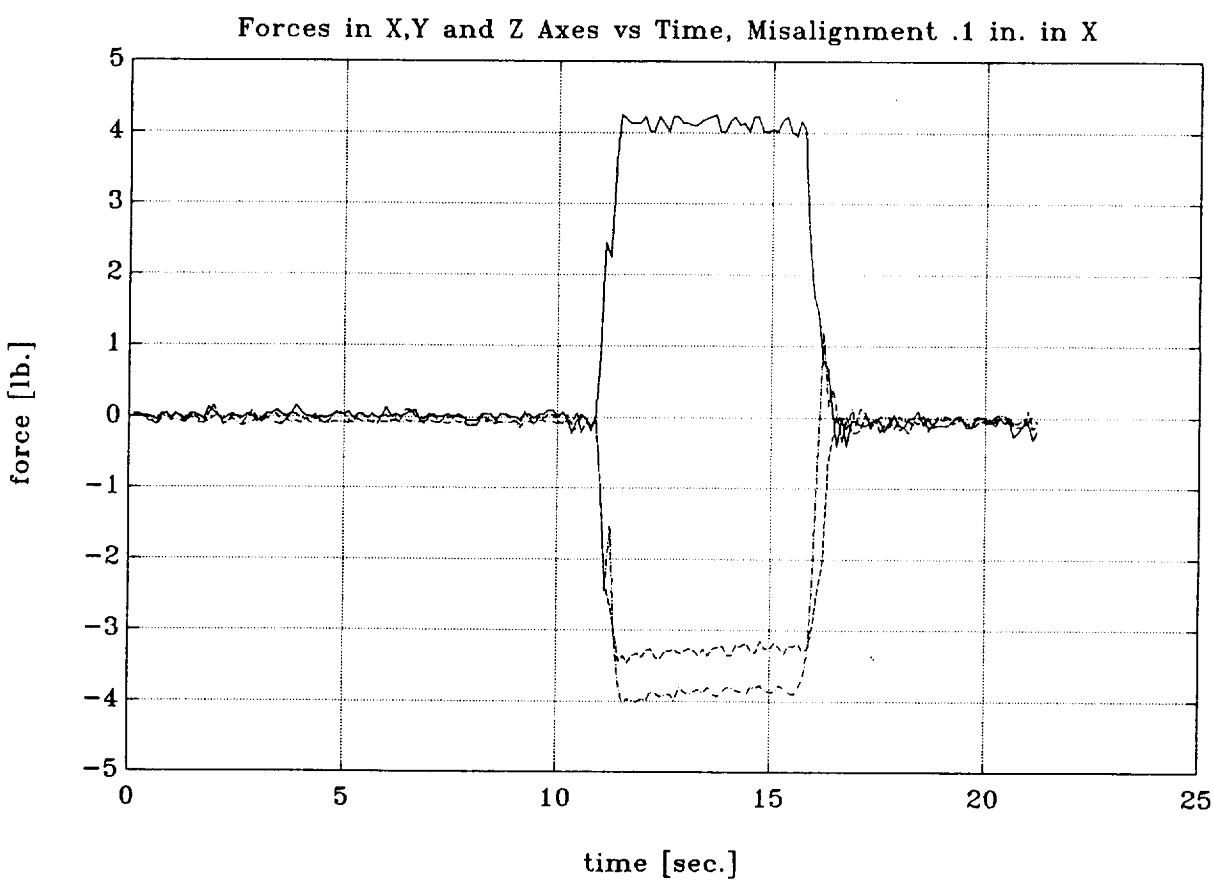

Figure OLDPIN6 Time histories of torques under 0.1 in. misalignment
dashed: T_x; *dashed-dotted:* T_y; *solid:* T_z

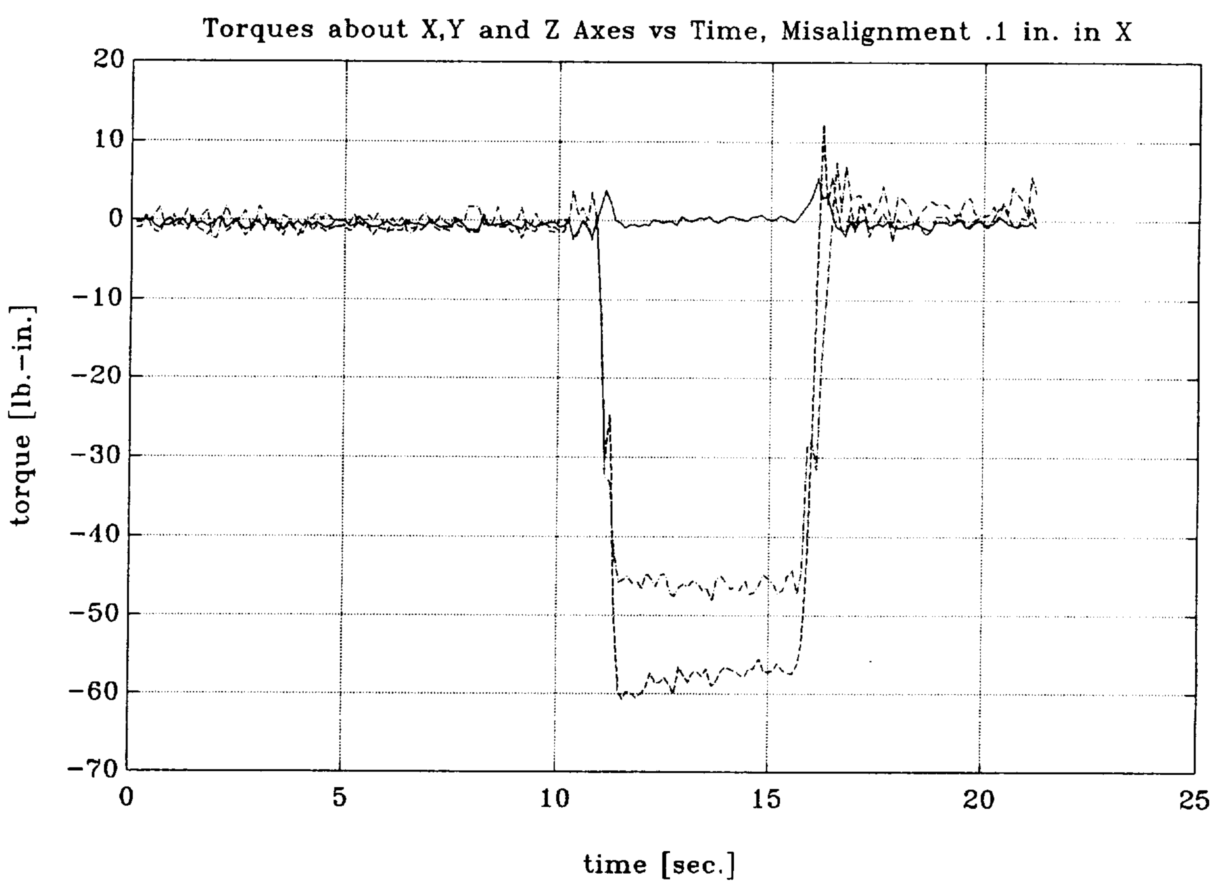

Figure OLDPIN7 Time histories of forces under 0.15 in. misalignment
dashed: F_x; *dashed-dotted:* F_y; *solid:* F_z

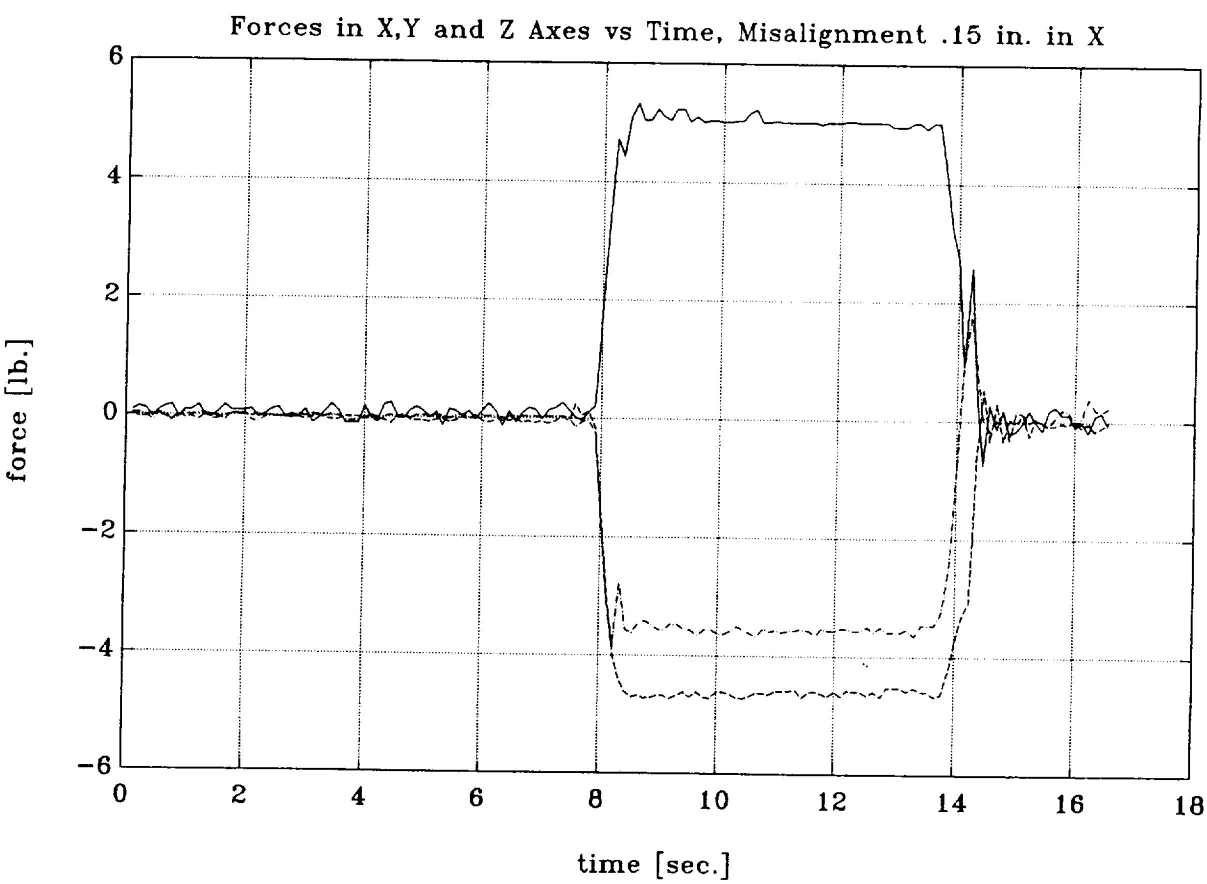

Figure OLDPIN8 Time histories of torques under 0.15 in. misalignment
dashed: T_x*; dashed-dotted:* T_y*; solid:* T_z

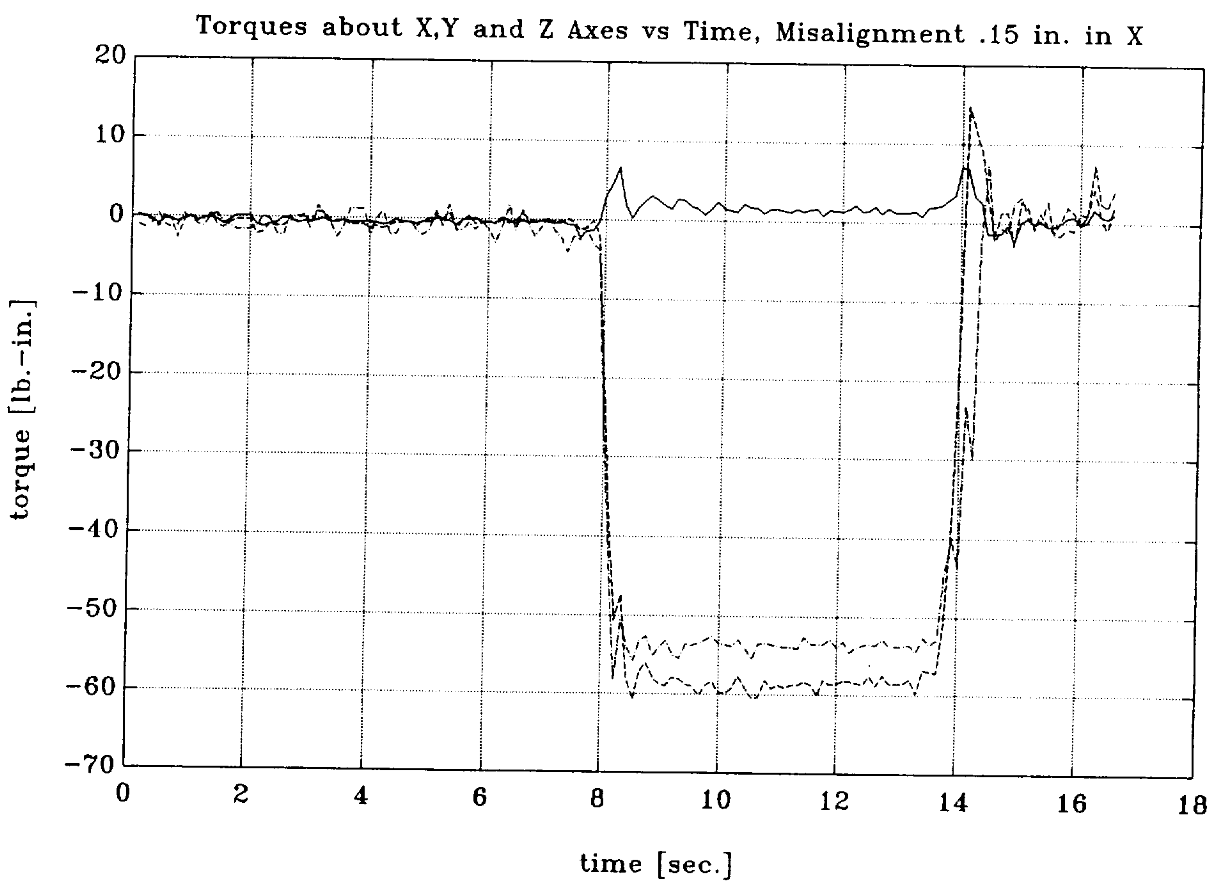

Figure OLDPIN9 Time histories of forces under 0.20 in. misalignment
dashed: F_x; *dashed-dotted:* F_y; *solid:* F_z

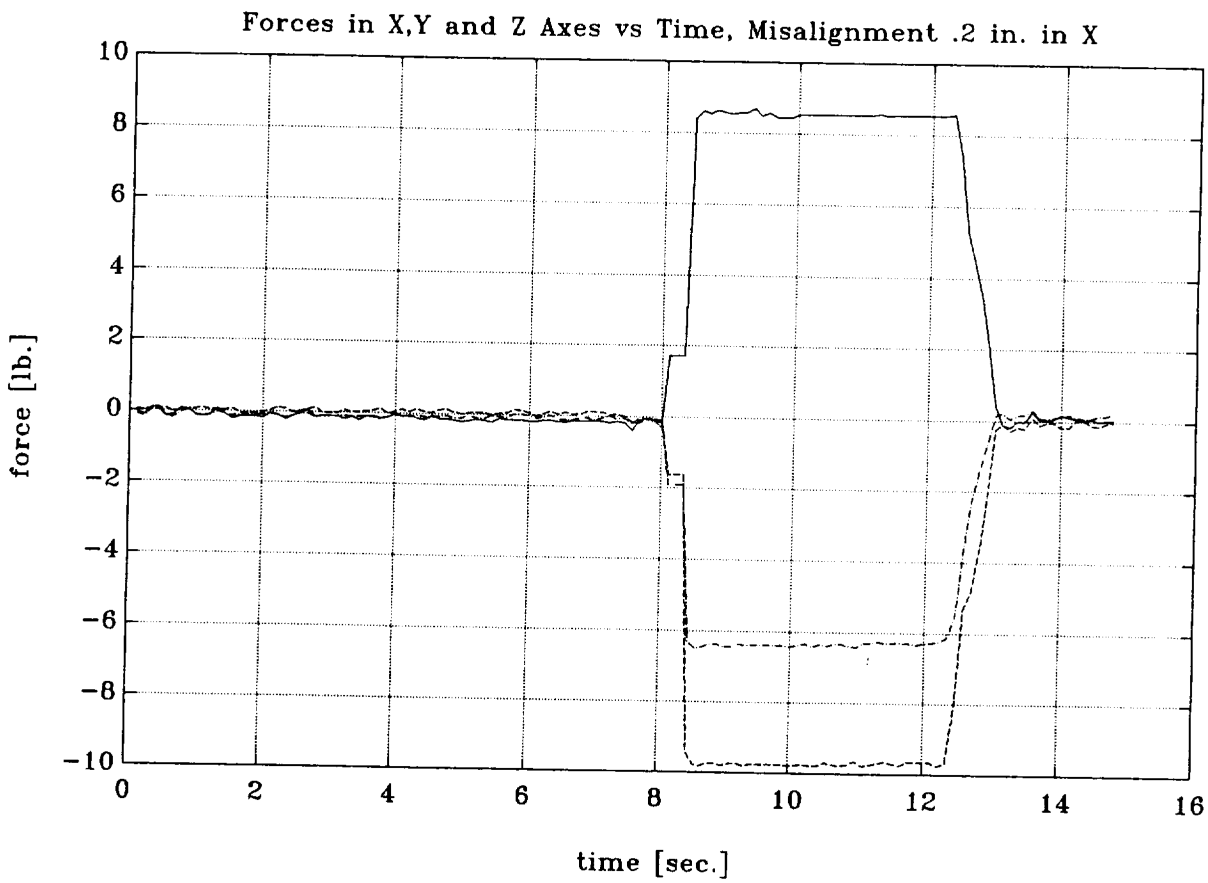

Figure OLDPIN10 Time histories of torques under 0.20 in. misalignment
dashed: T_x; *dashed-dotted:* T_y; *solid:* T_z

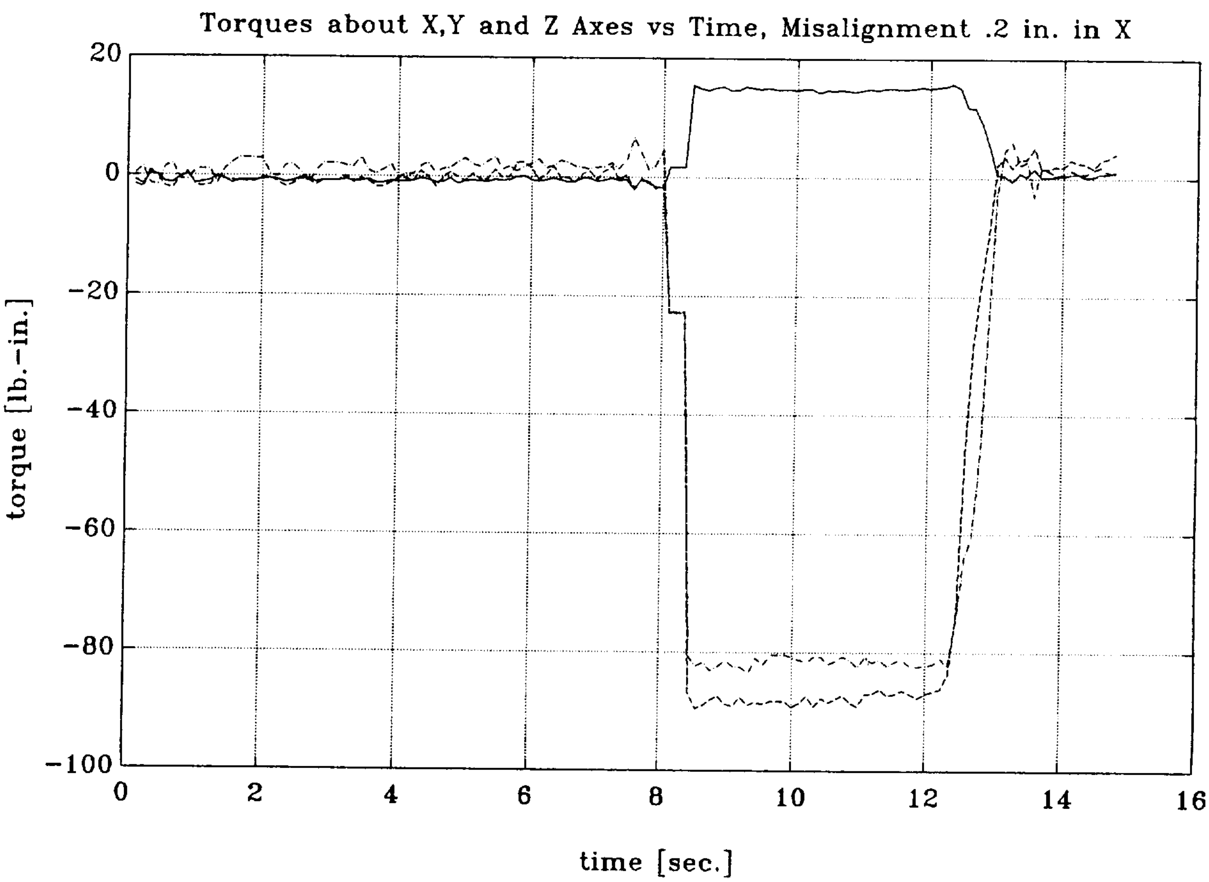

Figure OLDPIN11 Time histories of forces under -0.05 in. misalignment
dashed: F_x; *dashed-dotted:* F_y; *solid:* F_z

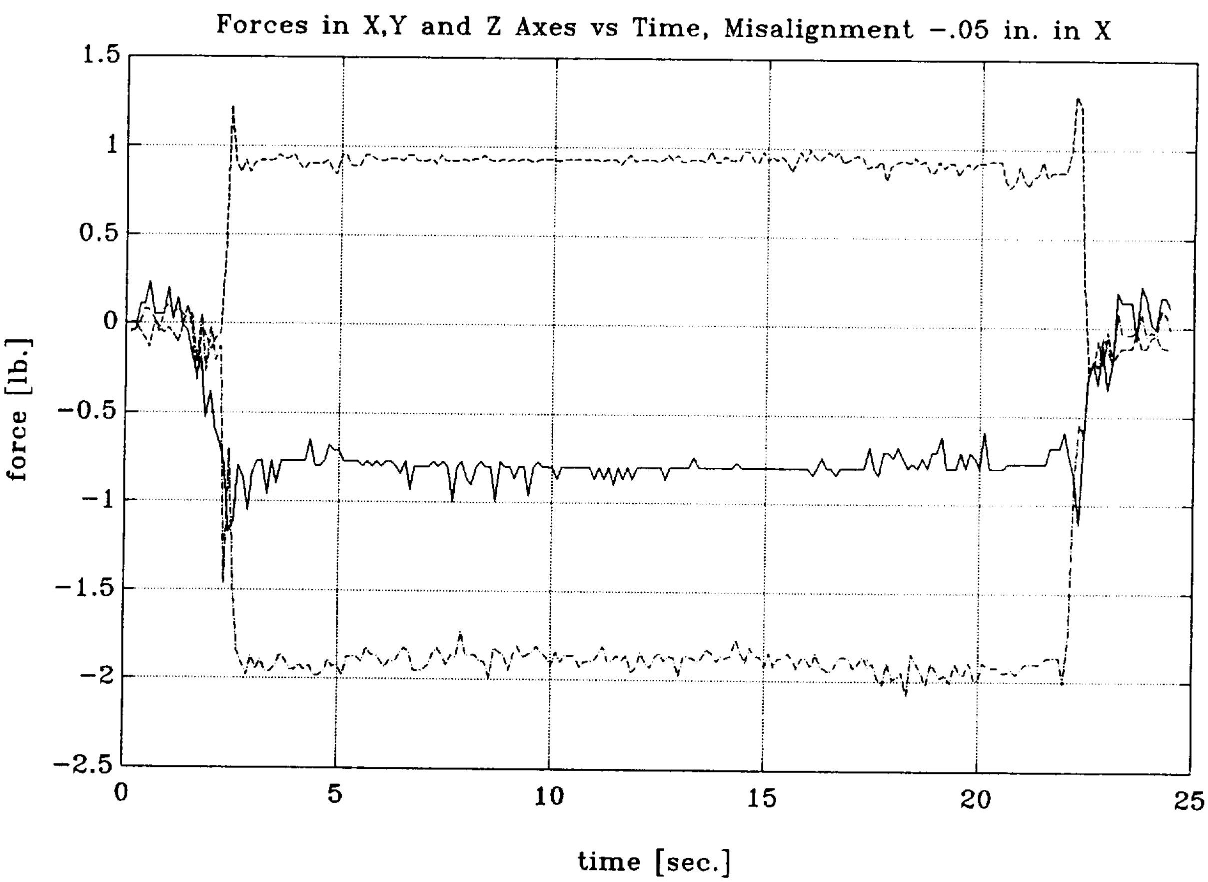

Figure OLDPIN12 Time histories of torques under -0.05 in. misalignment
dashed: T_x; *dashed-dotted:* T_y; *solid:* T_z

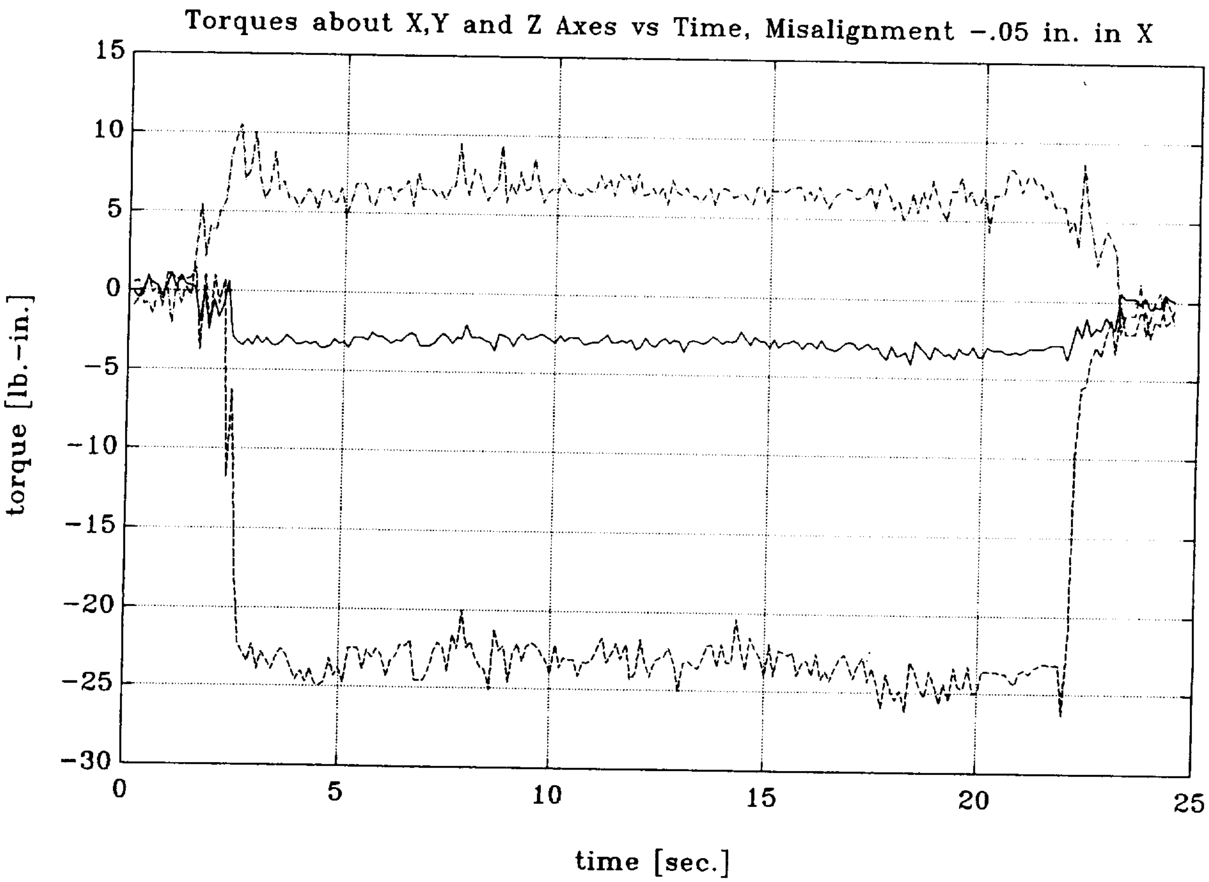

Figure OLDPIN13 Time histories of forces under -0.1 in. misalignment
dashed: F_x; *dashed-dotted:* F_y; *solid:* F_z

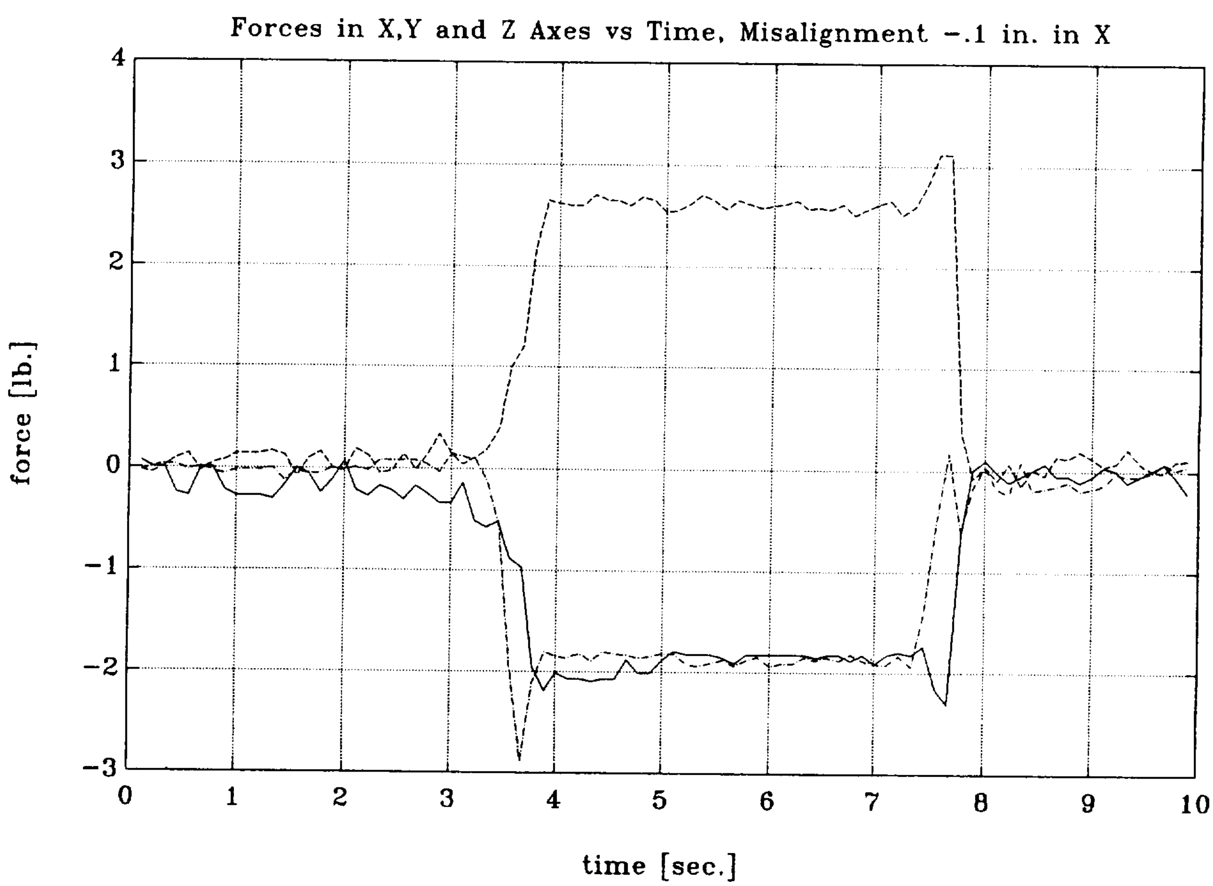

Figure OLDPIN14 Time histories of torques under -0.1 in. misalignment
dashed: T_x; dashed-dotted: T_y; solid: T_z

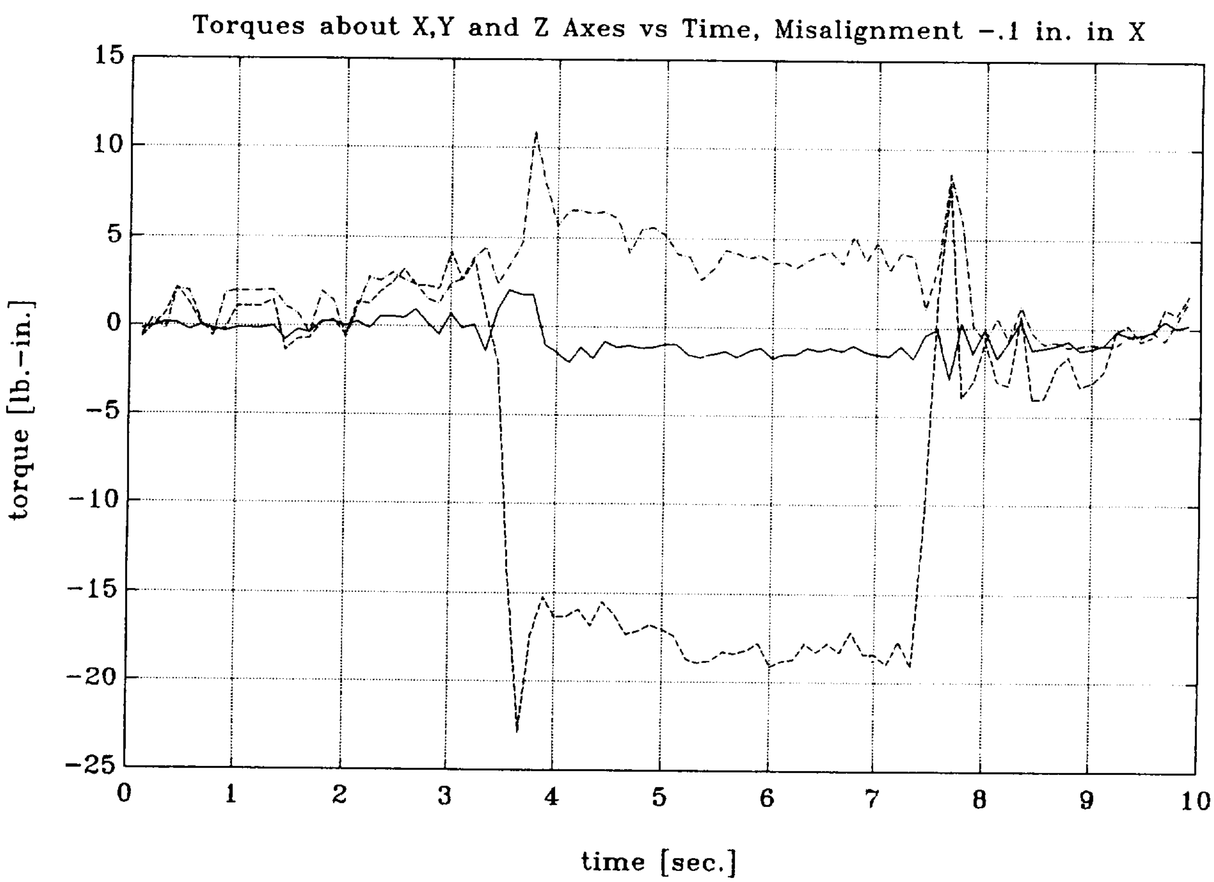

Figure OLDPIN15 Time histories of forces under -0.15 in. misalignment
dashed: F_x; *dashed-dotted:* F_y; *solid:* F_z

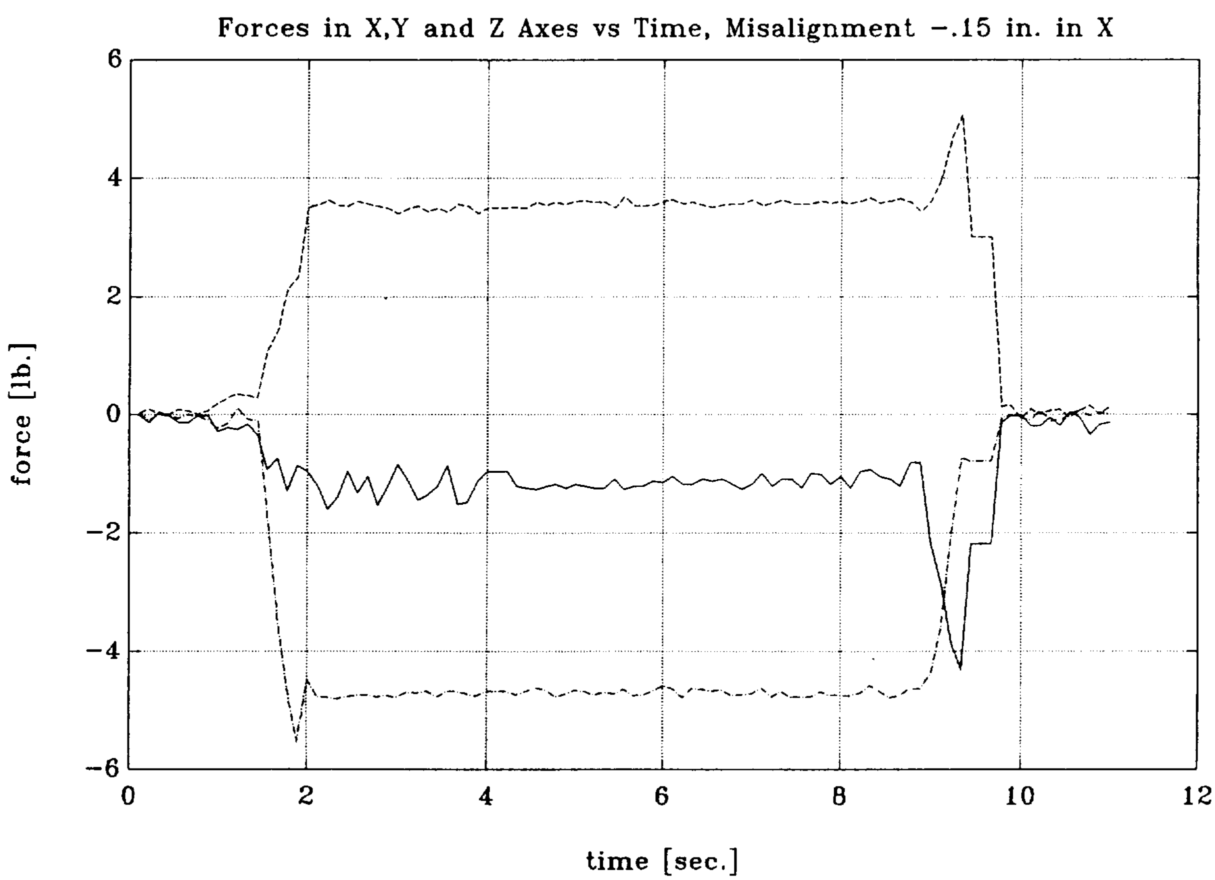

Figure OLDPIN16 Time histories of torques under -0.15 in. misalignment
dashed: T_x*; dashed-dotted:* T_y*; solid:* T_z

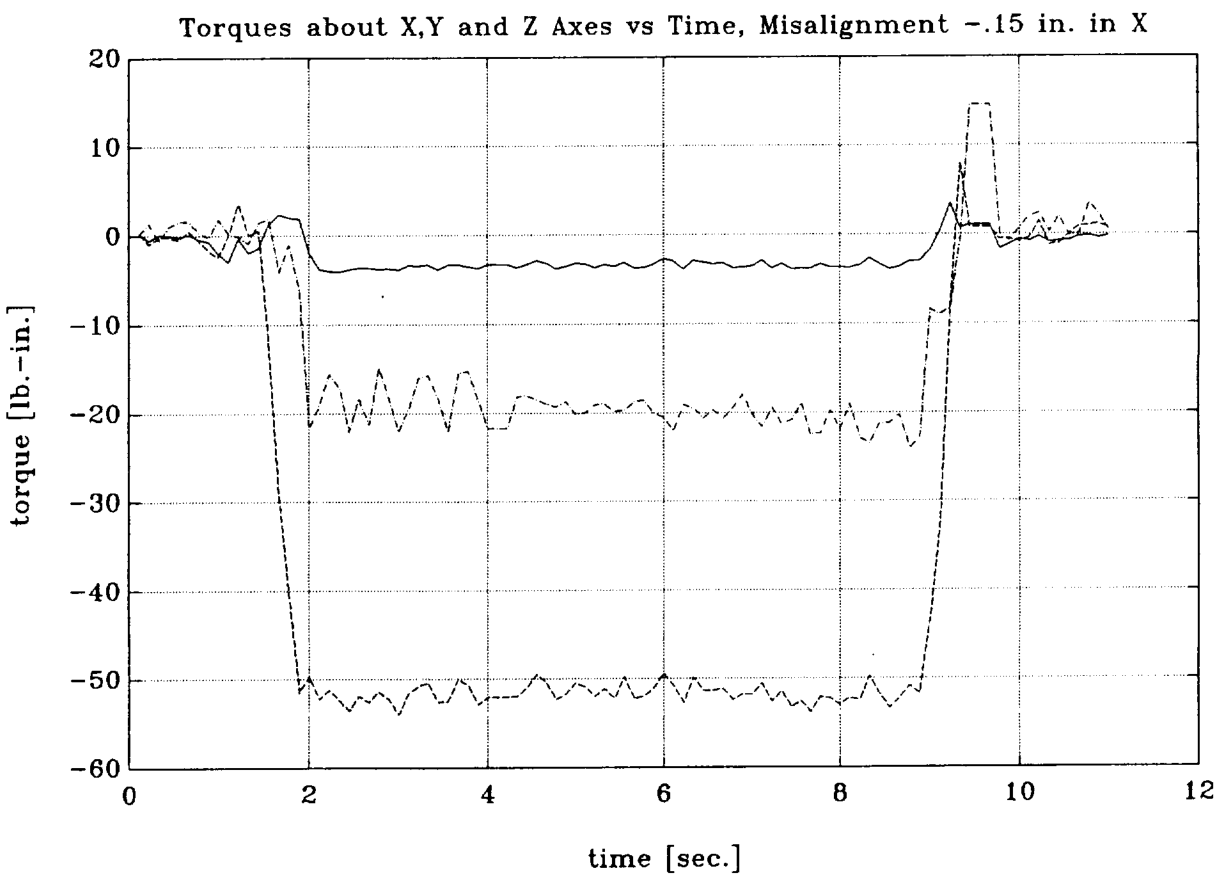

Figure OLDPIN17 Time histories of forces under -0.20 in. misalignment
dashed: F_x*; dashed-dotted:* F_y*; solid:* F_z

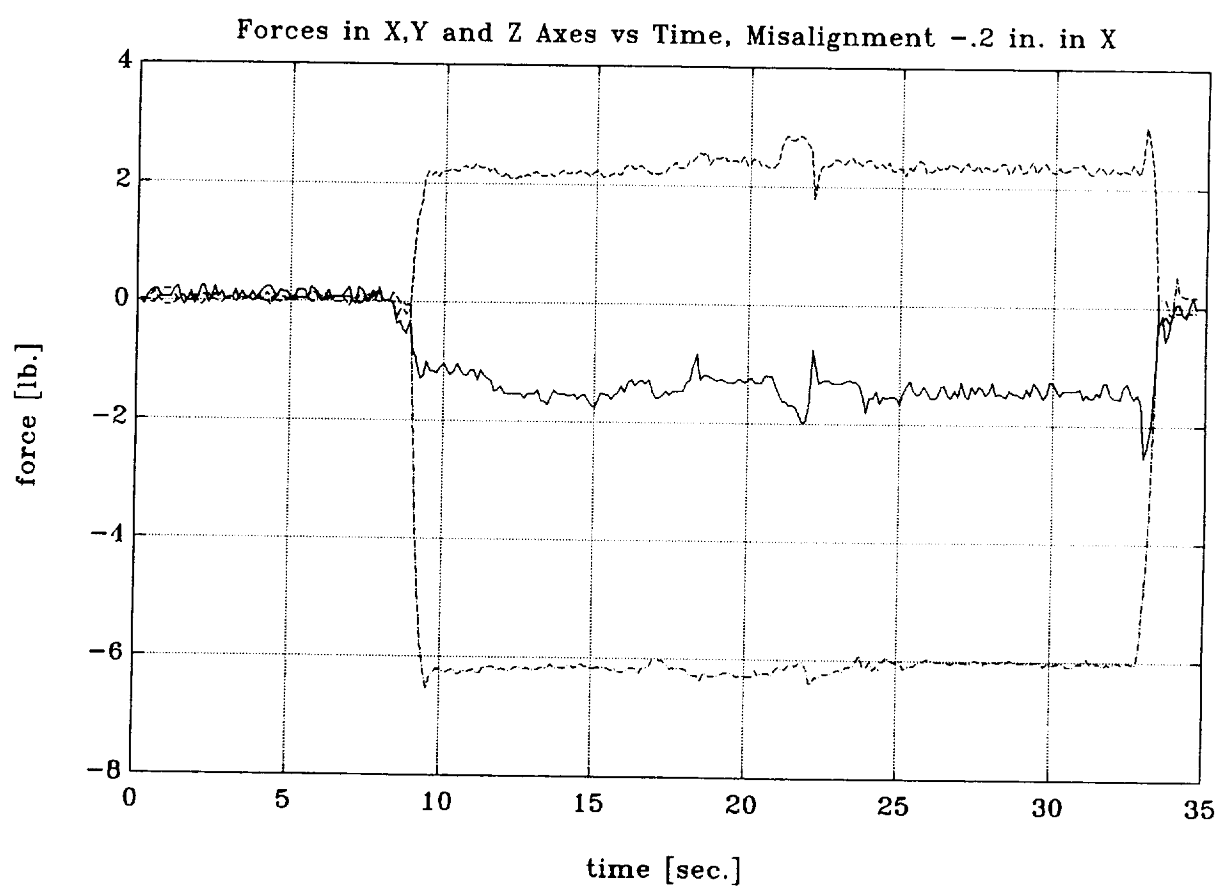

Figure OLDPIN18 Time histories of torques under -0.20 in. misalignment
dashed: T_x*; dashed-dotted:* T_y*; solid:* T_z

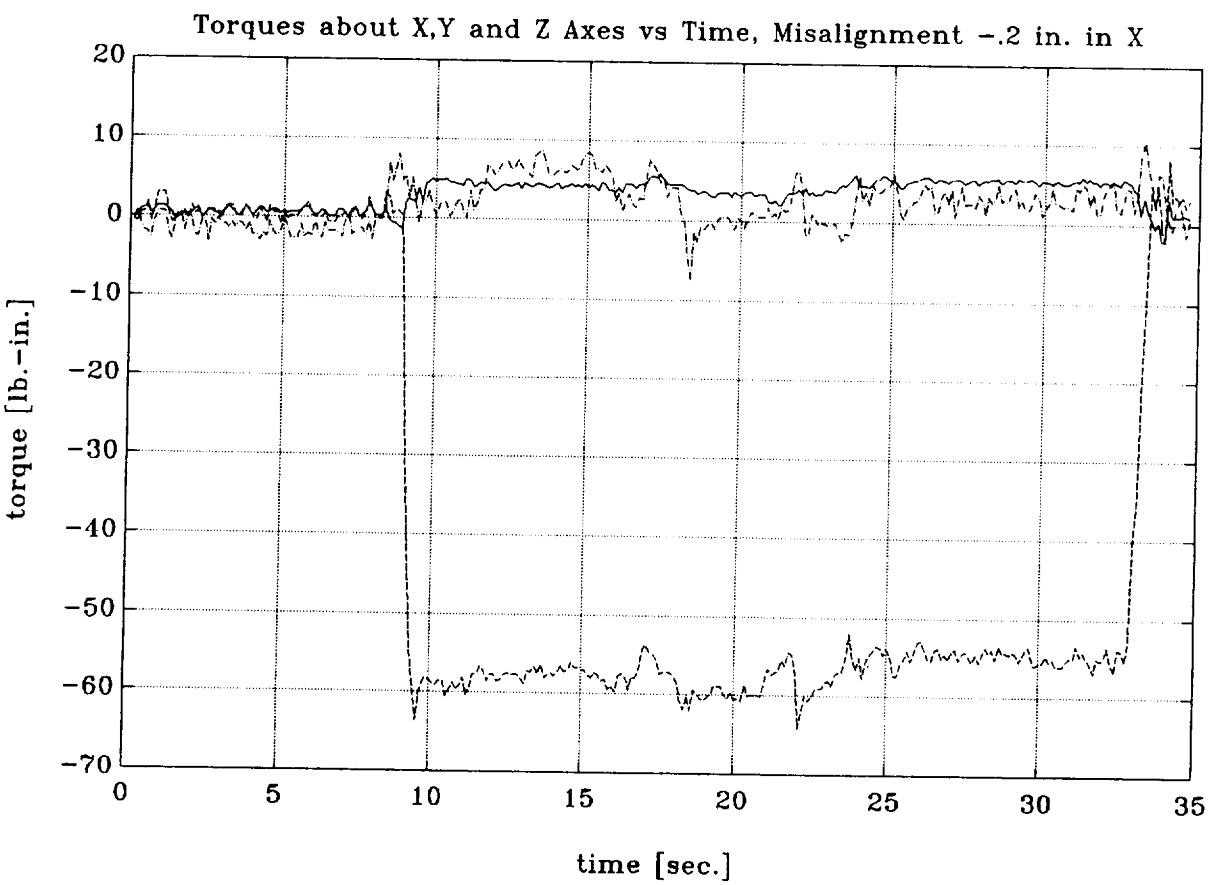

Figure NEWPIN1 Time histories of forces under perfect alignment
dashed: F_x; *dashed-dotted:* F_y; *solid:* F_z

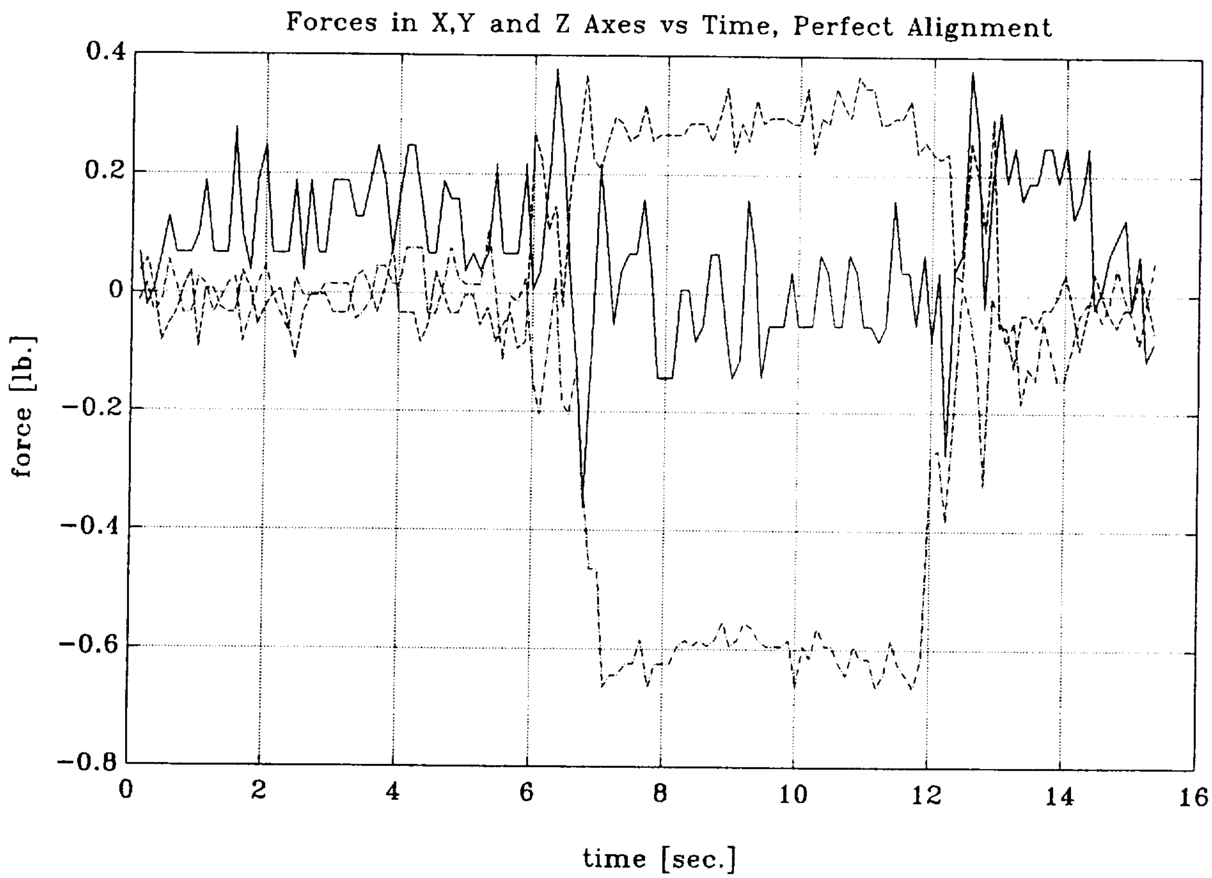

Figure NEWPIN2 Time histories of torques under perfect alignment
dashed: T_x; *dashed-dotted:* T_y; *solid:* T_z

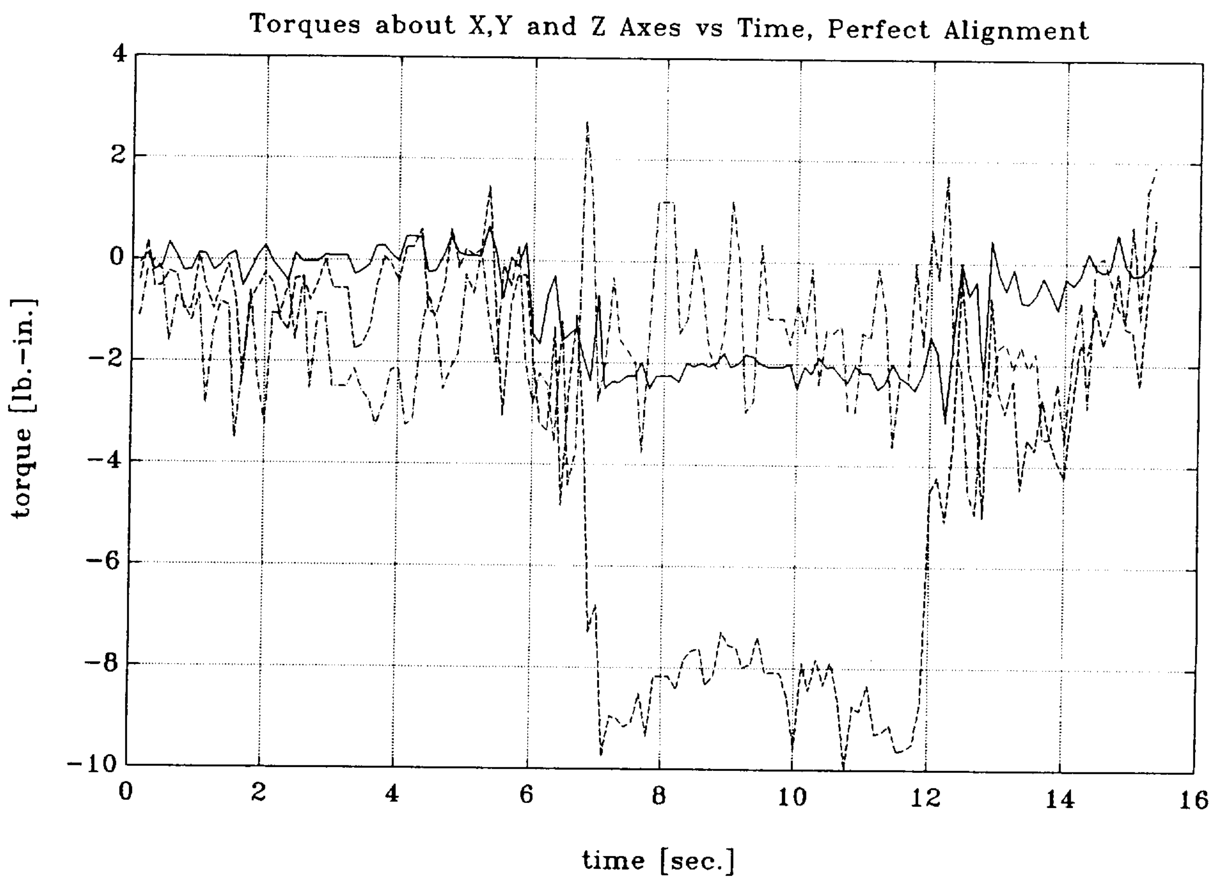

Figure NEWPIN3 Time histories of forces under 0.05 in. misalignment
dashed: F_x; *dashed-dotted:* F_y; *solid:* F_z

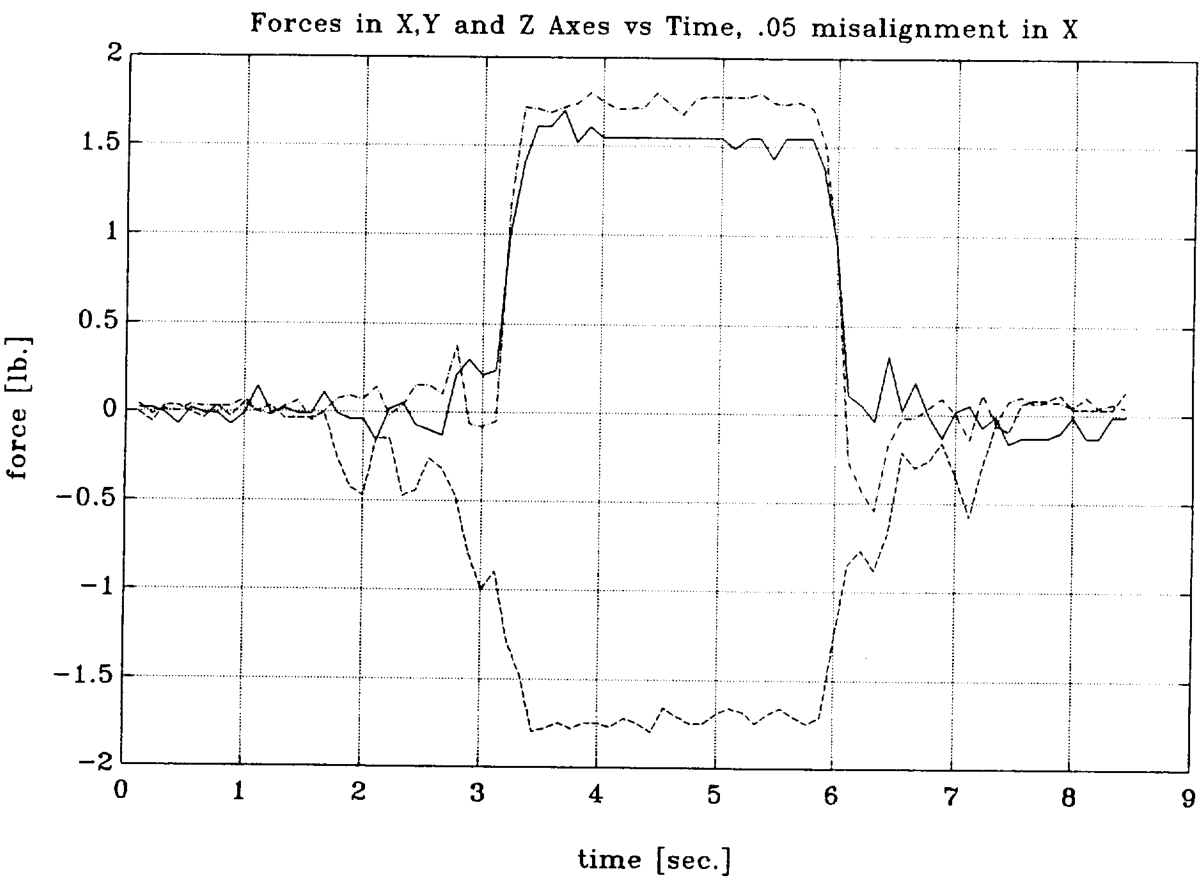

Figure NEWPIN4 Time histories of torques under 0.05 in. misalignment
dashed: T_x; *dashed-dotted:* T_y; *solid:* T_z

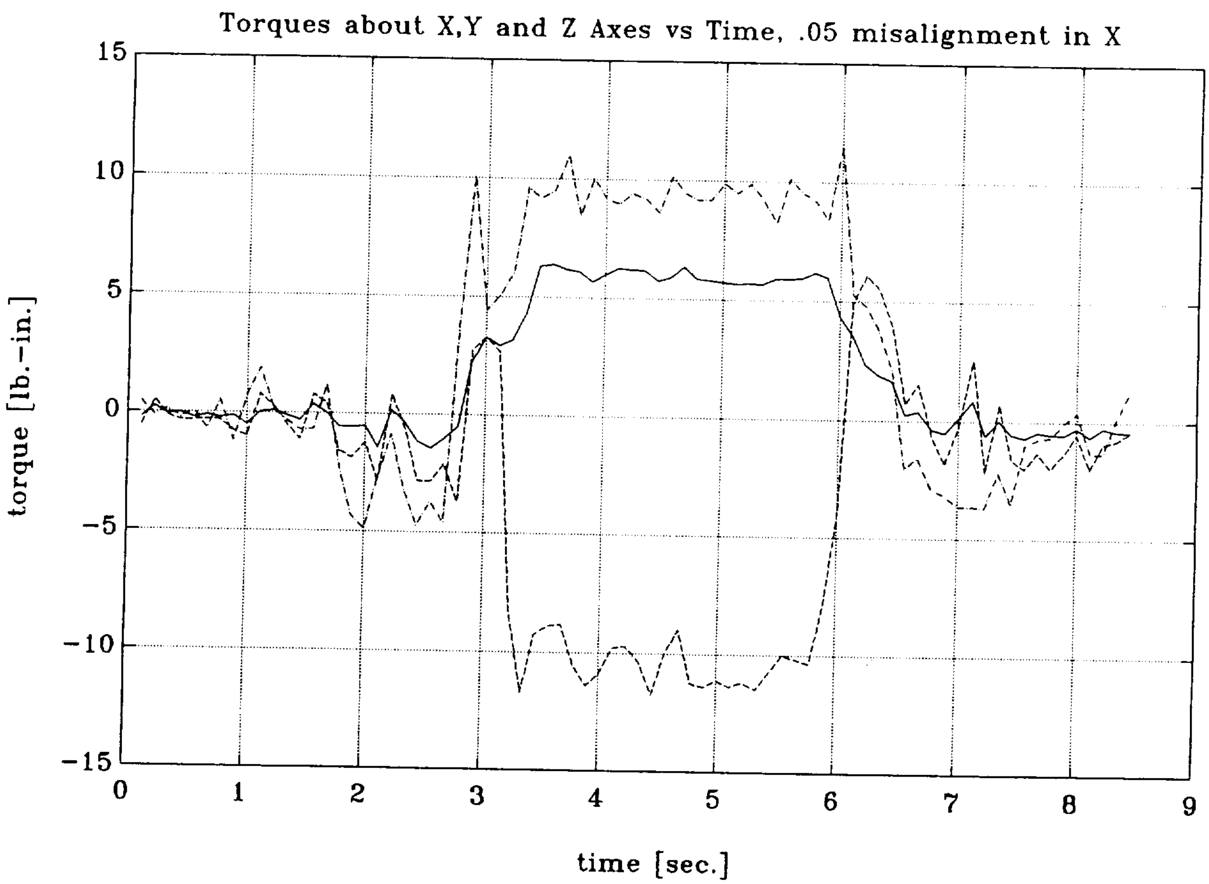

Figure NEWPIN5 Time histories of forces under 0.1 in. misalignment
dashed: F_x; *dashed-dotted:* F_y; *solid:* F_z

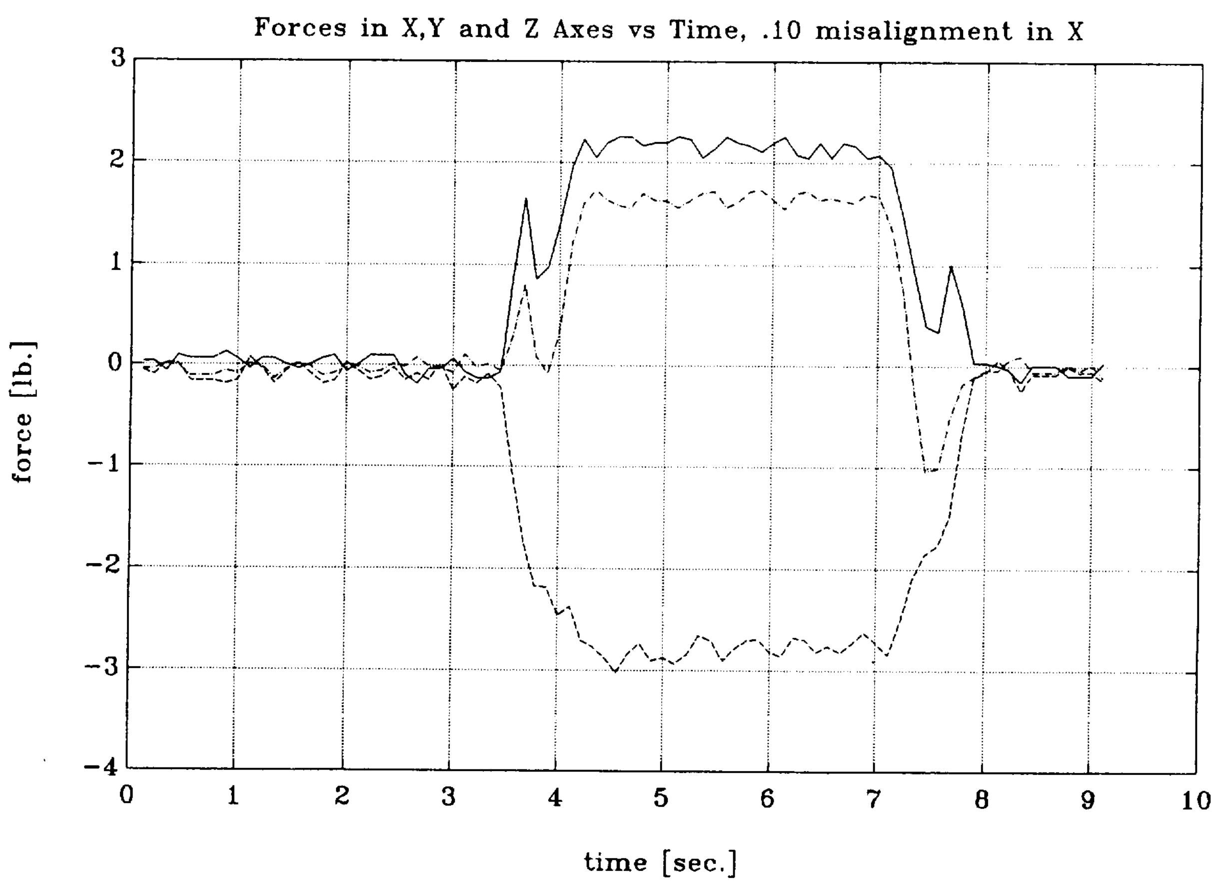

Figure NEWPIN6 Time histories of torques under 0.1 in. misalignment
dashed: T_x; *dashed-dotted:* T_y; *solid:* T_z

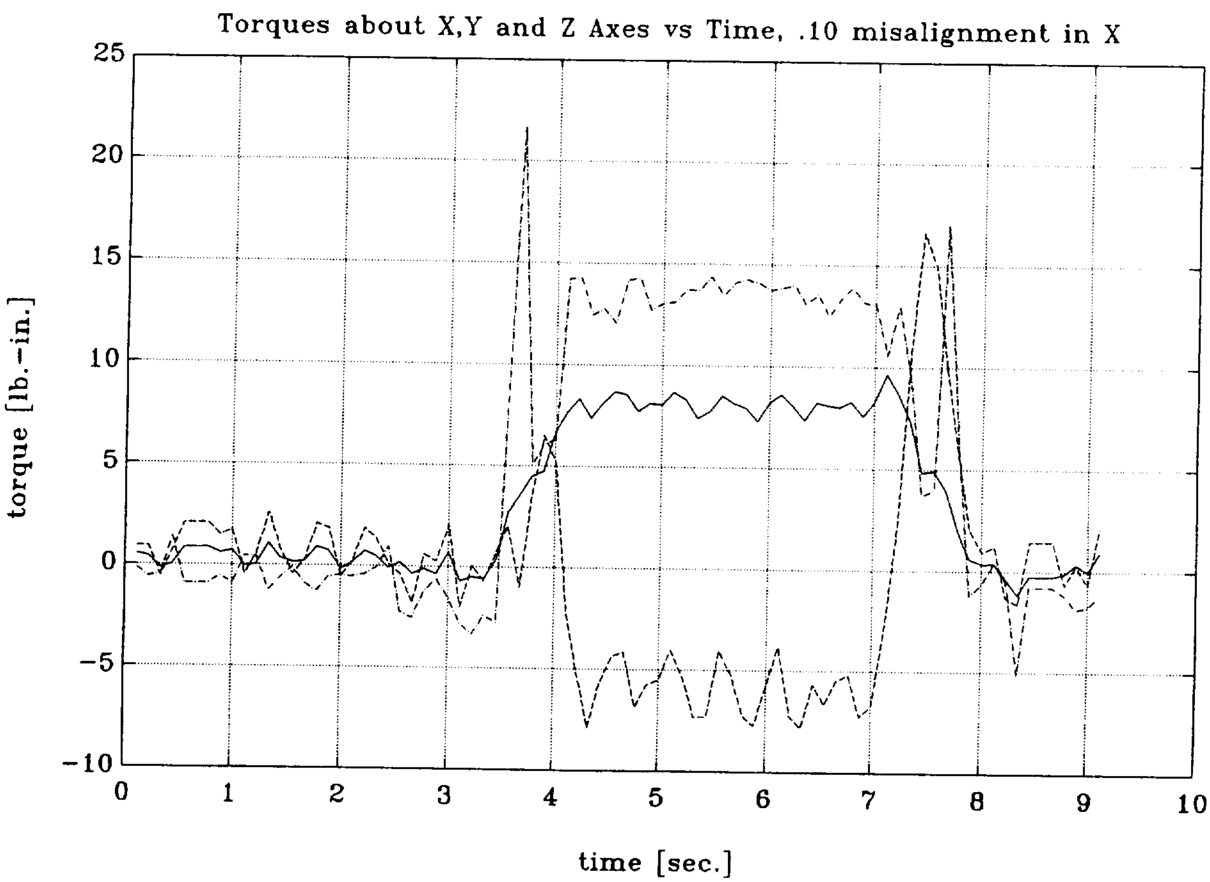

Figure NEWPIN7 Time histories of forces under 0.15 in. misalignment
dashed: F_x; *dashed-dotted:* F_y; *solid:* F_z

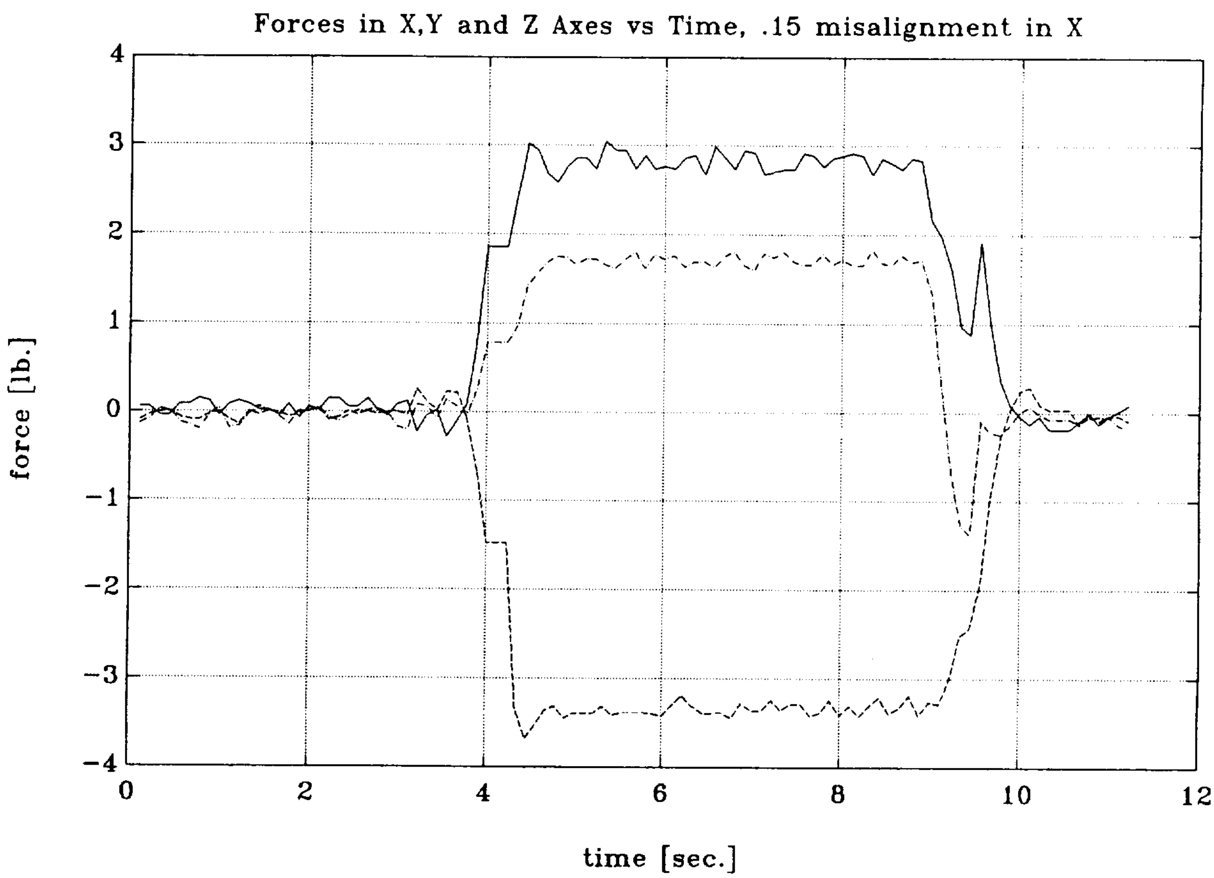

Figure NEWPIN8 Time histories of torques under 0.15 in. misalignment
dashed: T_x*; dashed-dotted:* T_y*; solid:* T_z

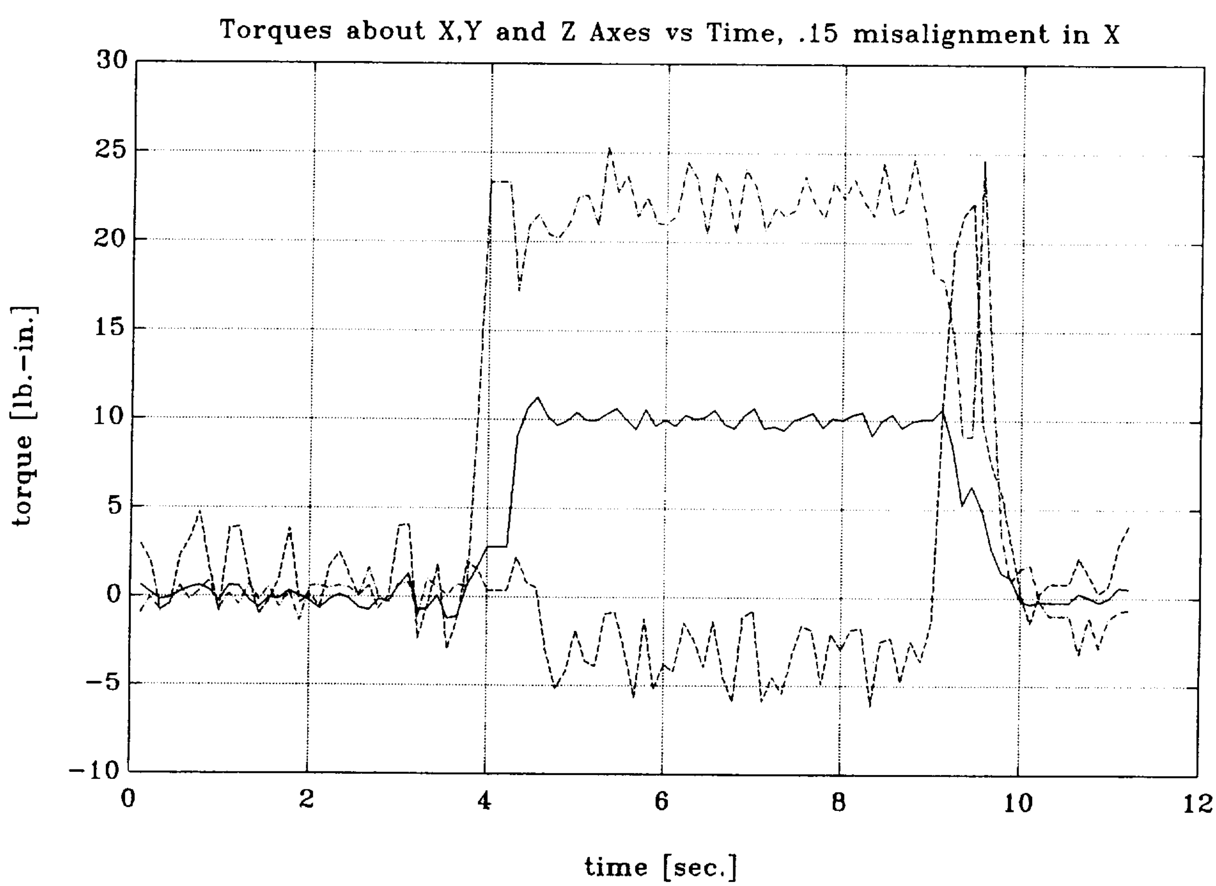

Figure NEWPIN9 Time histories of forces under 0.20 in. misalignment
dashed: F_x; *dashed-dotted:* F_y; *solid:* F_z

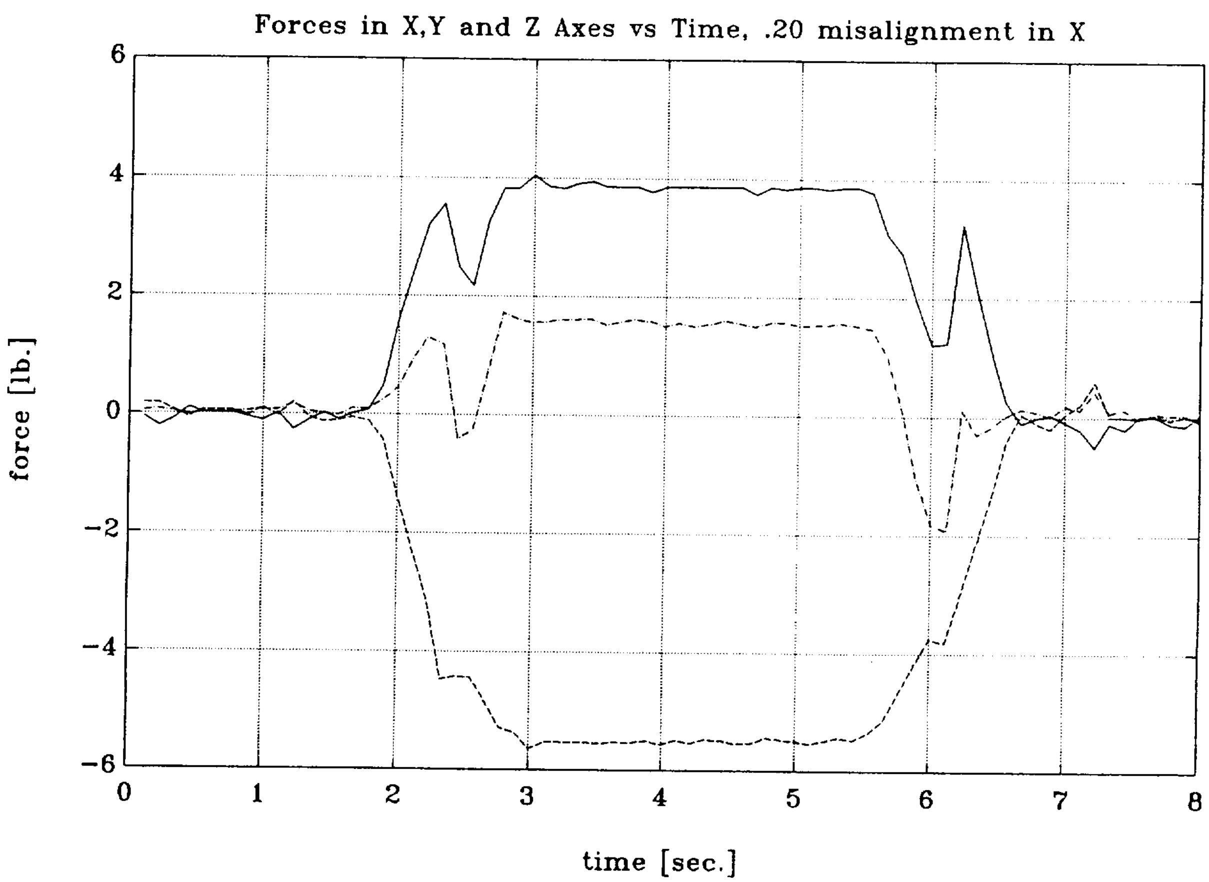

Figure NEWPIN10 Time histories of torques under 0.20 in. misalignment
dashed: T_x; *dashed-dotted:* T_y; *solid:* T_z

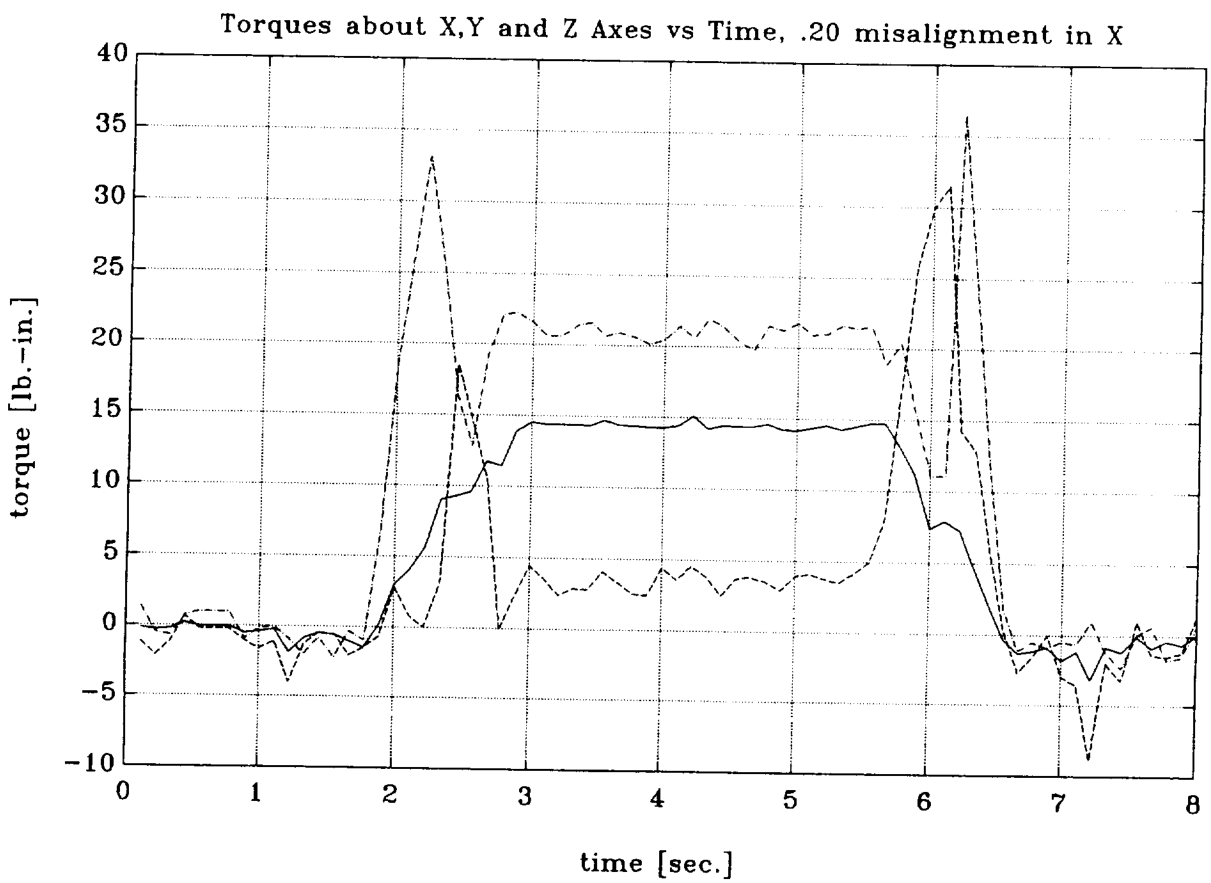

Figure NEWPIN11 Time histories of forces under -0.05 in. misalignment
dashed: F_x*; dashed-dotted:* F_y*; solid:* F_z

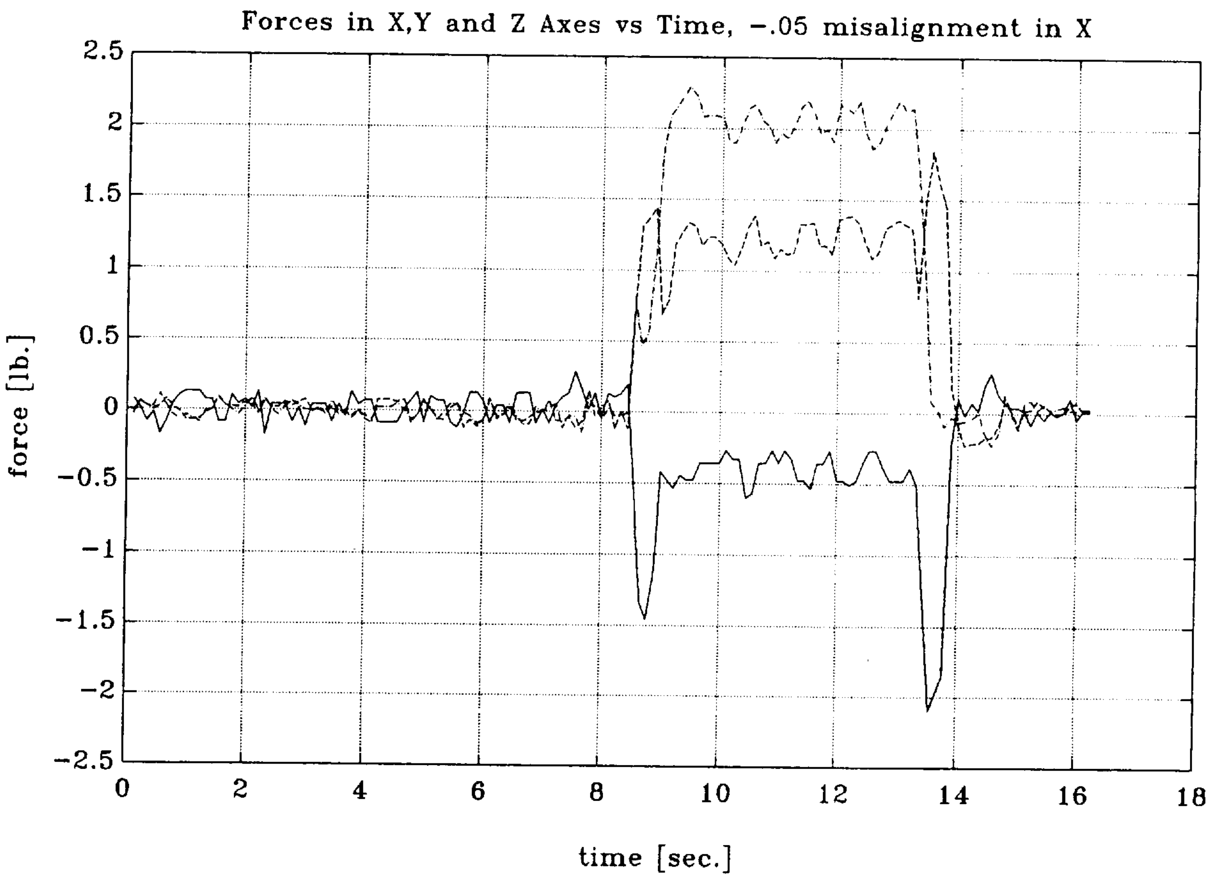

Figure NEWPIN12 Time histories of torques under -0.05 in. misalignment
dashed: T_x; *dashed-dotted:* T_y; *solid:* T_z

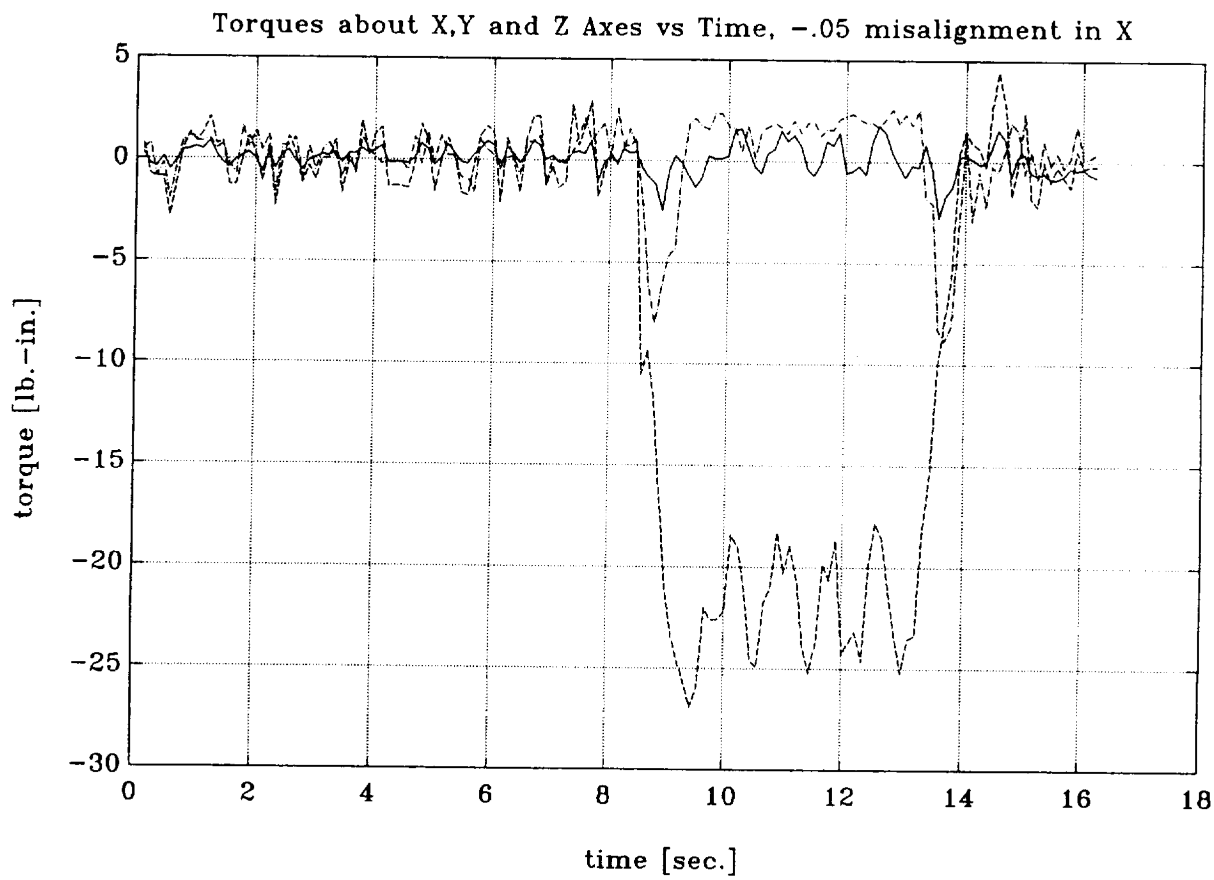

Figure NEWPIN13 Time histories of forces under -0.1 in. misalignment
dashed: F_x*; dashed-dotted:* F_y*; solid:* F_z

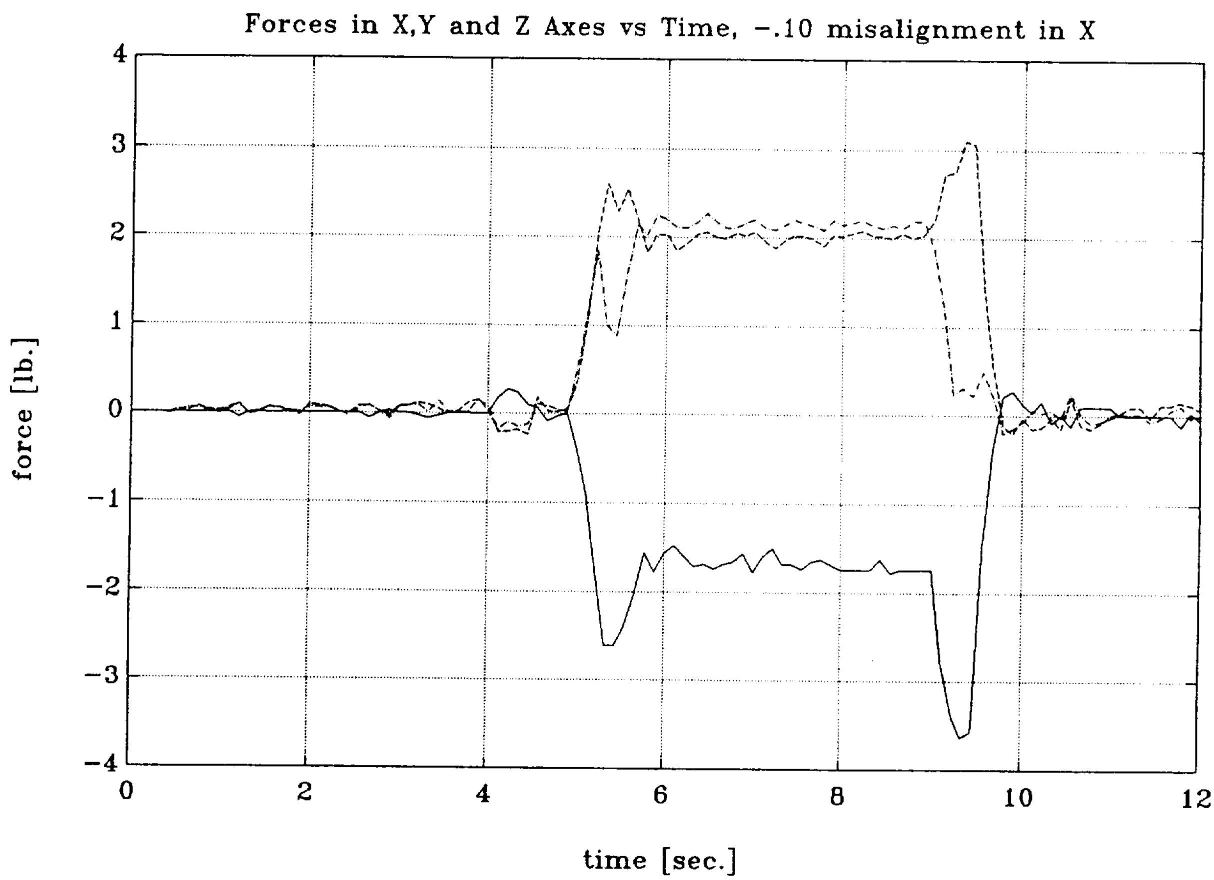

Figure NEWPIN14 Time histories of torques under -0.1 in. misalignment
dashed: T_x*; dashed-dotted:* T_y*; solid:* T_z

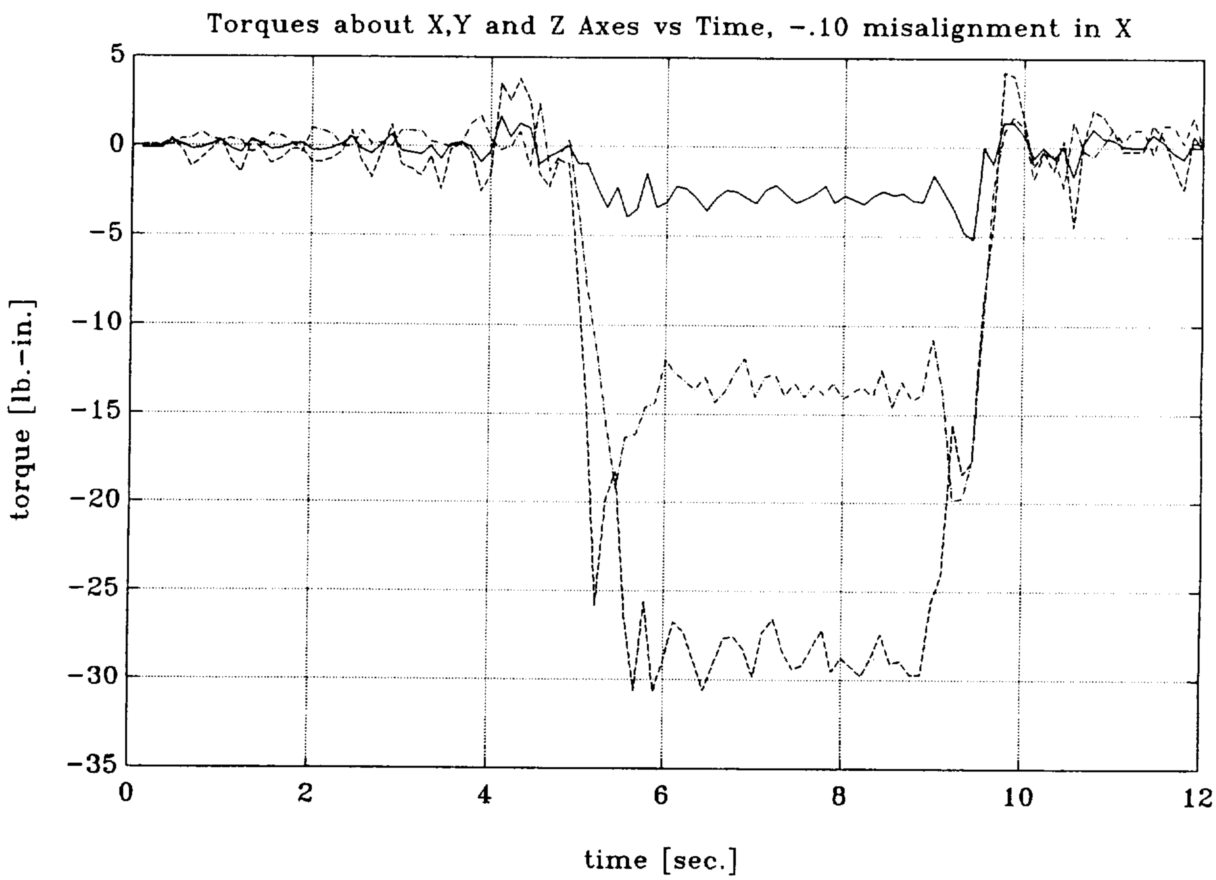

Figure NEWPIN15 Time histories of forces under -0.15 in. misalignment
dashed: F_x; *dashed-dotted:* F_y; *solid:* F_z

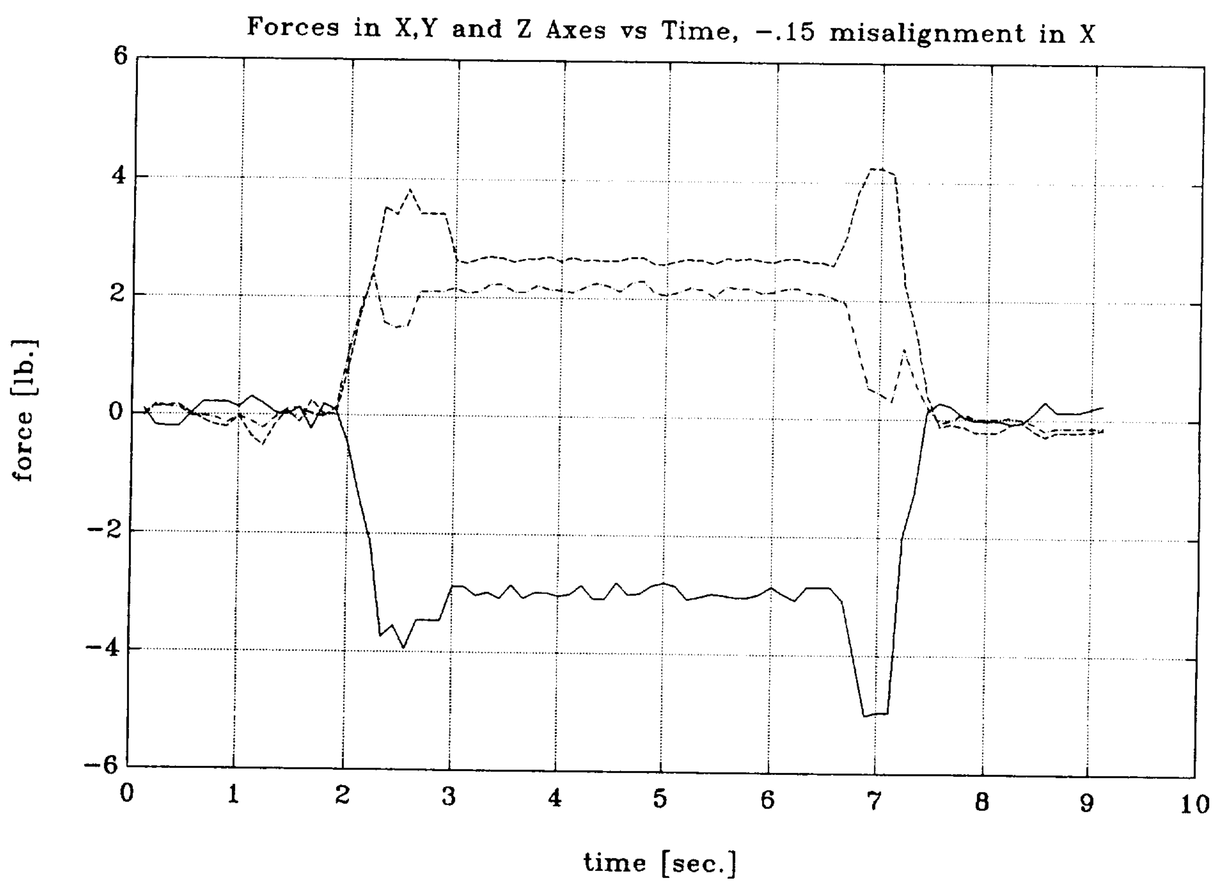

Figure NEWPIN16 Time histories of torques under -0.15 in. misalignment
dashed: T_x*; dashed-dotted:* T_y*; solid:* T_z

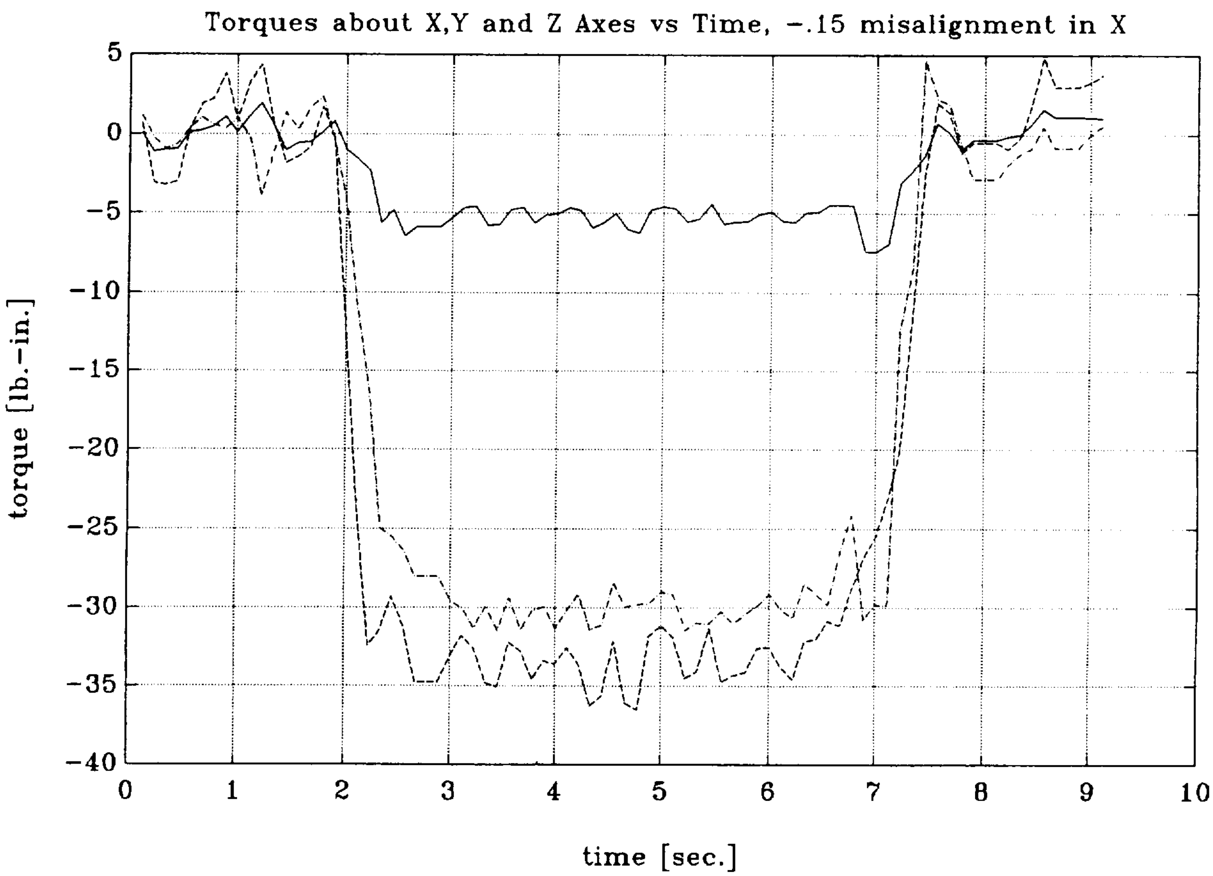

Figure NEWPIN17 Time histories of forces under -0.20 in. misalignment
dashed: F_x*; dashed-dotted:* F_y*; solid:* F_z

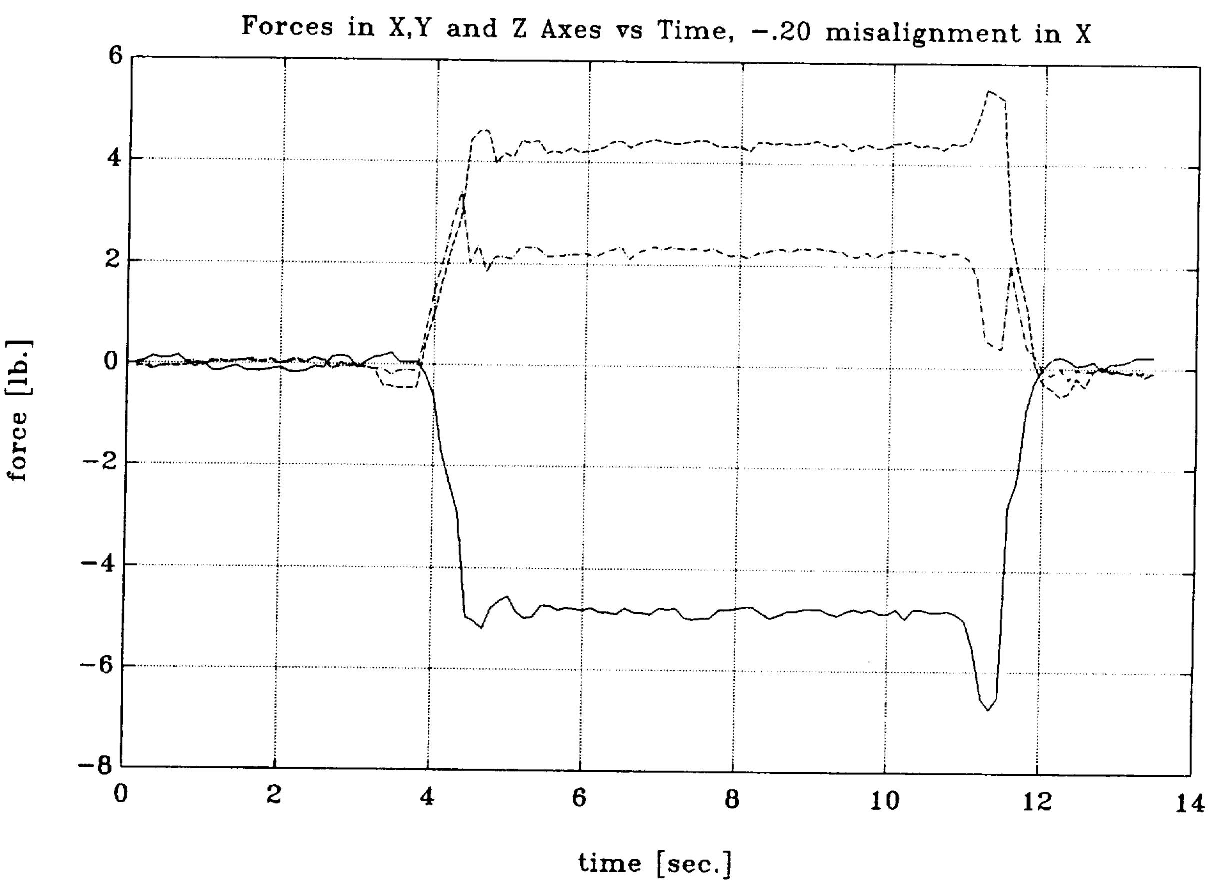

Figure NEWPIN18 Time histories of torques under -0.20 in. misalignment
dashed: T_x; *dashed-dotted:* T_y; *solid:* T_z

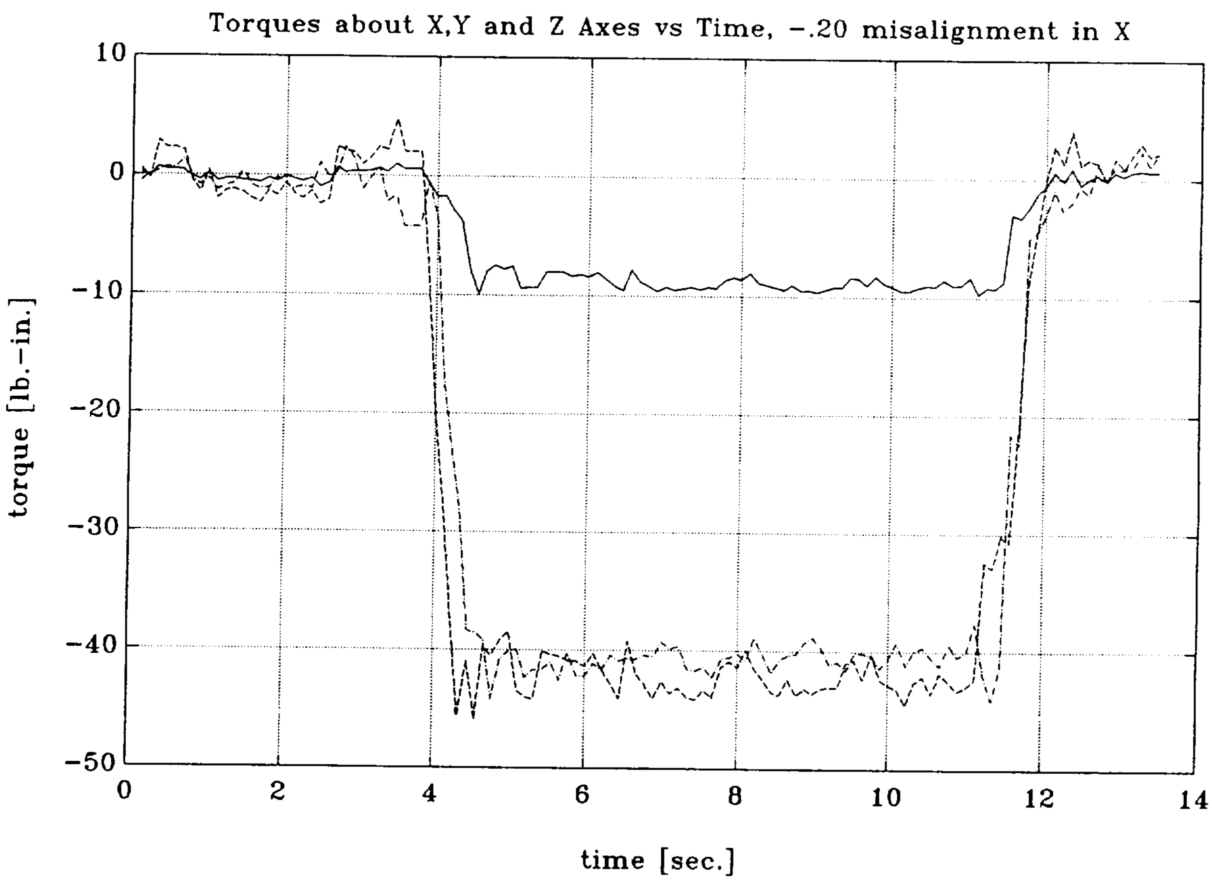

Figure SRACK1 Time histories of forces under perfect alignment
dashed: F_x; dashed-dotted: F_y; solid: F_z

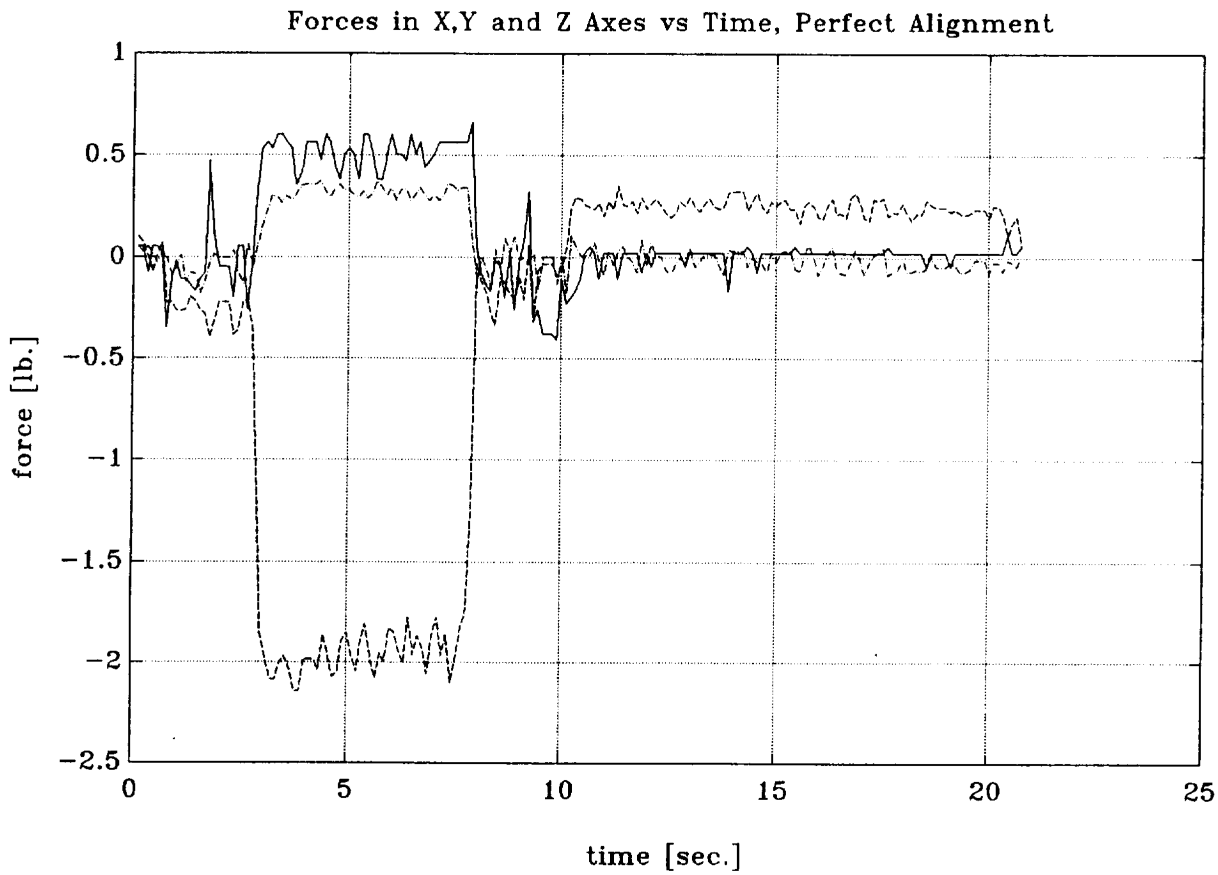

Figure SRACK2 Time histories of torques under perfect alignment
dashed: T_x*; dashed-dotted:* T_y*; solid:* T_z

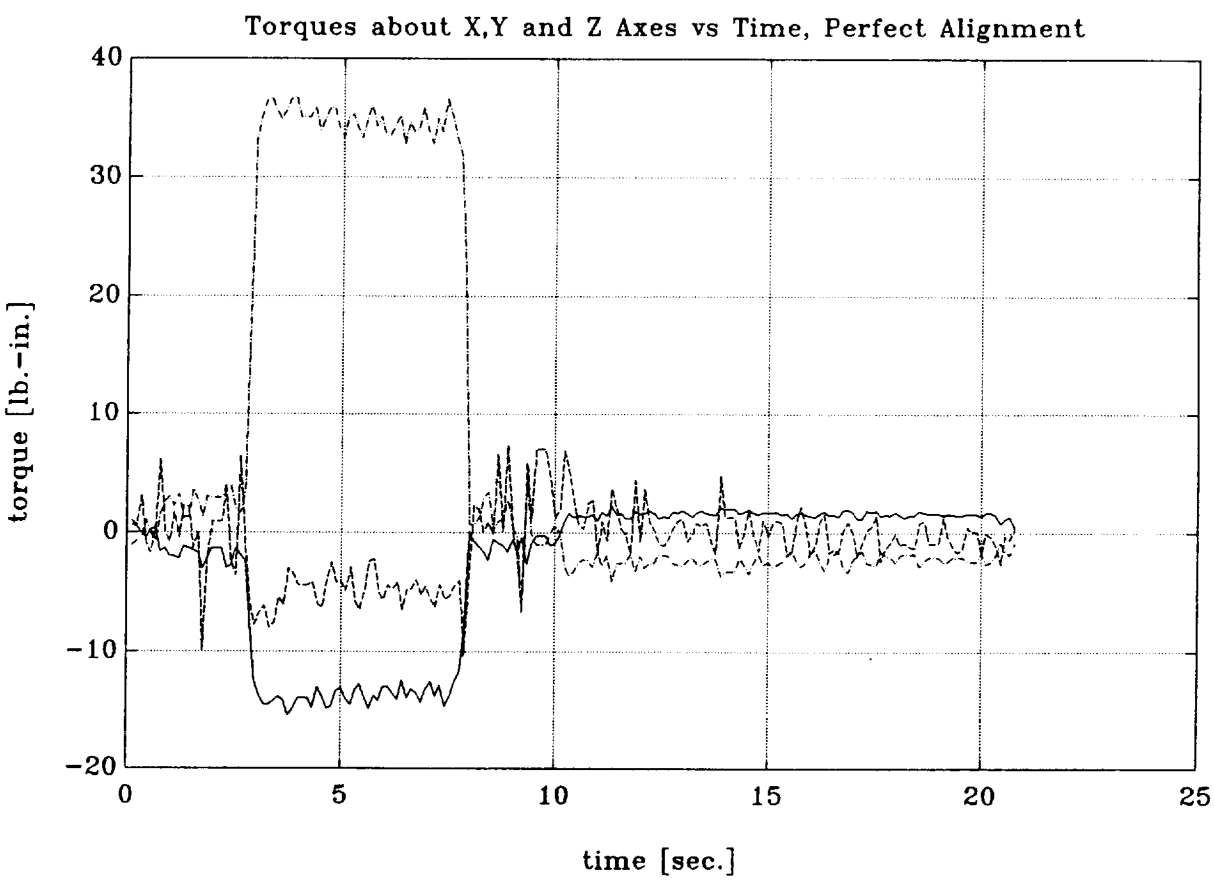

Figure SRACK3 Time histories of forces under 0.05 in. misalignment
dashed: F_x; *dashed-dotted:* F_y; *solid:* F_z

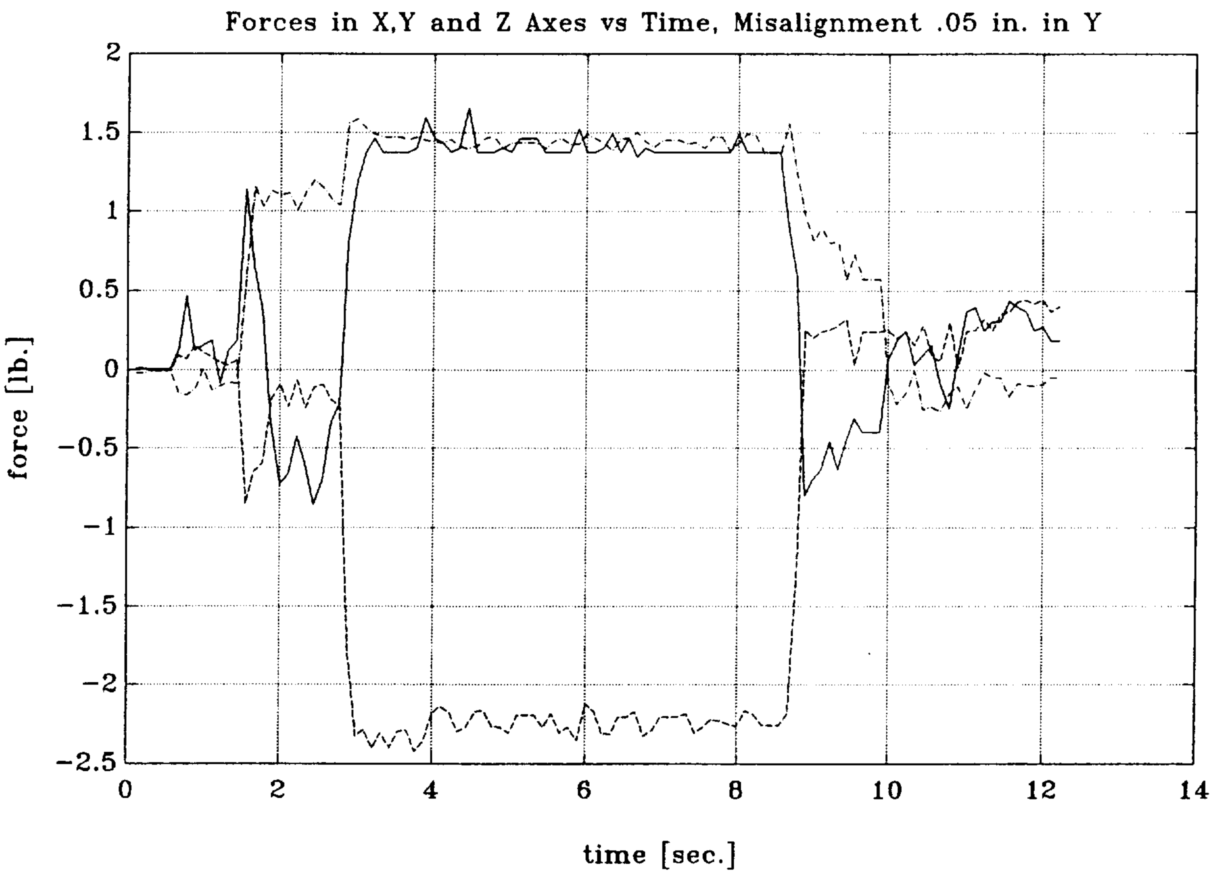

Figure SRACK4 Time histories of torques under 0.05 in. misalignment
dashed: T_x*; dashed-dotted:* T_y*; solid:* T_z

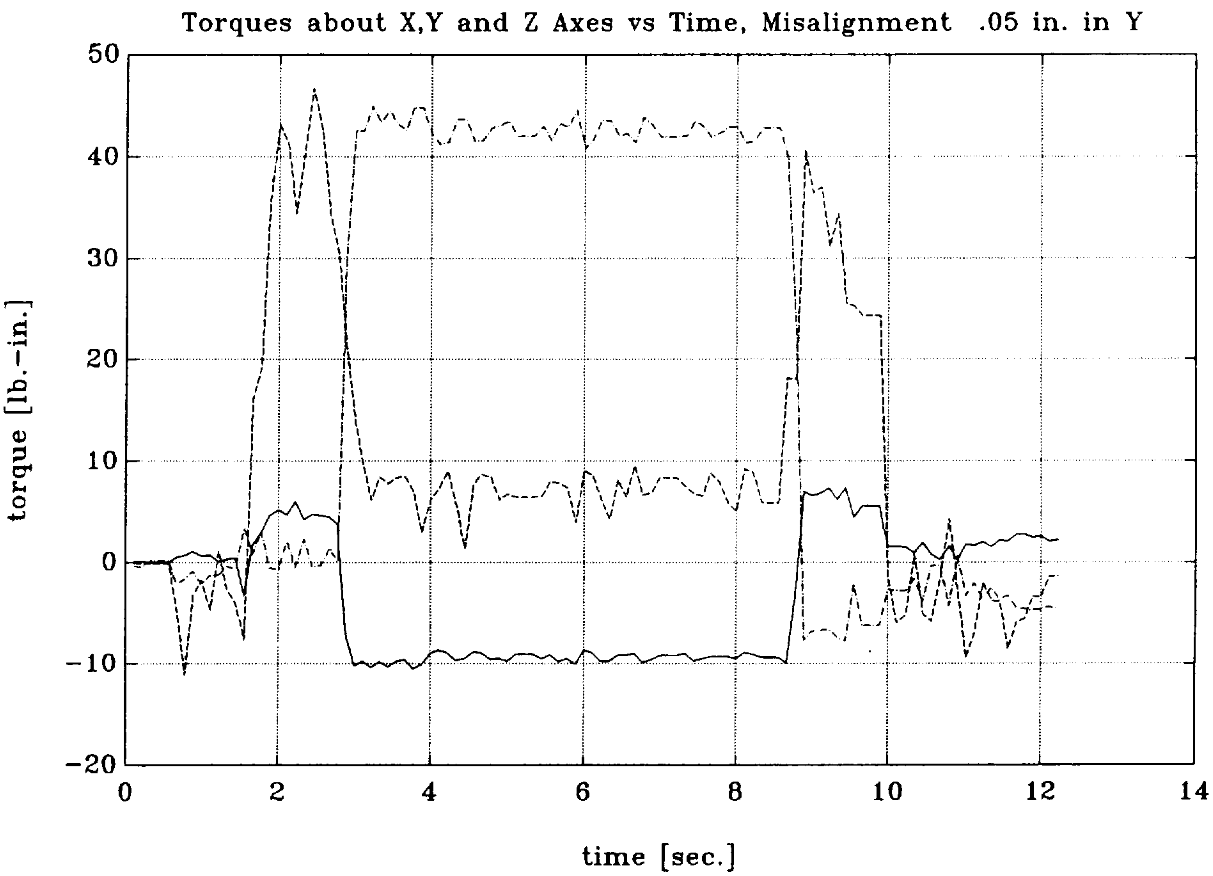

Figure SRACK5 Time histories of forces under 0.1 in. misalignment
dashed: F_x; *dashed-dotted:* F_y; *solid:* F_z

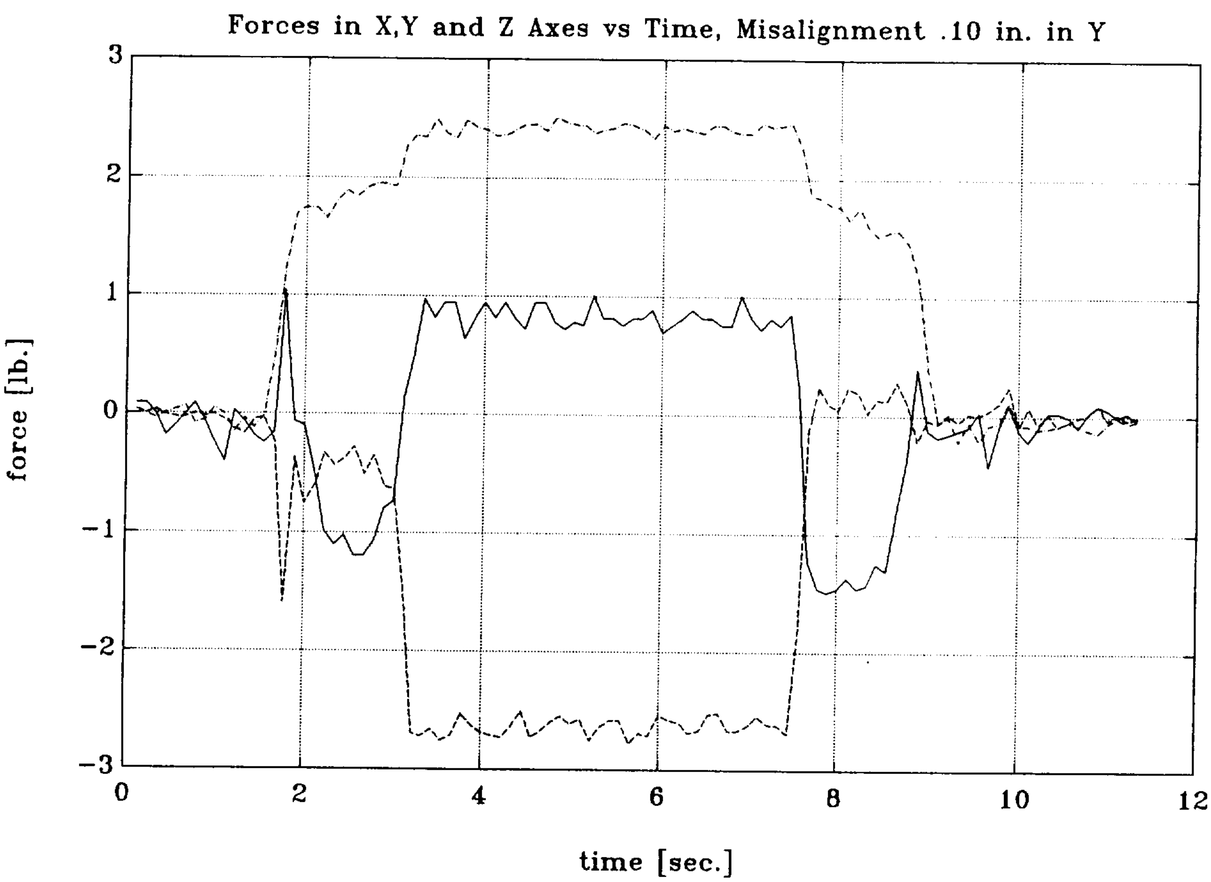

Figure SRACK6 Time histories of torques under 0.1 in. misalignment
dashed: T_x; *dashed-dotted:* T_y; *solid:* T_z

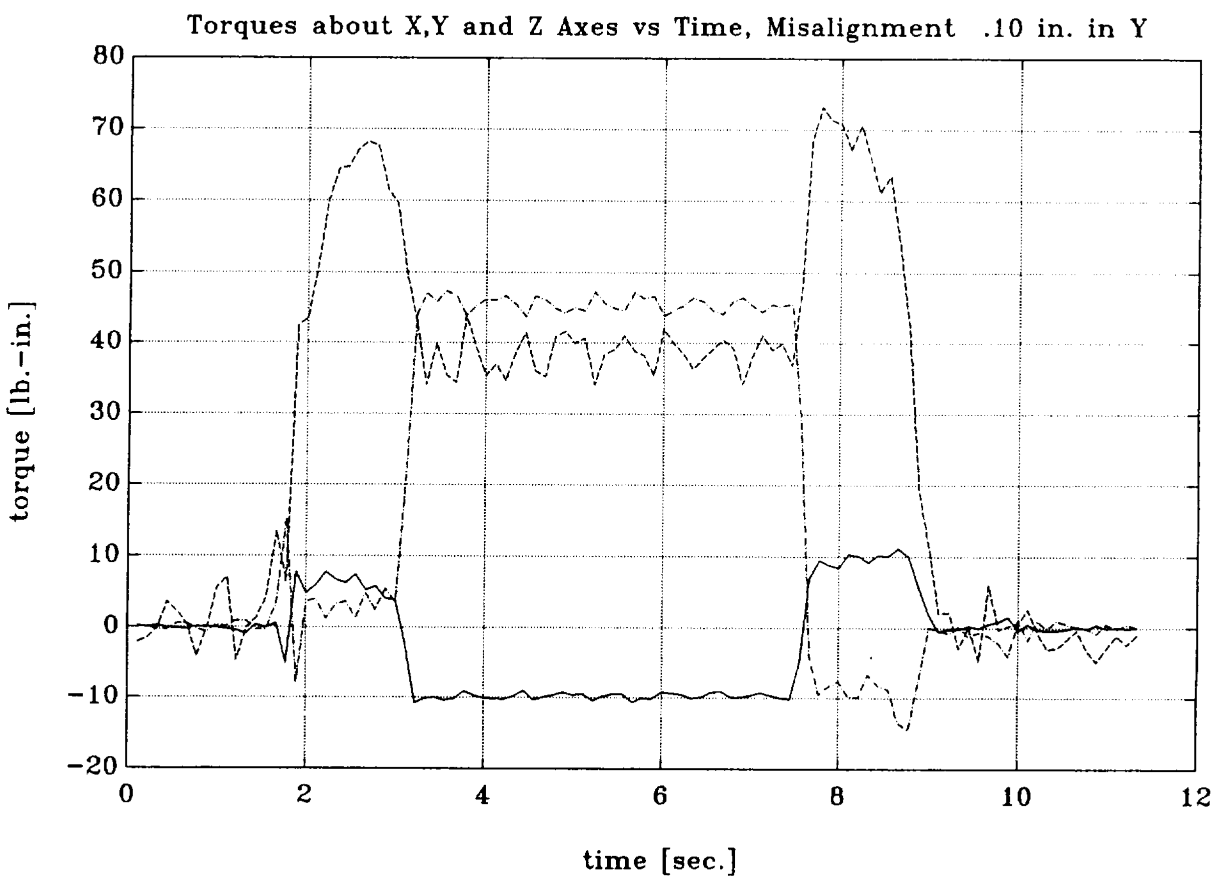

Figure SRACK7 Time histories of forces under 0.15 in. misalignment
dashed: F_x; dashed-dotted: F_y; solid: F_z

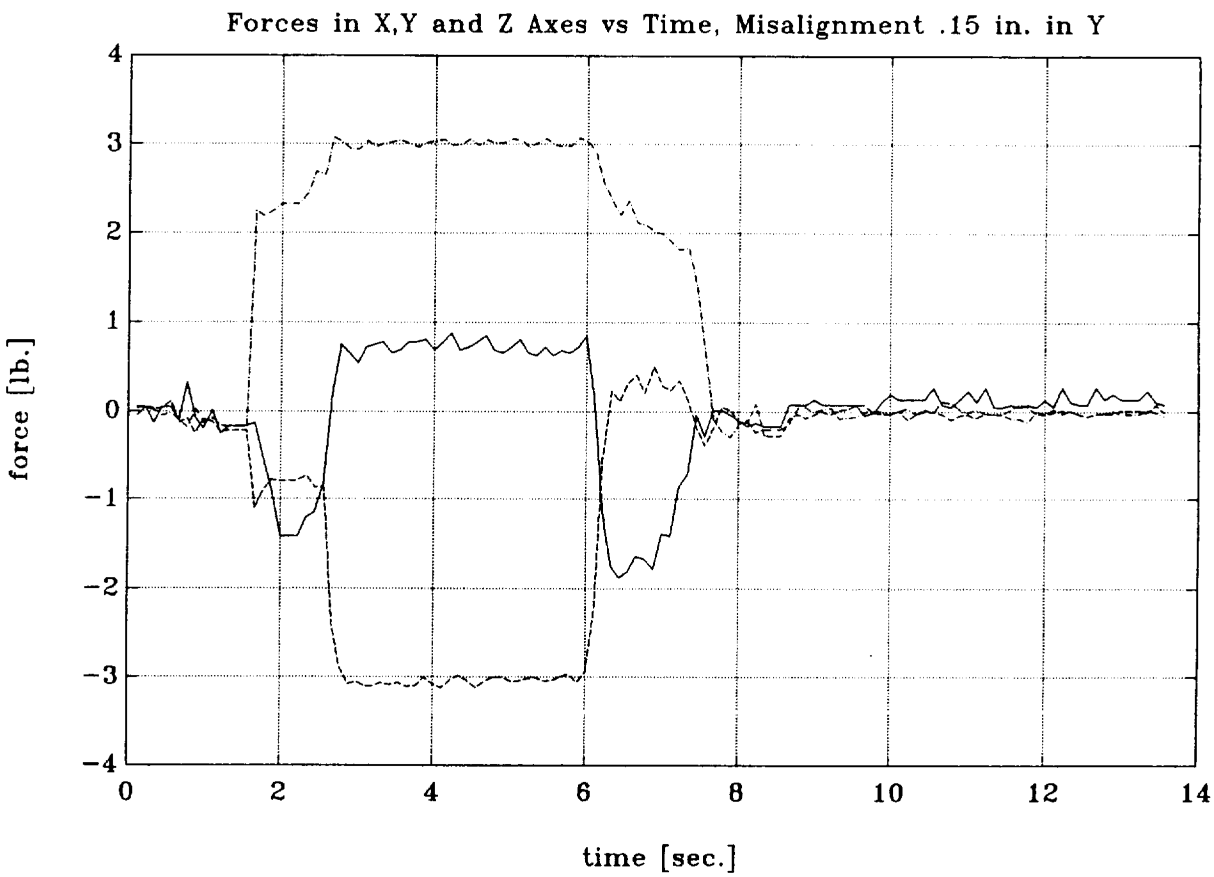

Figure SRACK8 Time histories of torques under 0.15 in. misalignment
dashed: T_x; dashed-dotted: T_y; solid: T_z

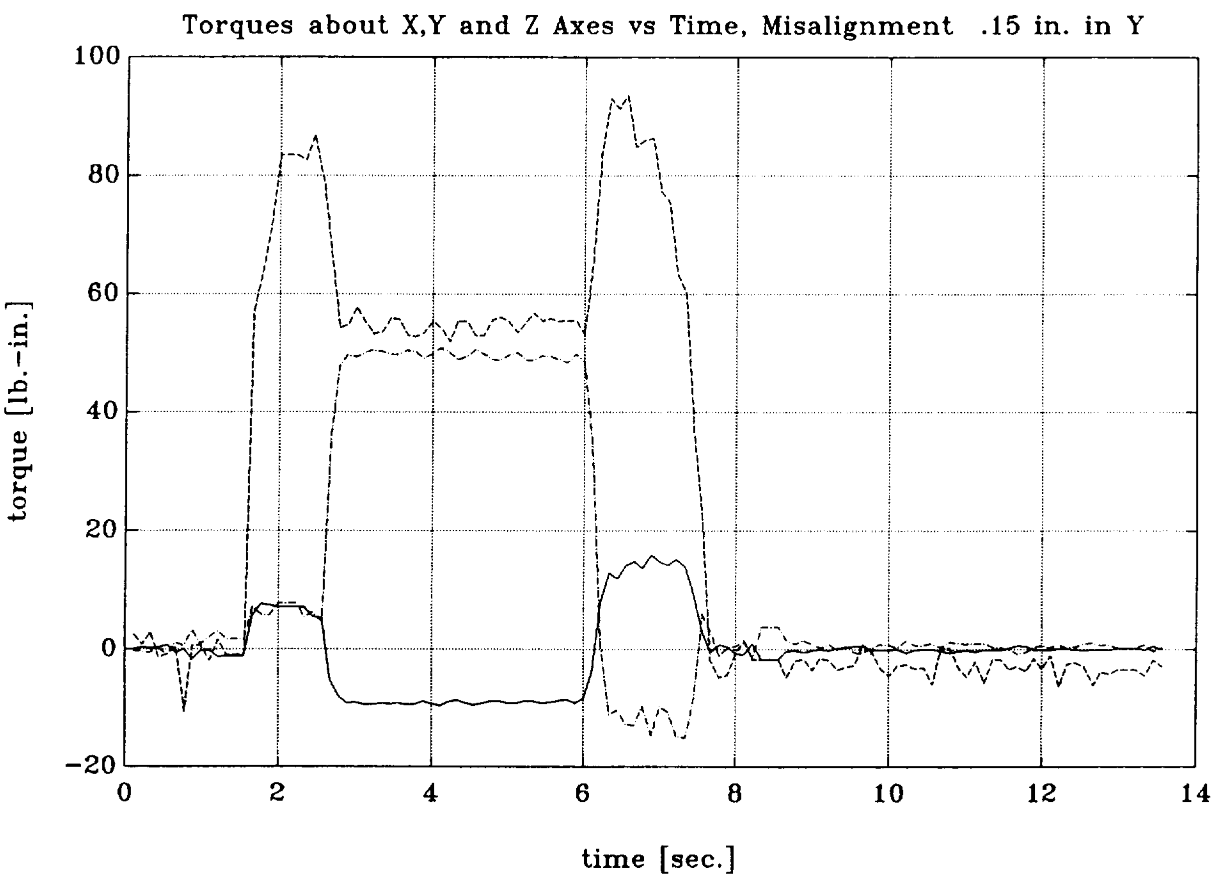

Figure SRACK9 Time histories of forces under 0.20 in. misalignment
dashed: F_x; dashed-dotted: F_y; solid: F_z

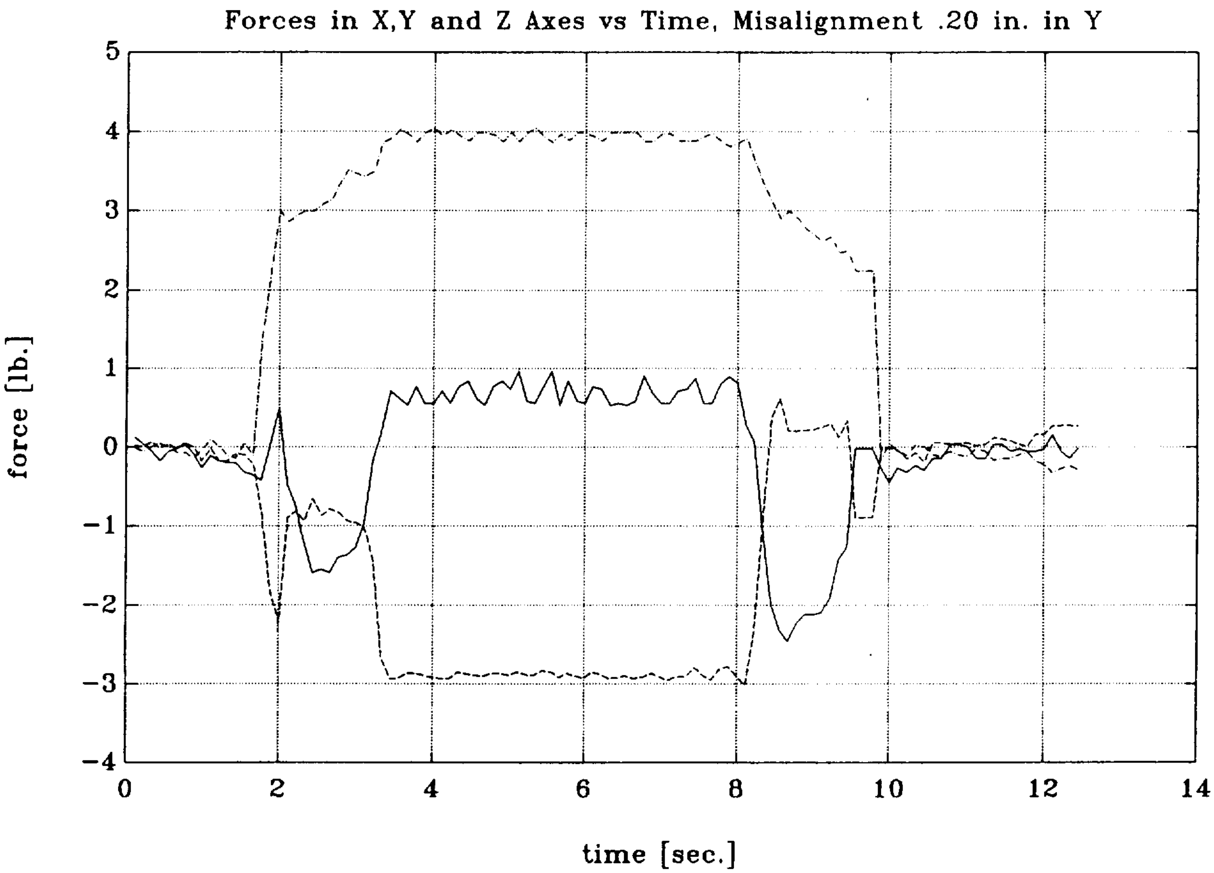

Figure SRACK10 Time histories of torques under 0.20 in. misalignment
dashed: T_x*; dashed-dotted:* T_y*; solid:* T_z

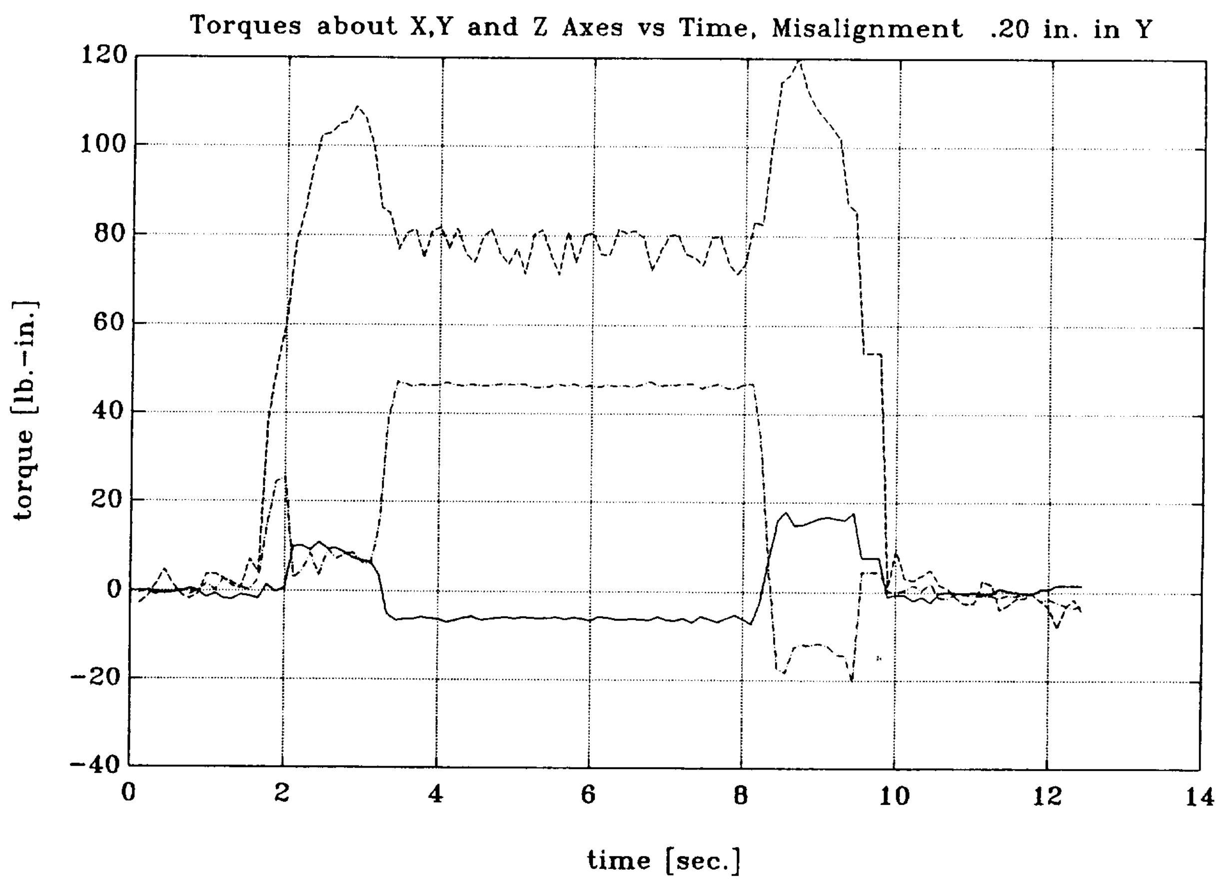

Figure SRACK11 Time histories of forces under 0.25 in. misalignment
dashed: F_x; *dashed-dotted:* F_y; *solid:* F_z

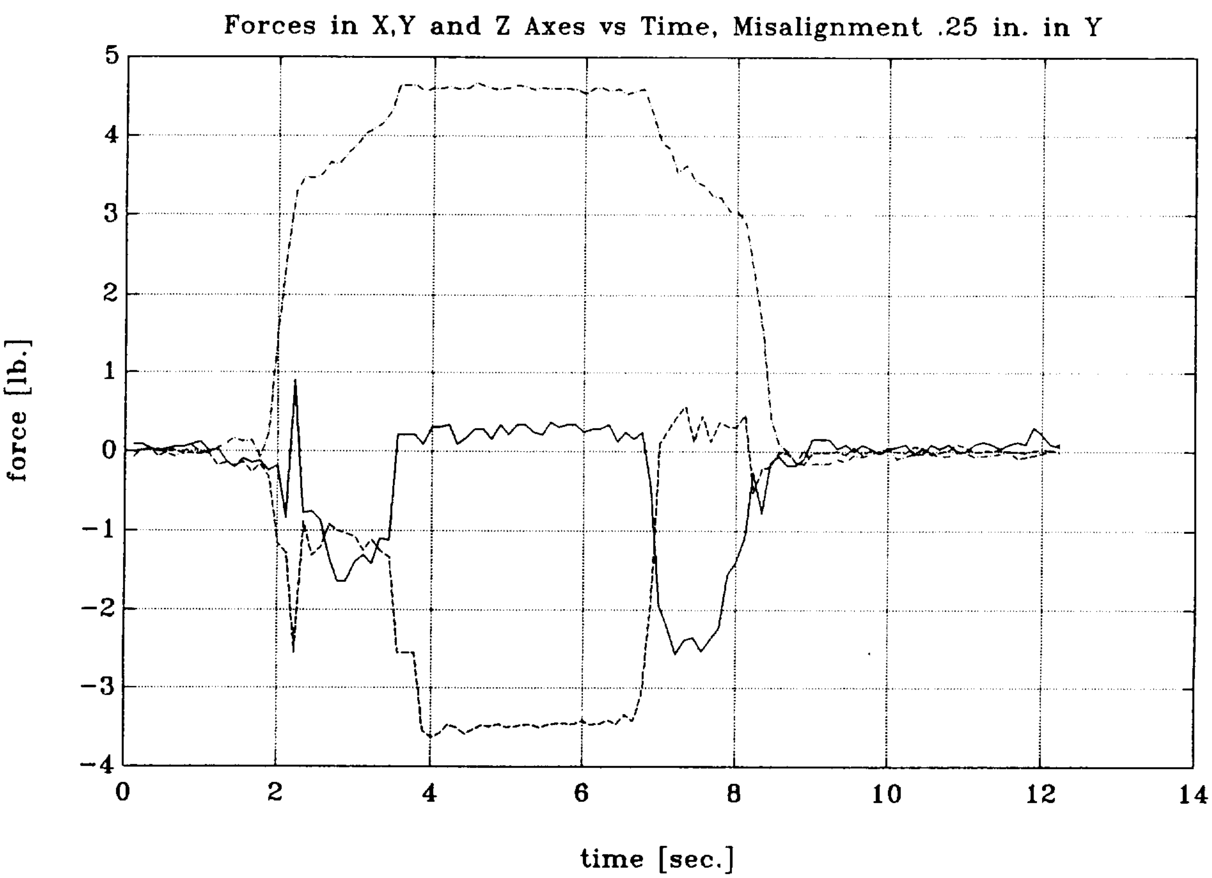

Figure SRACK12 Time histories of torques under 0.25 in. misalignment
dashed: T_x; *dashed-dotted:* T_y; *solid:* T_z

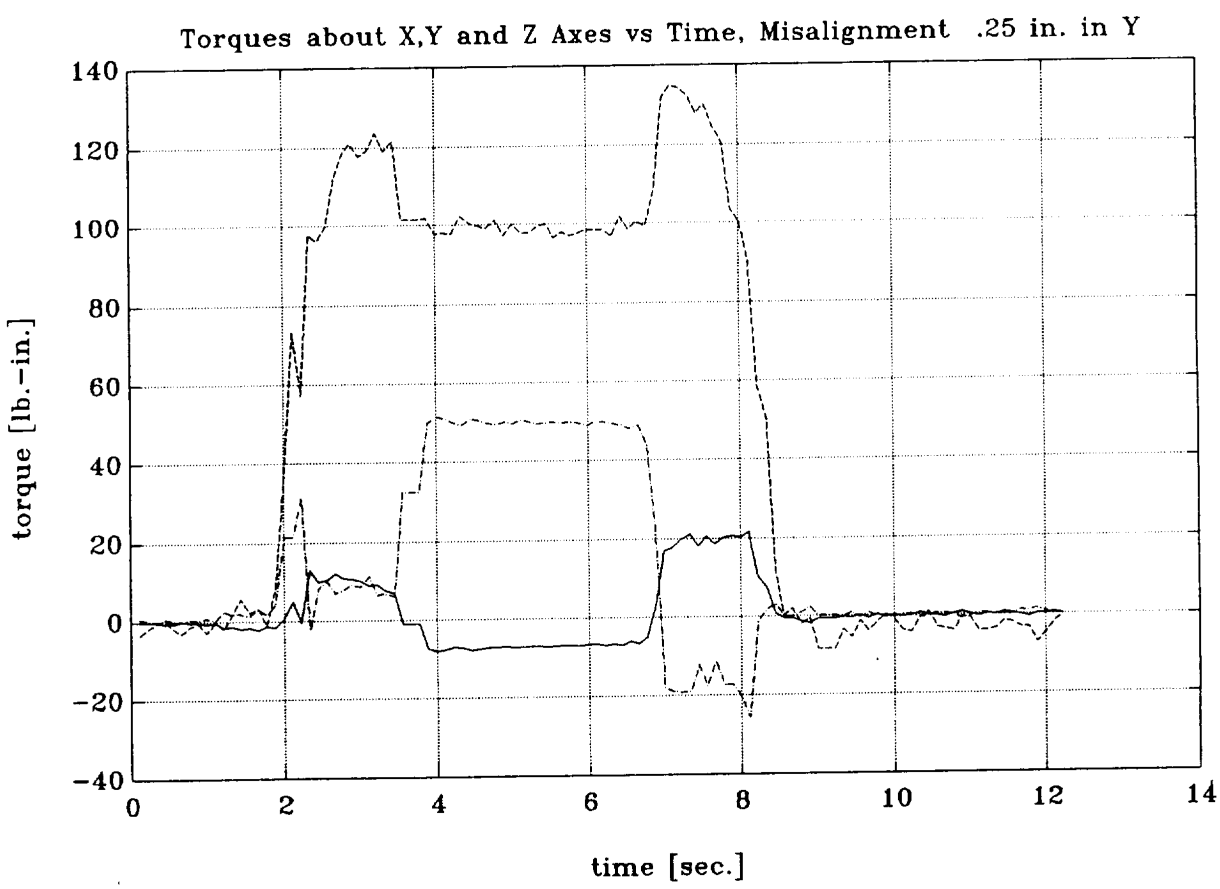

Figure SRACK13 Time histories of forces under 0.30 in. misalignment
dashed: F_x; dashed-dotted: F_y; solid: F_z

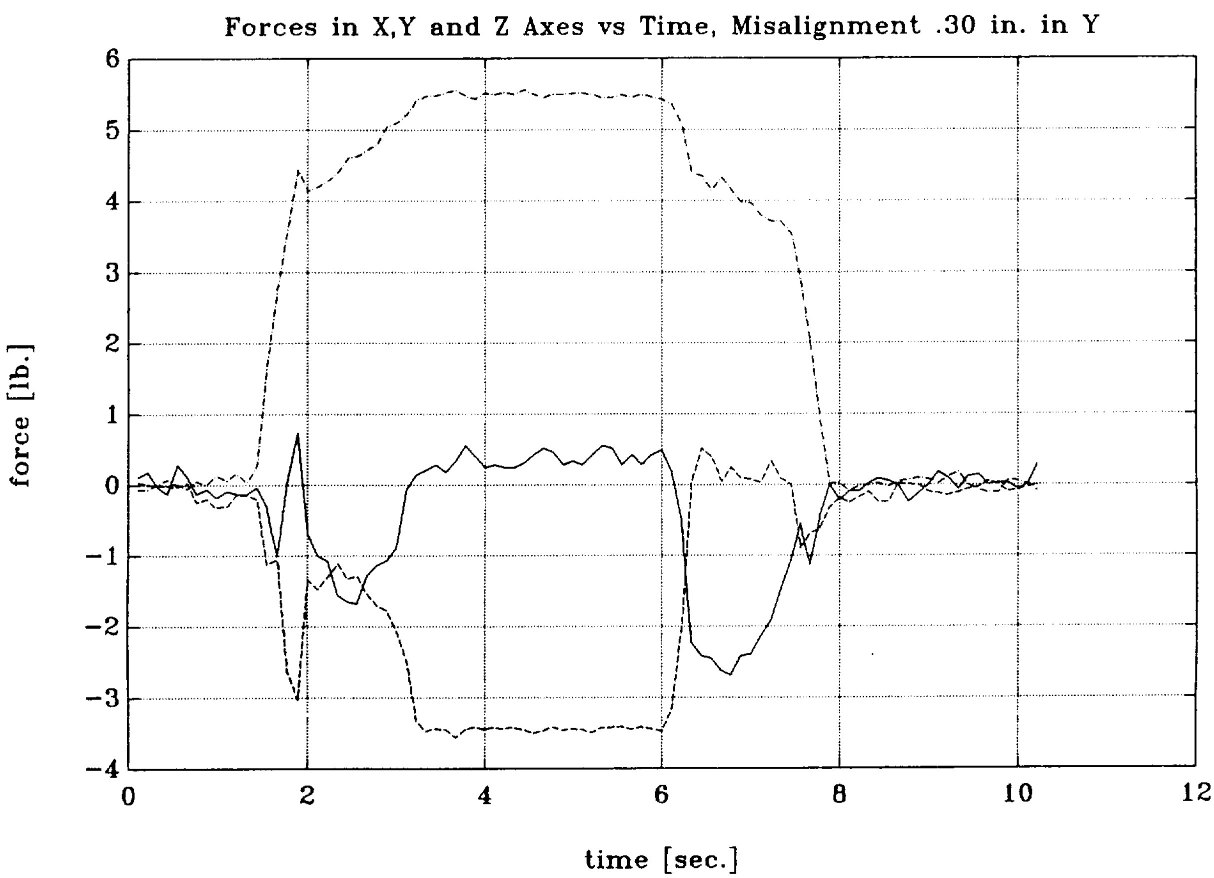

Figure SRACK14 Time histories of torques under 0.30 in. misalignment
dashed: T_x*; dashed-dotted:* T_y*; solid:* T_z

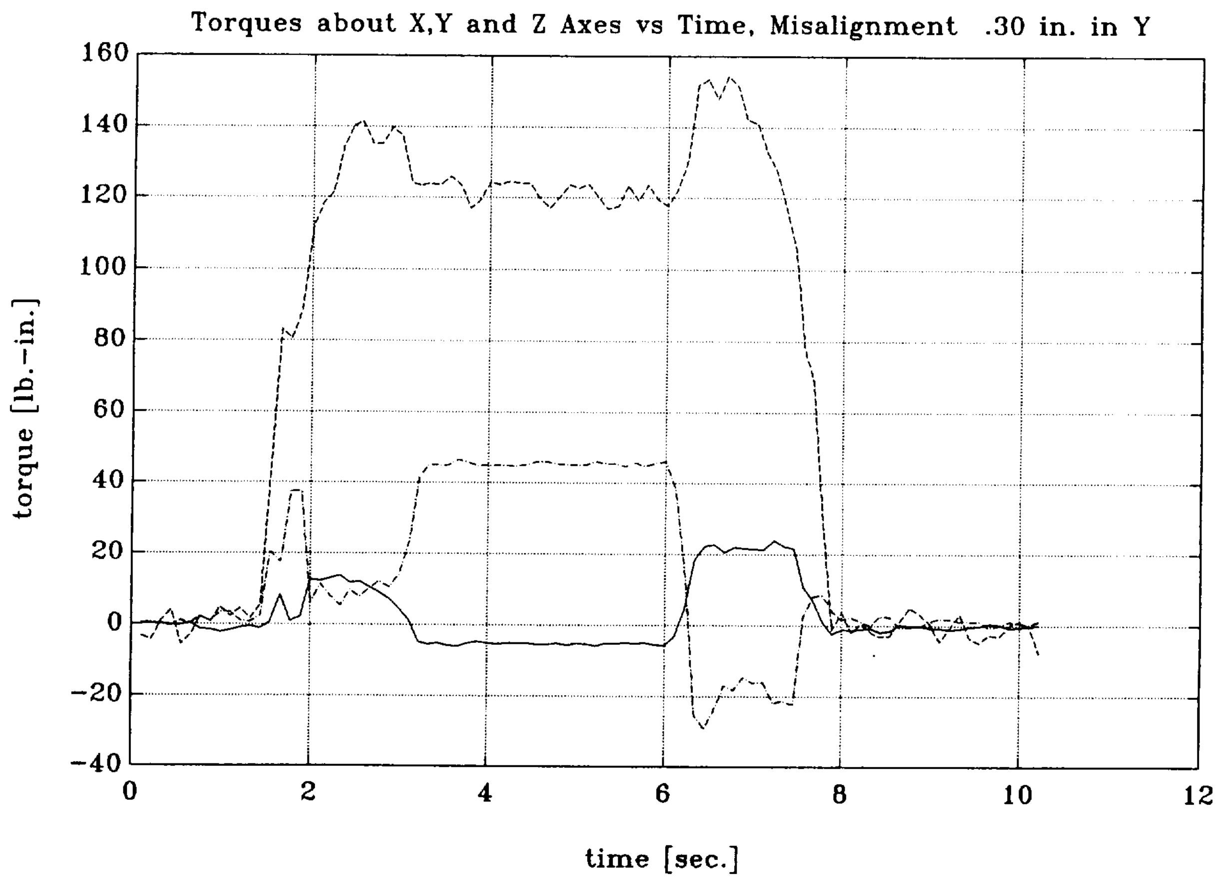

Figure SRACK15 Time histories of forces under -0.05 in. misalignment
dashed: F_x; dashed-dotted: F_y; solid: F_z

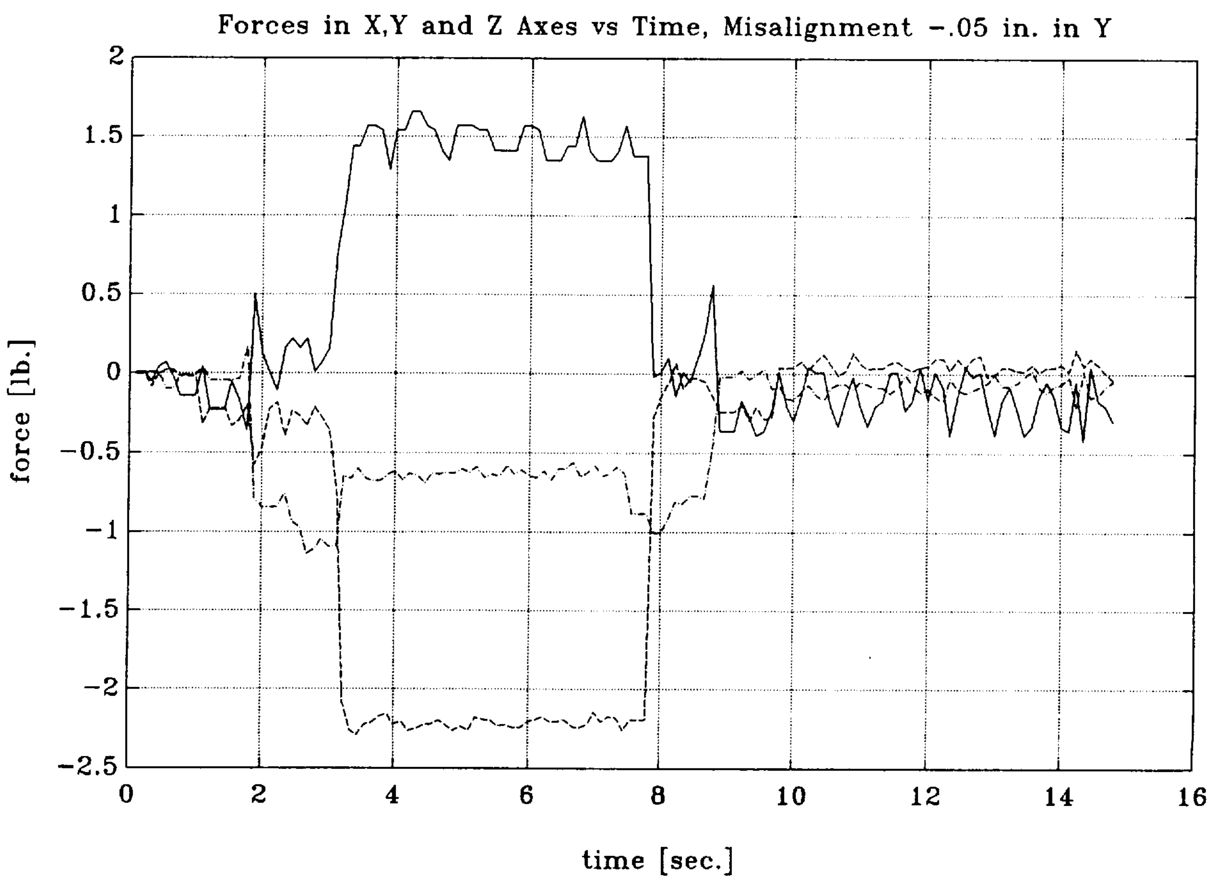

Figure SRACK16 Time histories of torques under -0.05 in. misalignment
dashed: T_x; *dashed-dotted:* T_y; *solid:* T_z

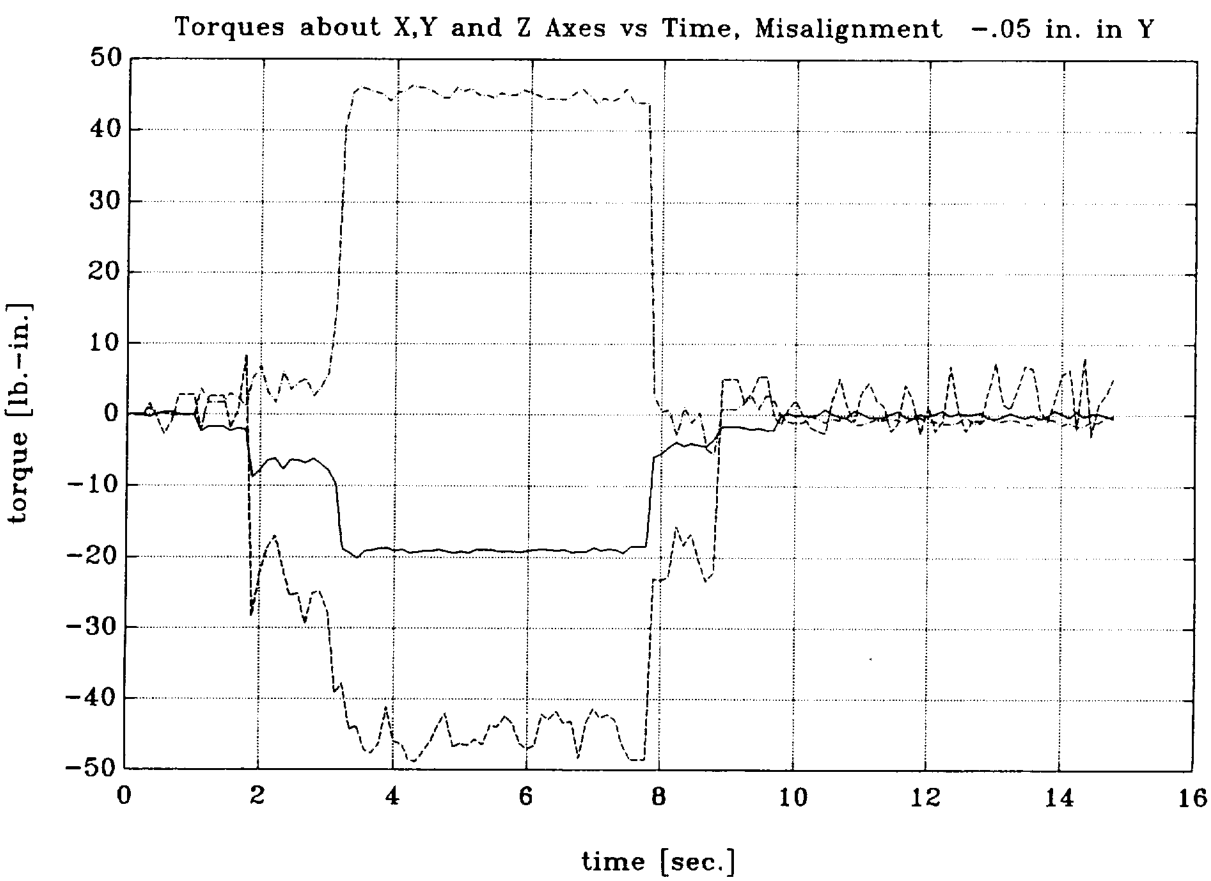

Figure SRACK17 Time histories of forces under -0.1 in. misalignment
dashed: F_x; *dashed-dotted:* F_y; *solid:* F_z

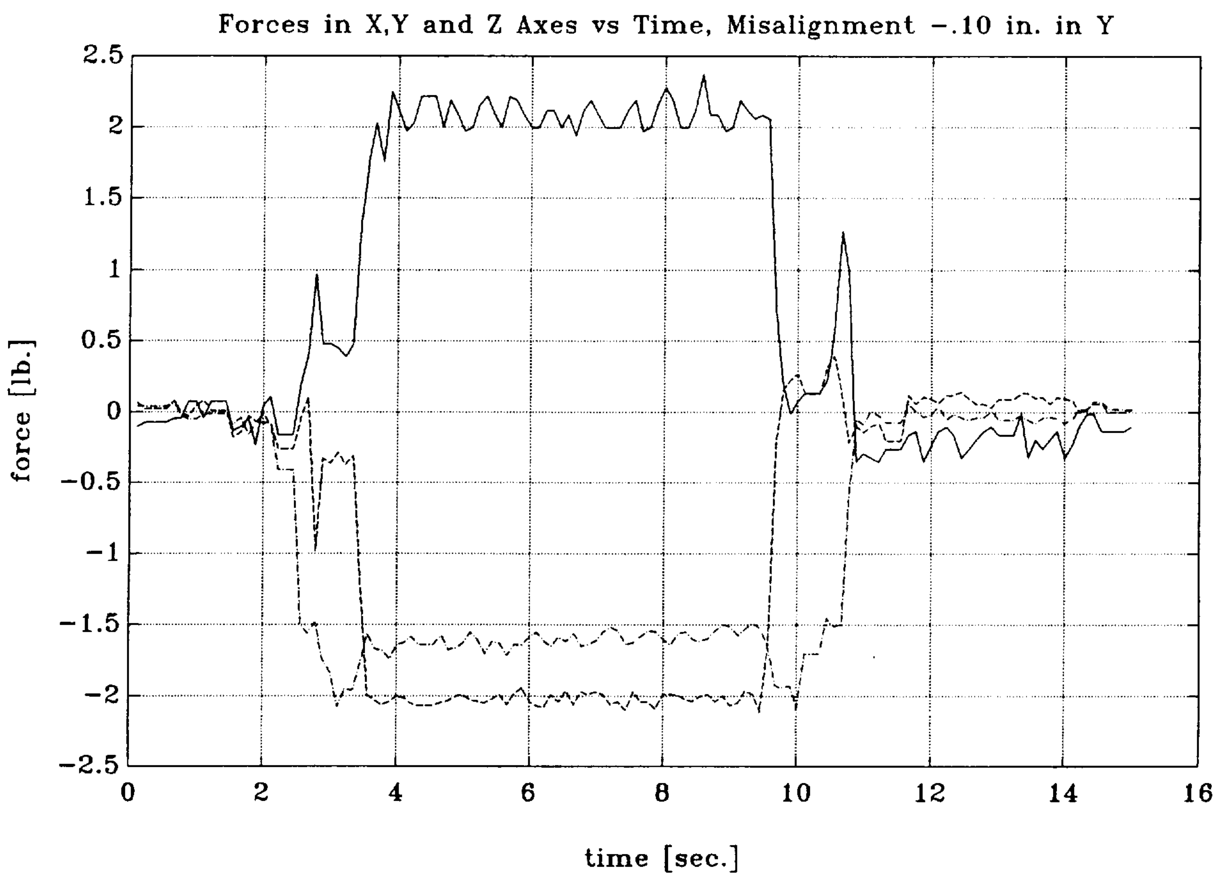

Figure SRACK18 Time histories of torques under -0.1 in. misalignment
dashed: T_x; *dashed-dotted:* T_y; *solid:* T_z

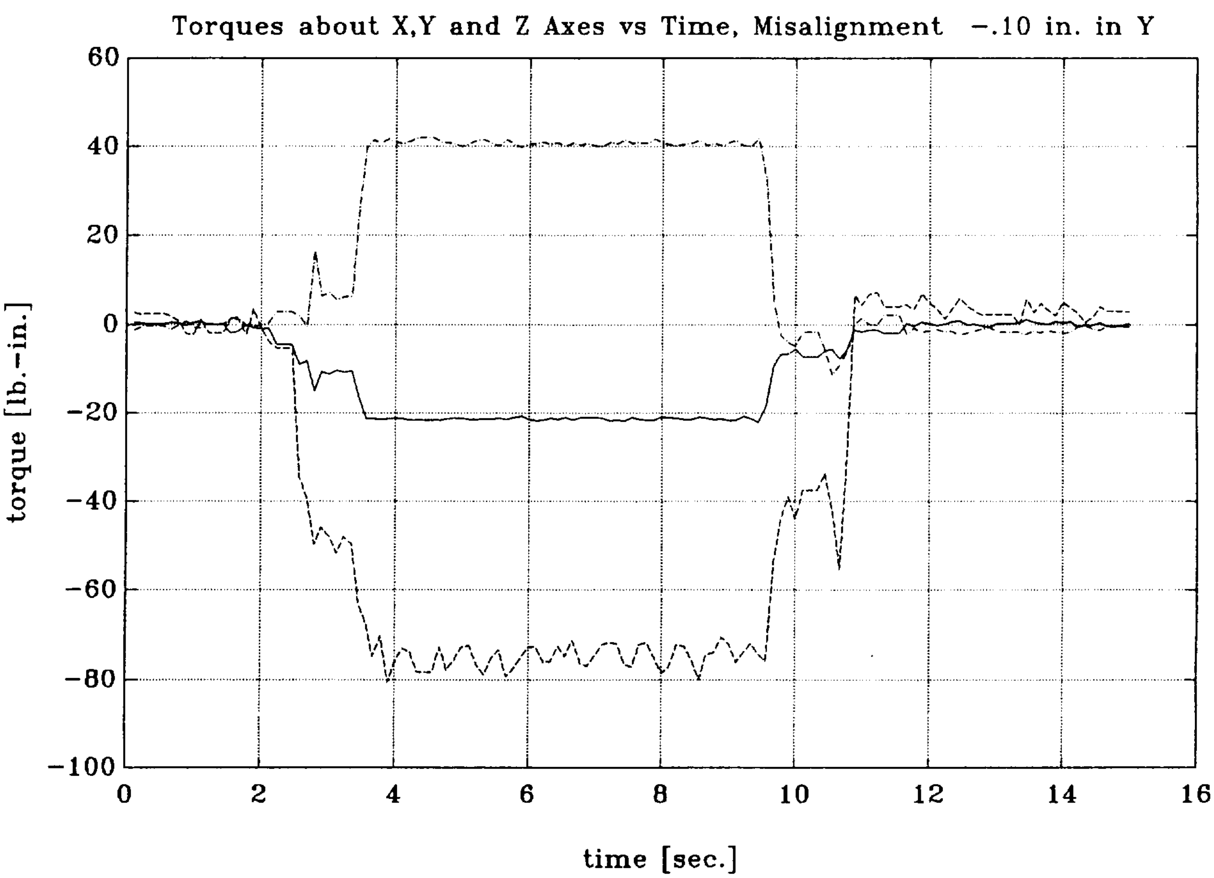

Figure SRACK19 Time histories of forces under -0.15 in. misalignment
dashed: F_x; *dashed-dotted:* F_y; *solid:* F_z

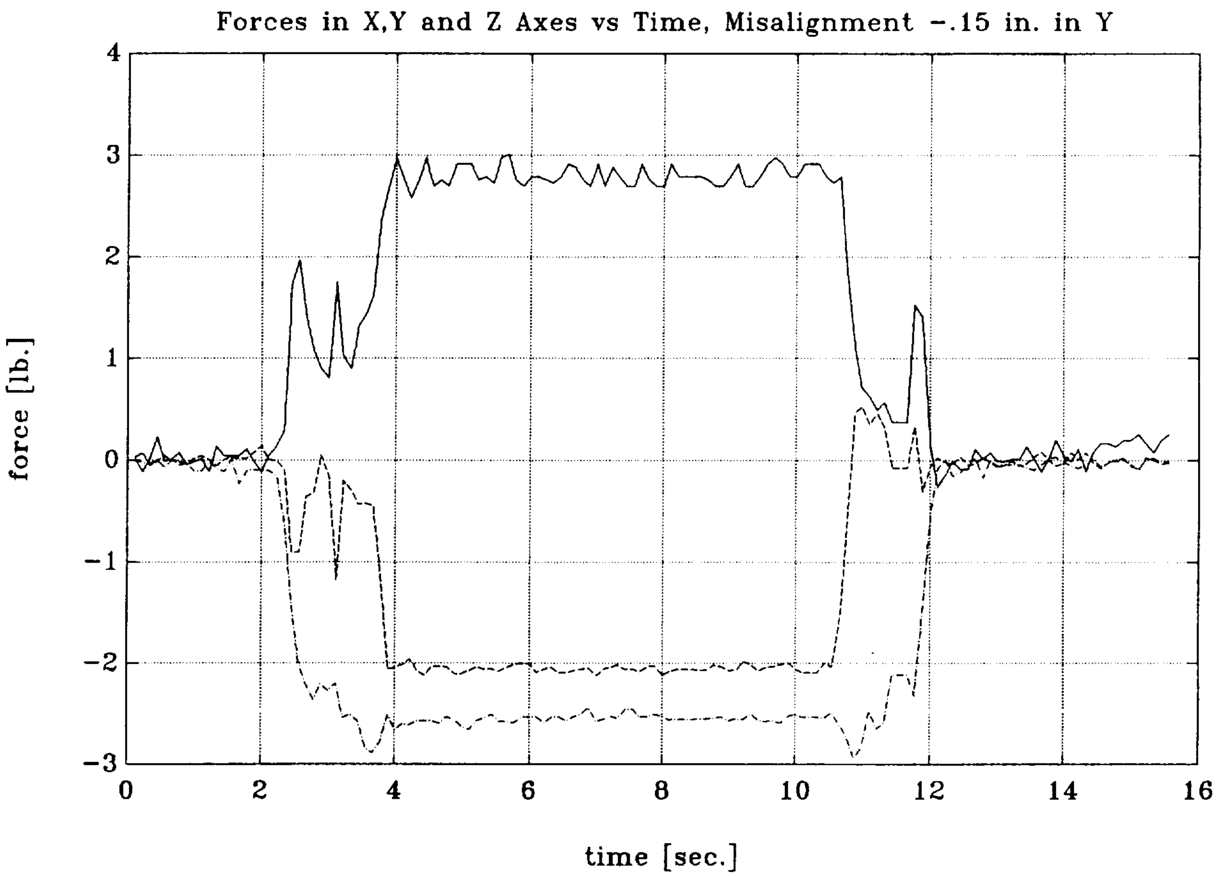

Figure SRACK20 Time histories of torques under -0.15 in. misalignment
dashed: T_x; *dashed-dotted:* T_y; *solid:* T_z

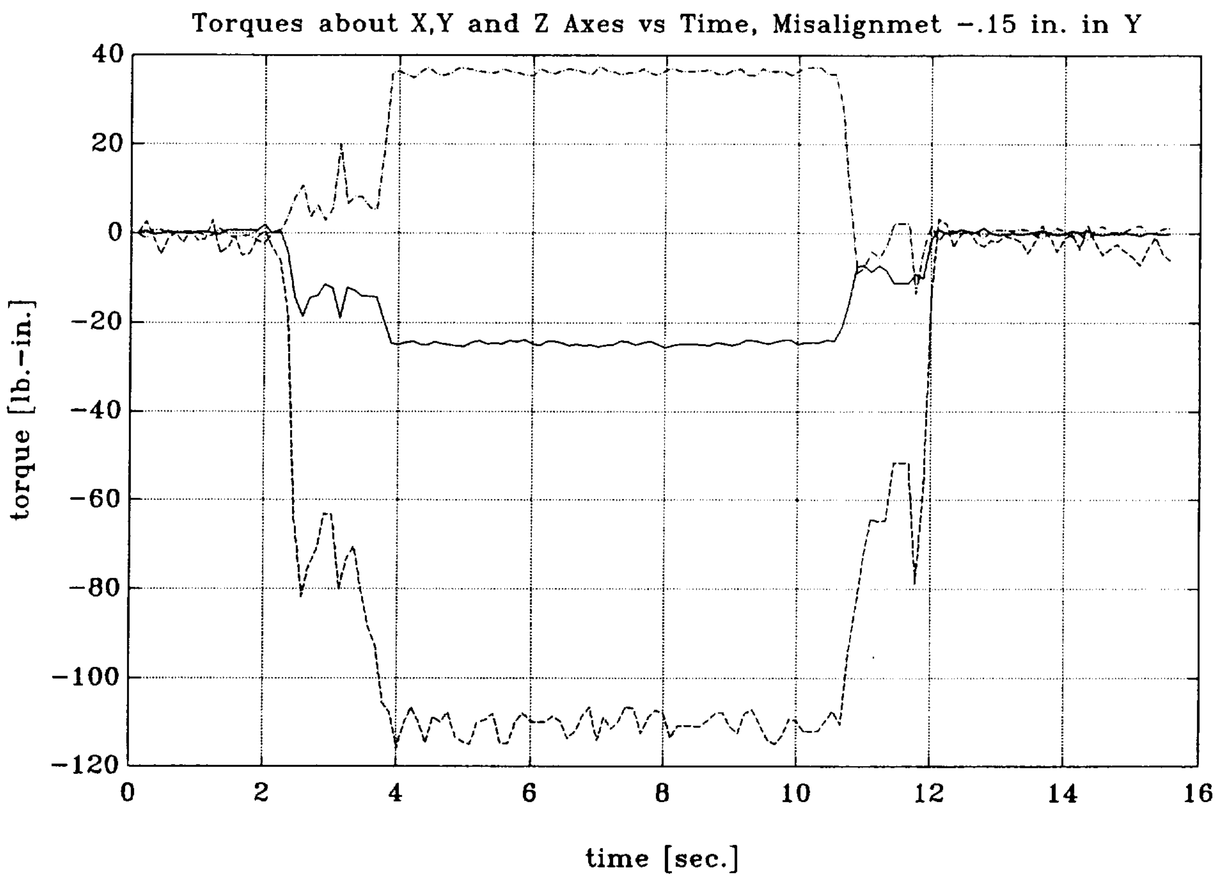

Figure SRACK21 Time histories of forces under -0.20 in. misalignment
dashed: F_x; dashed-dotted: F_y; solid: F_z

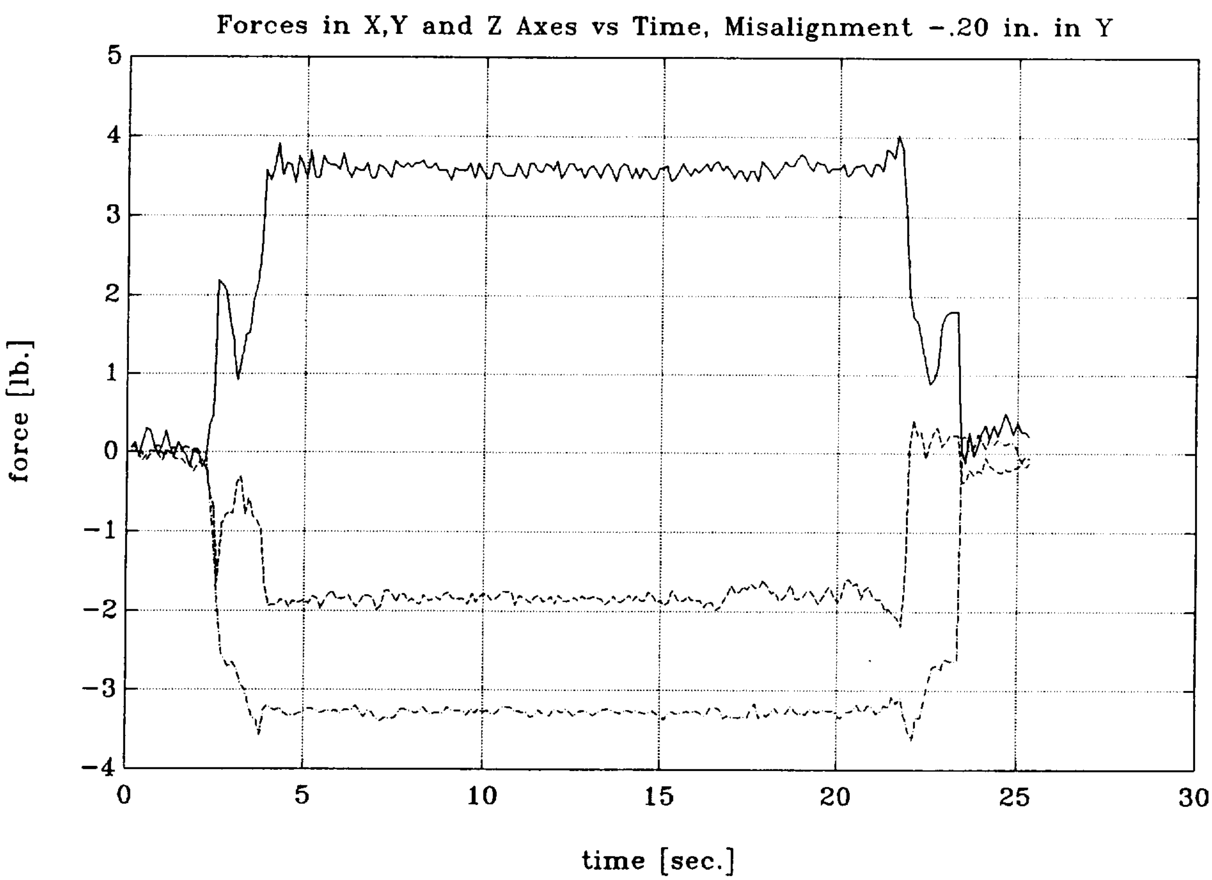

Figure SRACK22 Time histories of torques under -0.20 in. misalignment
dashed: T_x; dashed-dotted: T_y; solid: T_z

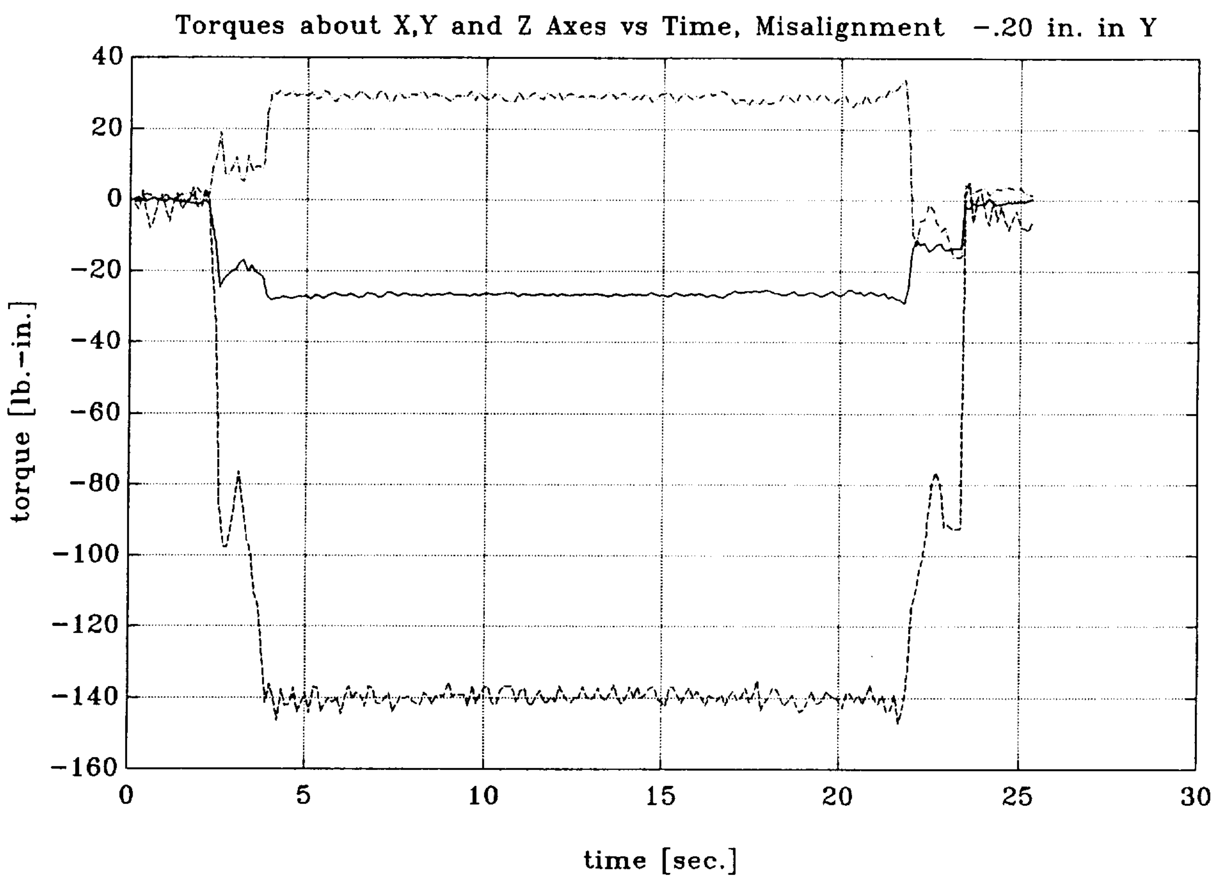

Figure SRACK23 Time histories of forces under -0.25 in. misalignment
dashed: F_x; dashed-dotted: F_y; solid: F_z

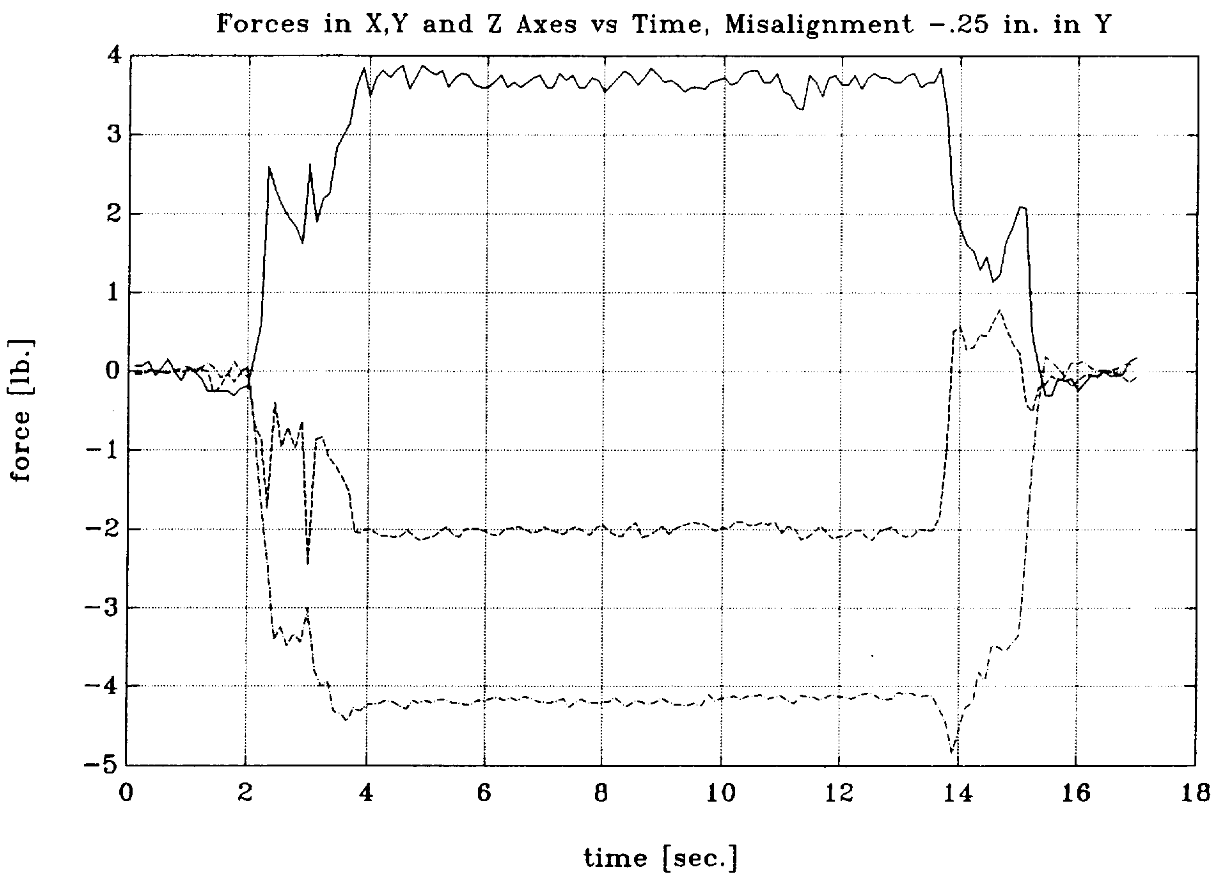

Figure SRACK24 Time histories of torques under -0.25 in. misalignment
dashed: T_x; *dashed-dotted:* T_y; *solid:* T_z

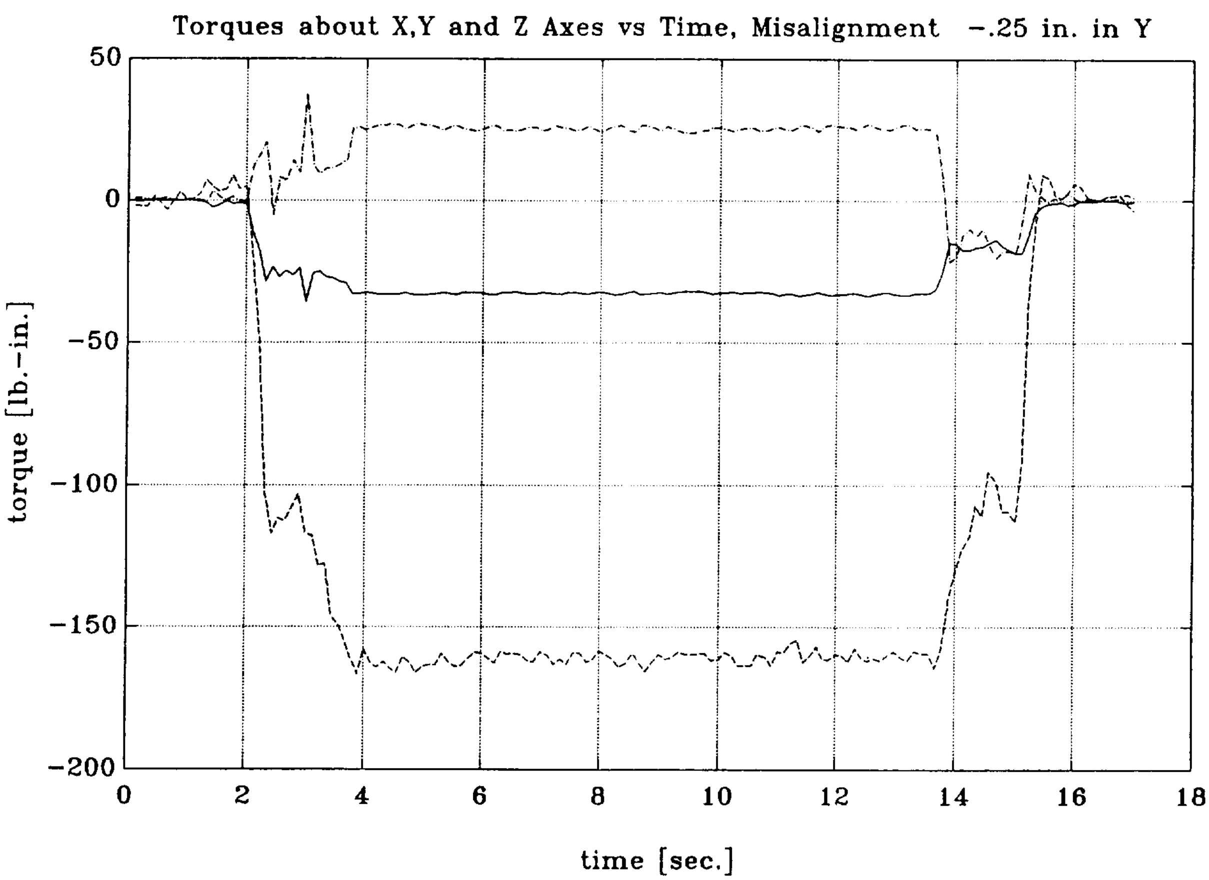

Figure SRACK25 Time histories of forces under -0.30 in. misalignment
dashed: F_x; *dashed-dotted:* F_y; *solid:* F_z

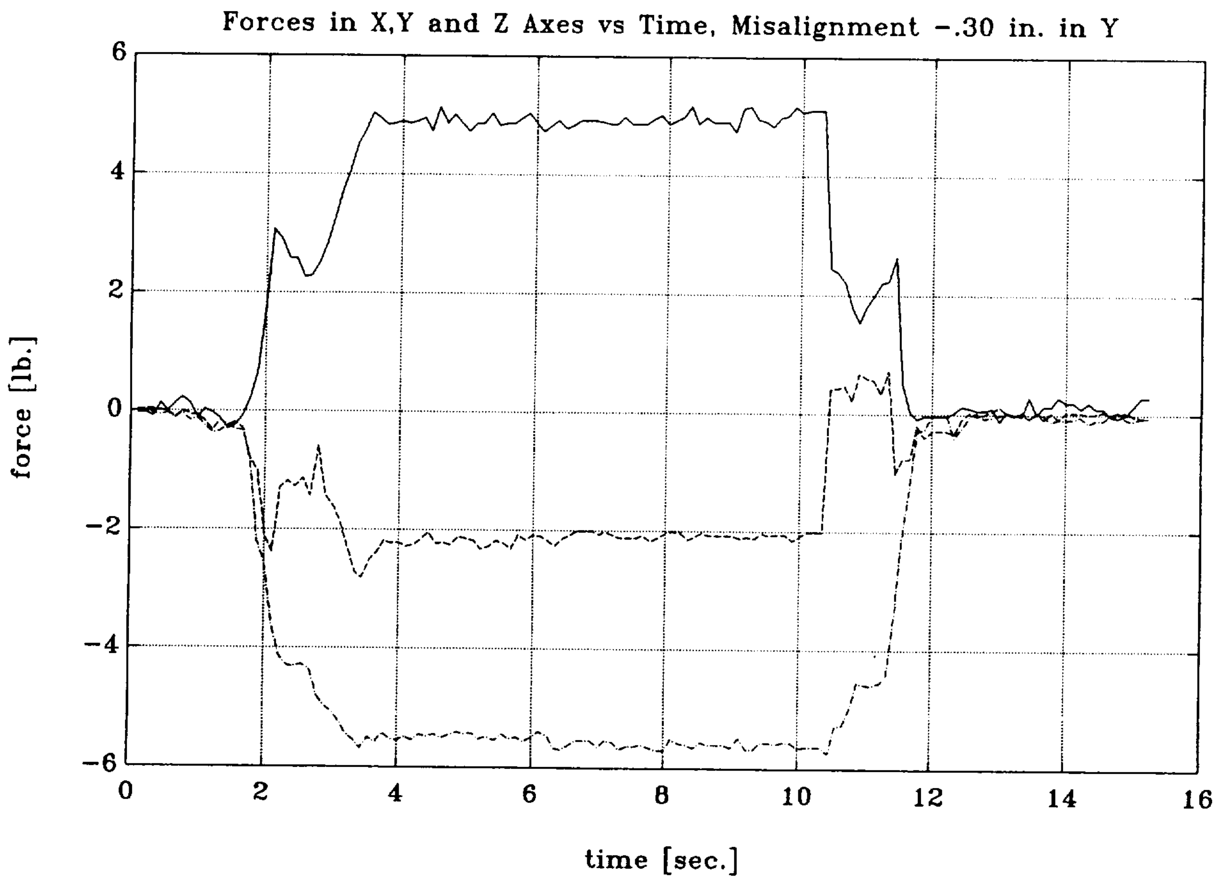

Figure SRACK26 Time histories of torques under -0.30 in. misalignment
dashed: T_x; *dashed-dotted:* T_y; *solid:* T_z

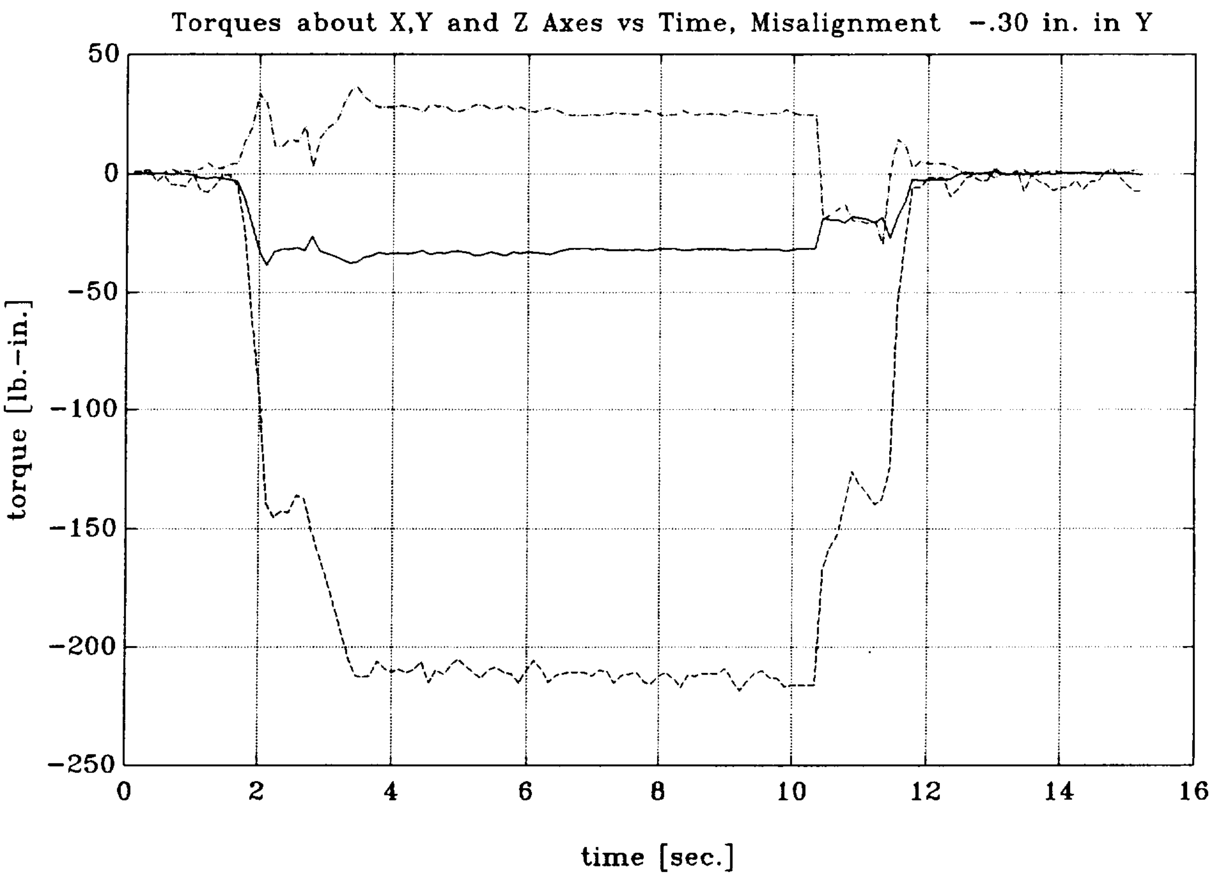

Figure SRACK1 Time histories of forces under perfect alignment
dashed: F_x; *dashed-dotted:* F_y; *solid:* F_z

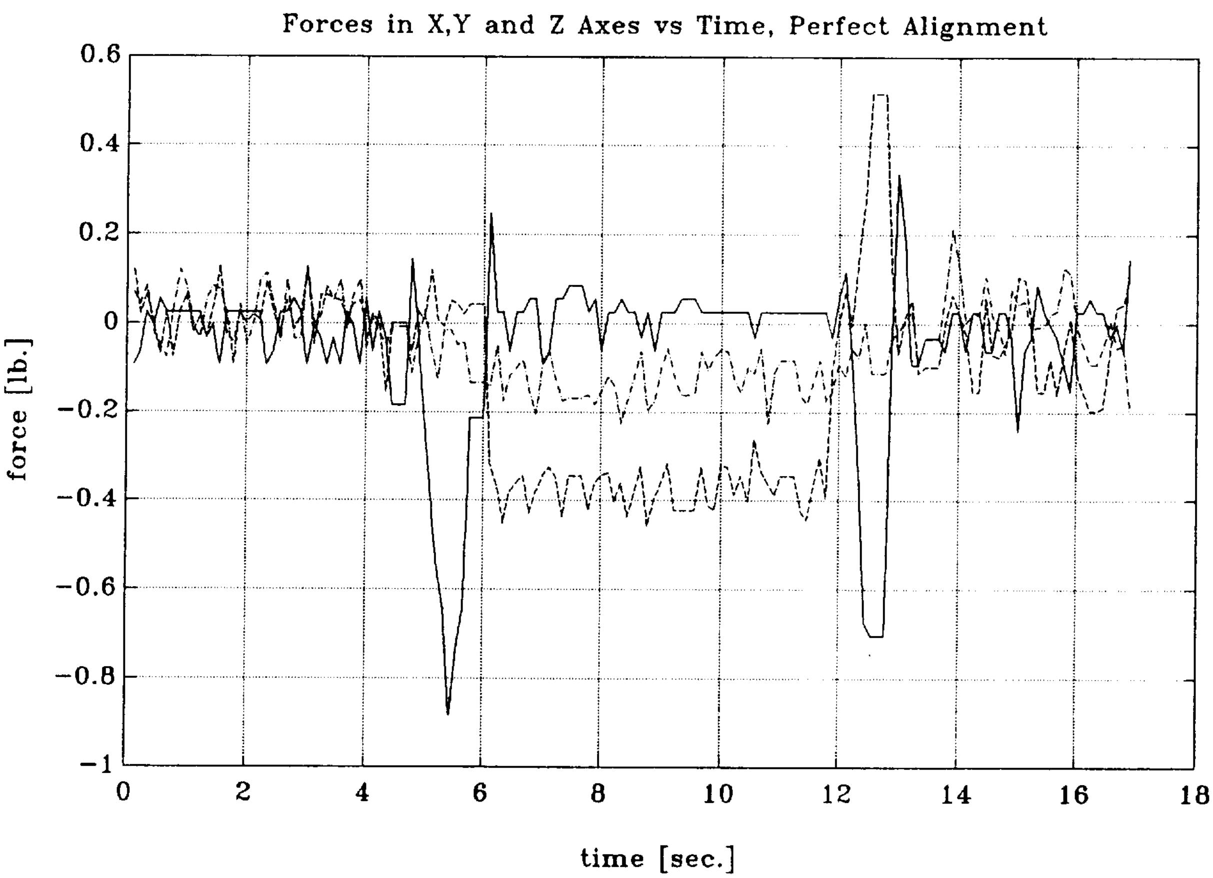

Figure SRACK2 Time histories of torques under perfect alignment
dashed: T_x; *dashed-dotted:* T_y; *solid:* T_z

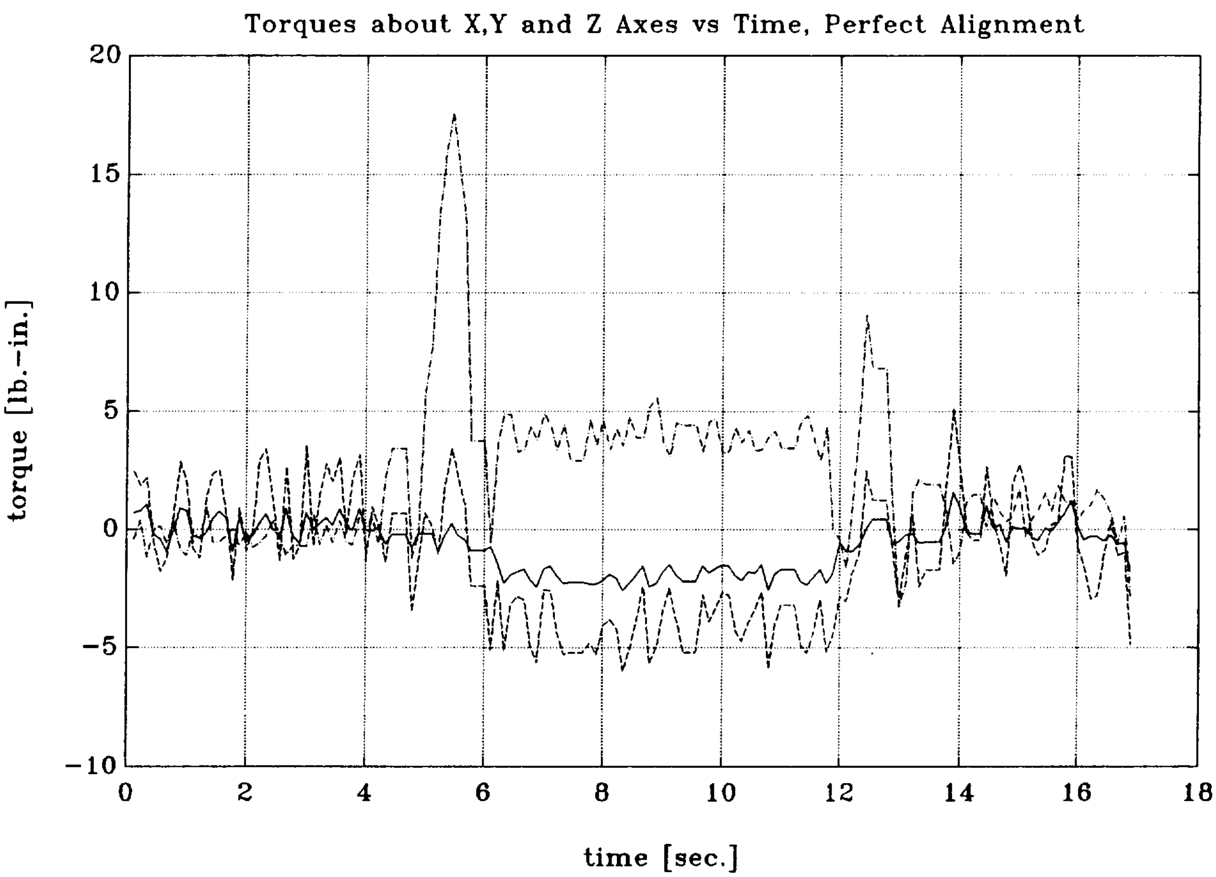

Figure SRACK3 Time histories of forces under 0.05 in. misalignment
dashed: F_x; *dashed-dotted:* F_y; *solid:* F_z

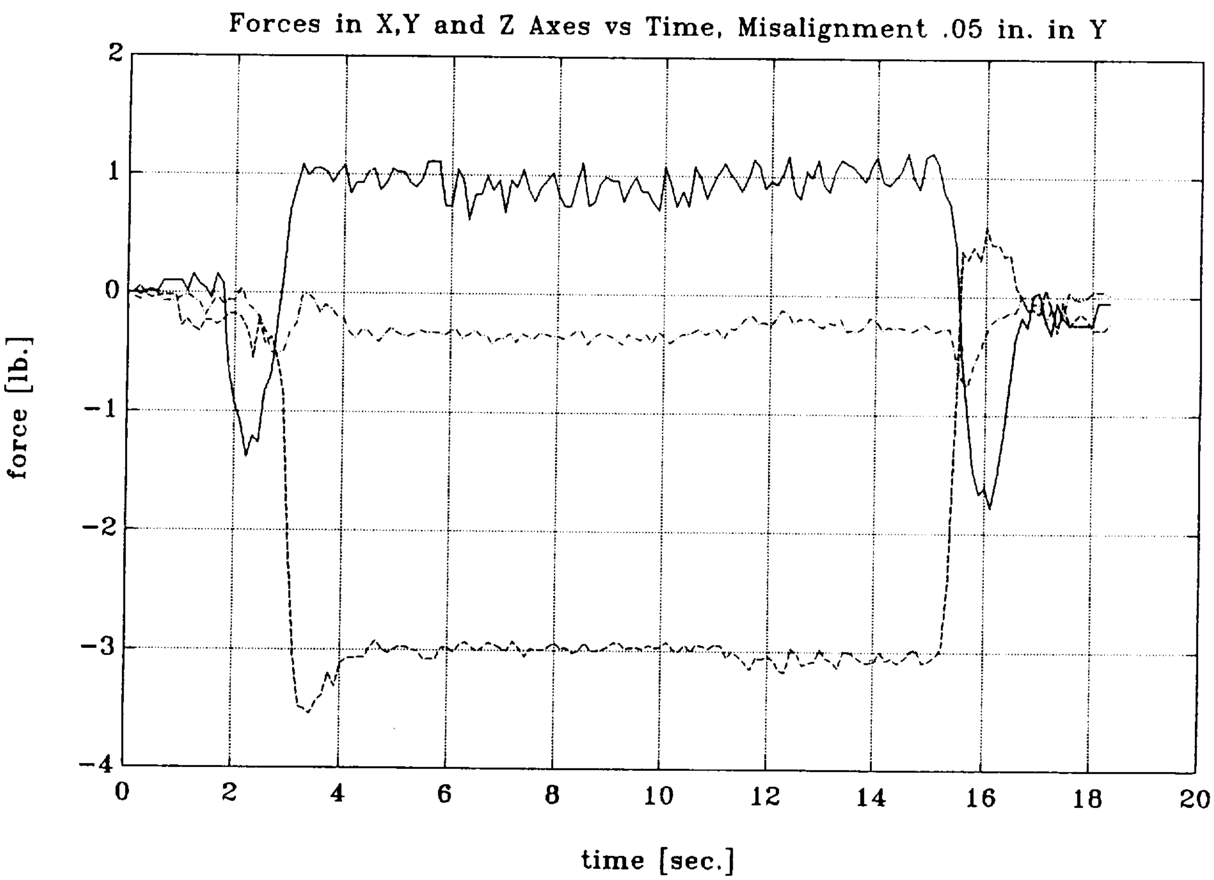

Figure HRACK4 Time histories of torques under 0.05 in. misalignment
dashed: T_x; *dashed-dotted:* T_y; *solid:* T_z

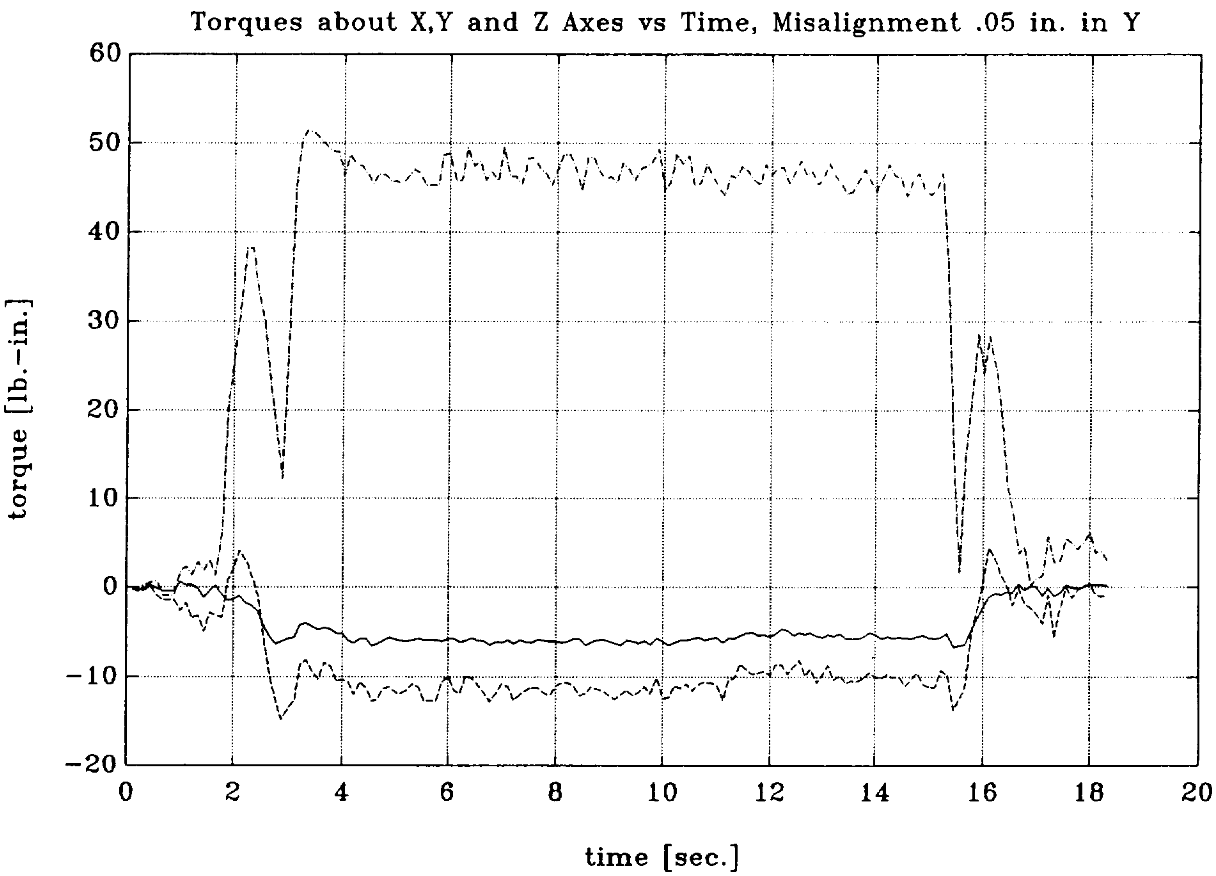

Figure HRACK5 Time histories of forces under 0.1 in. misalignment
dashed: F_x; *dashed-dotted:* F_y; *solid:* F_z

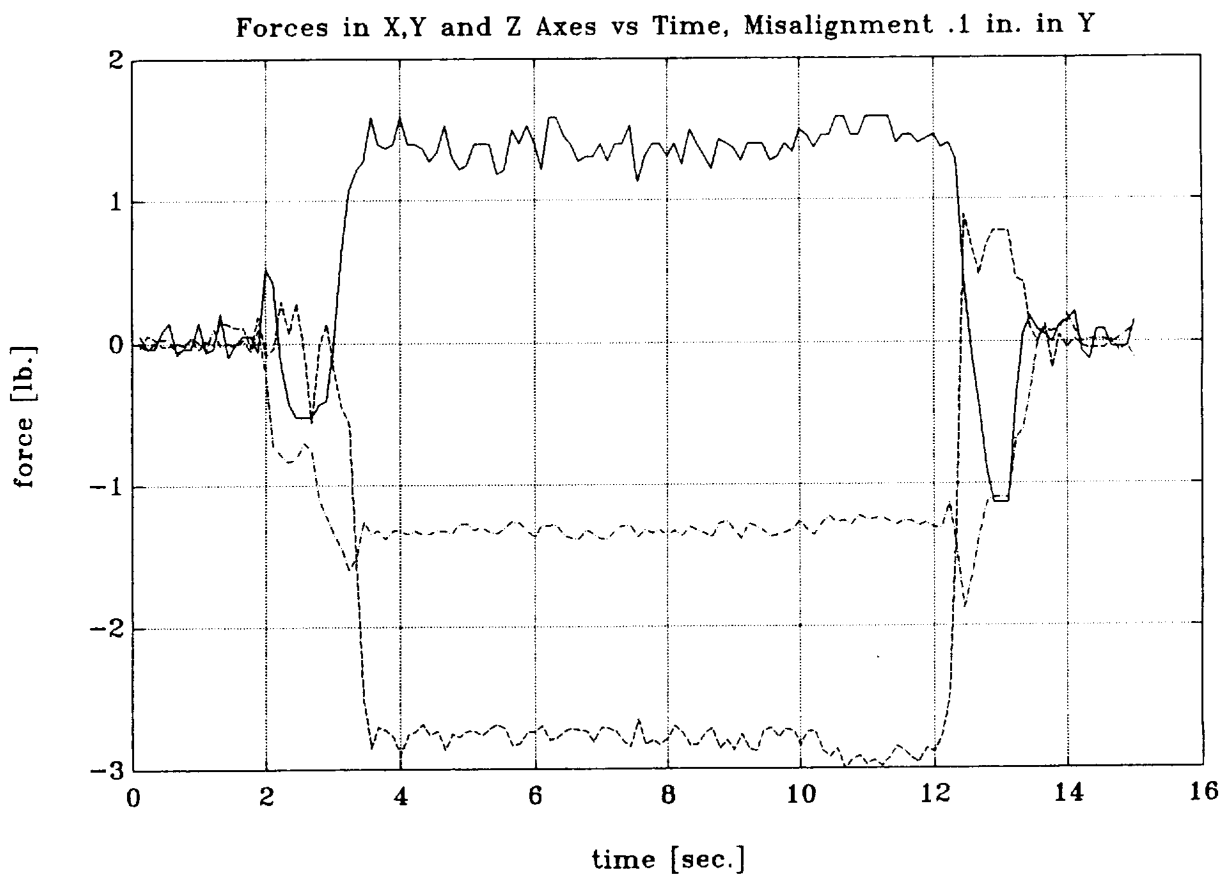

Figure HRACK6 Time histories of torques under 0.1 in. misalignment
dashed: T_x*; dashed-dotted:* T_y*; solid:* T_z

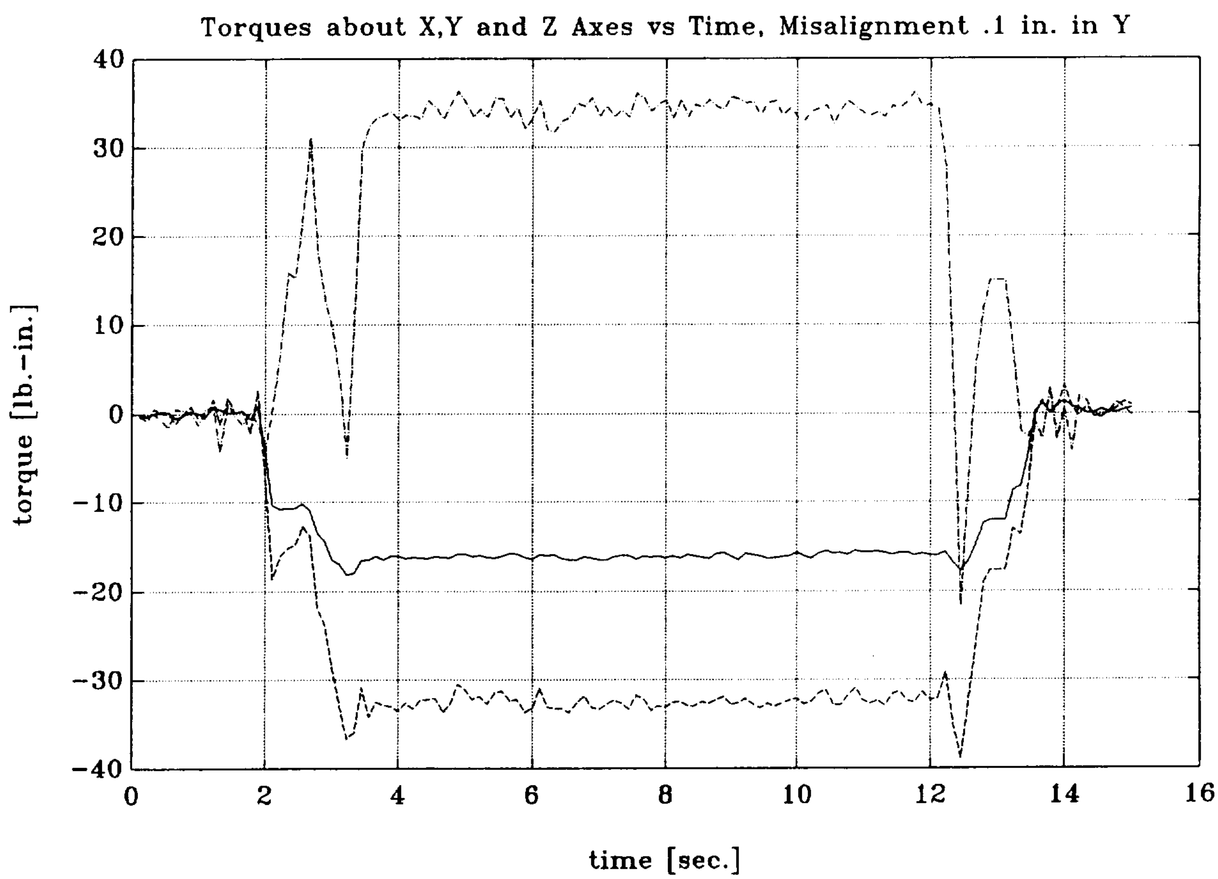

Figure HRACK7 Time histories of forces under 0.15 in. misalignment
dashed: F_x; *dashed-dotted:* F_y; *solid:* F_z

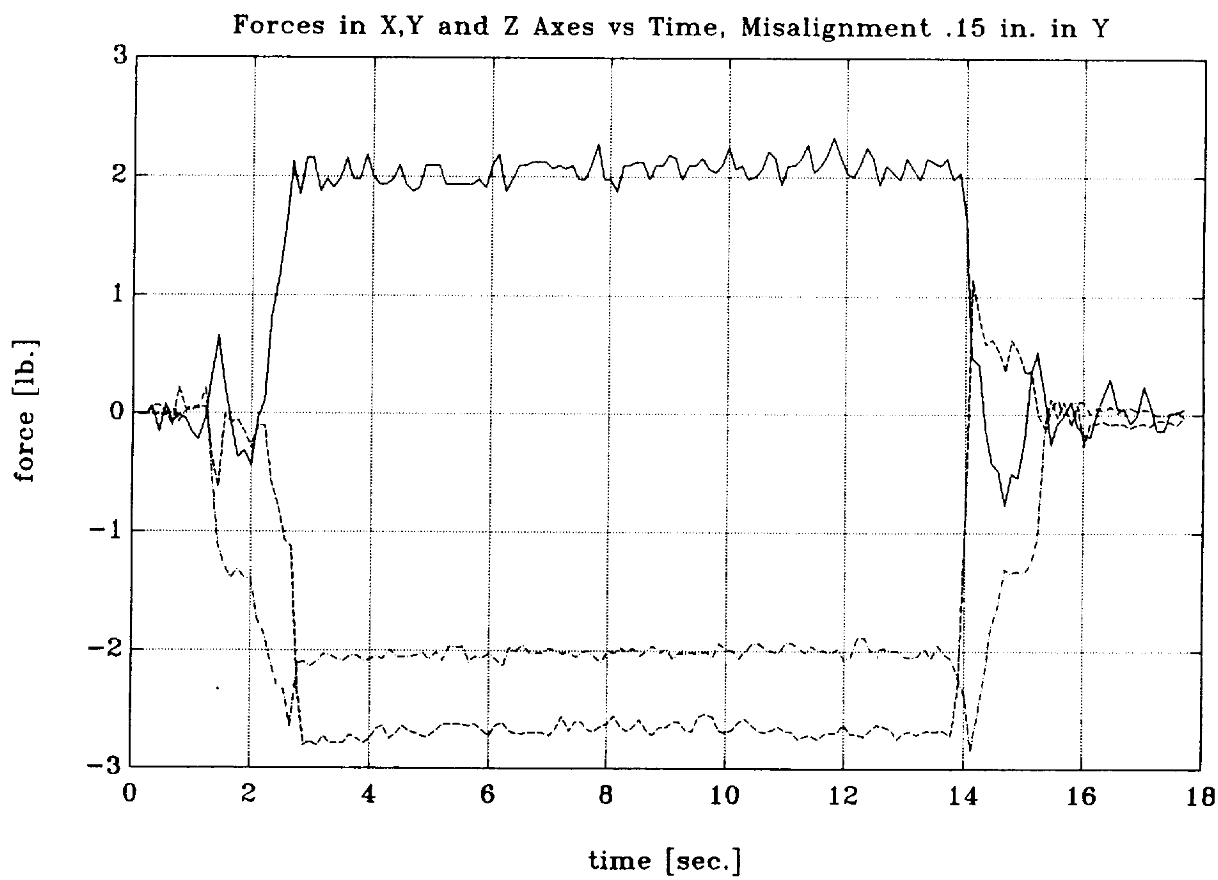

Figure HRACK8 Time histories of torques under 0.15 in. misalignment
dashed: T_x; *dashed-dotted:* T_y; *solid:* T_z

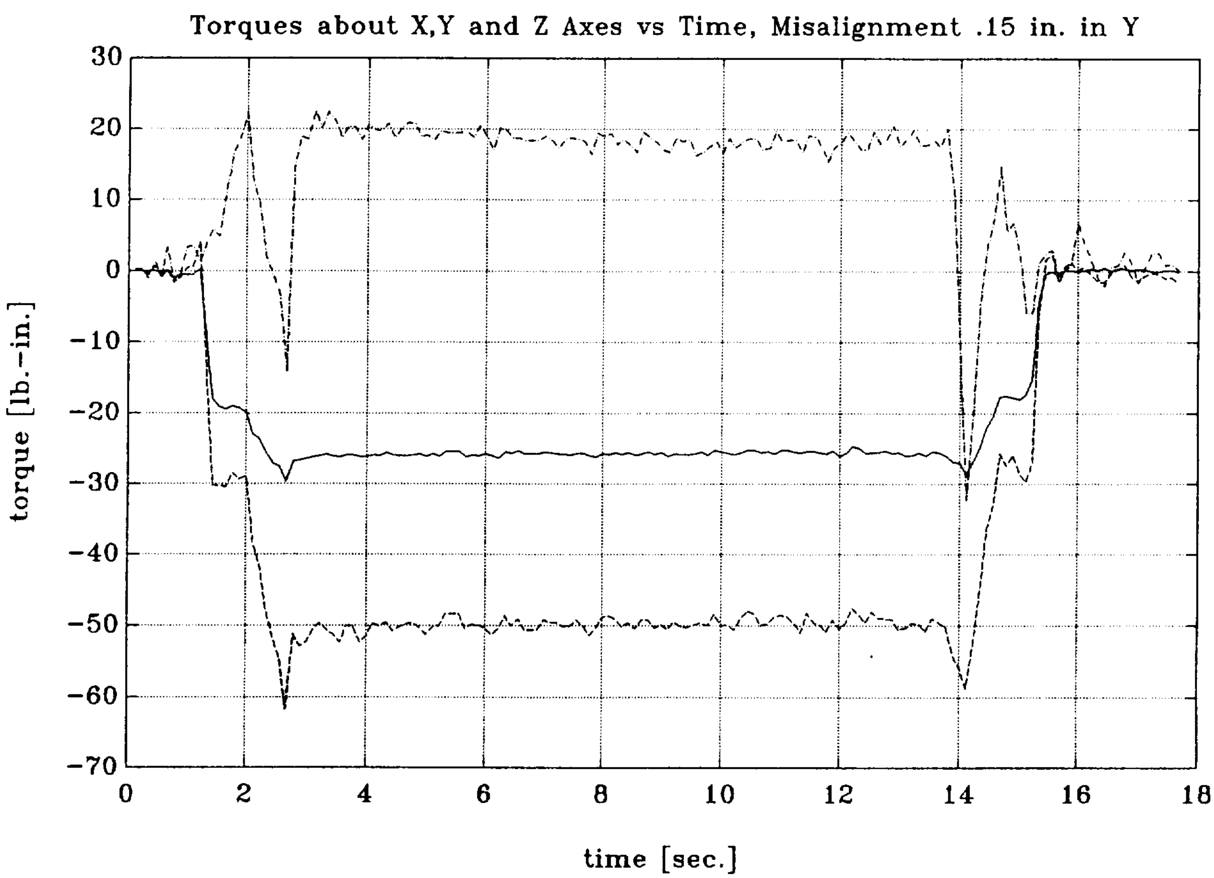

Figure HRACK9 Time histories of forces under 0.20 in. misalignment
dashed: F_x; dashed-dotted: F_y; solid: F_z

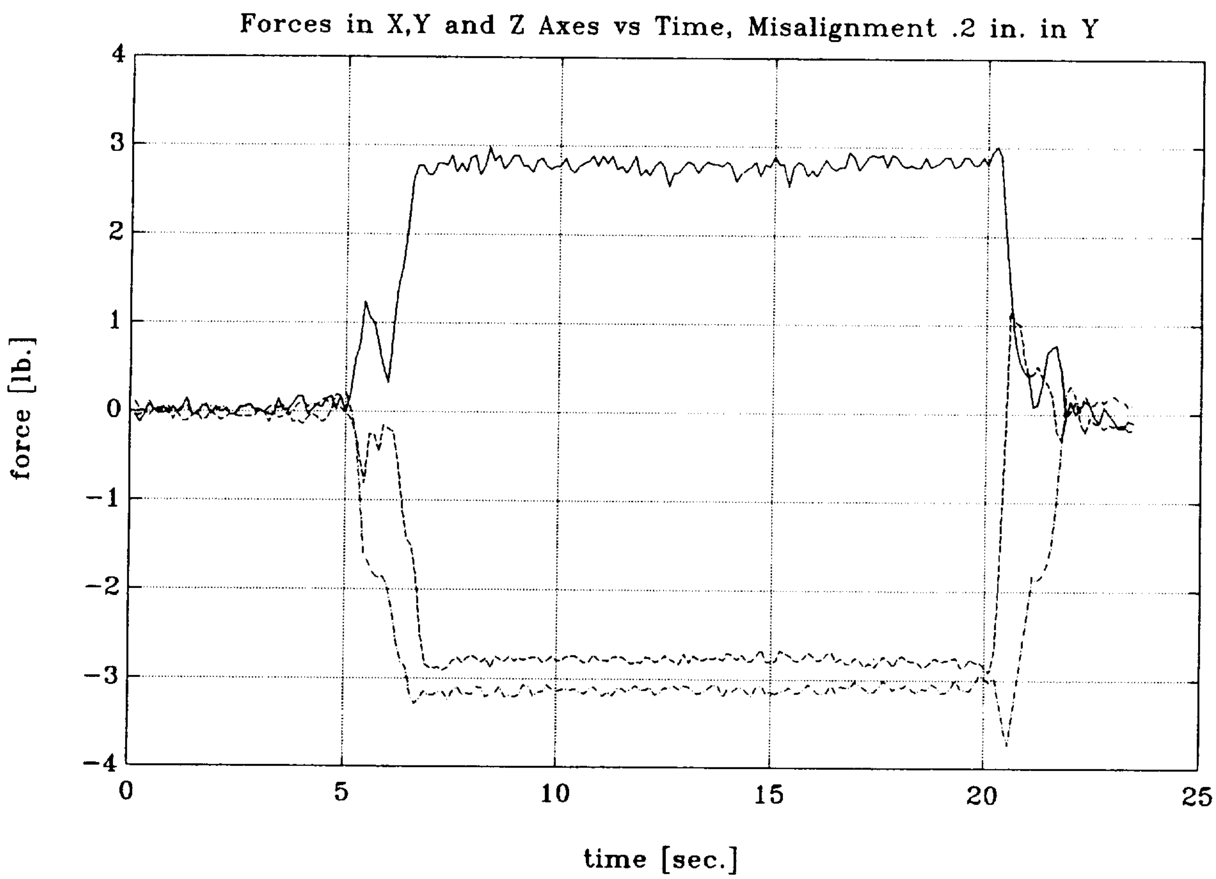

Figure HRACK10 Time histories of torques under 0.20 in. misalignment
dashed: T_x*; dashed-dotted:* T_y*; solid:* T_z

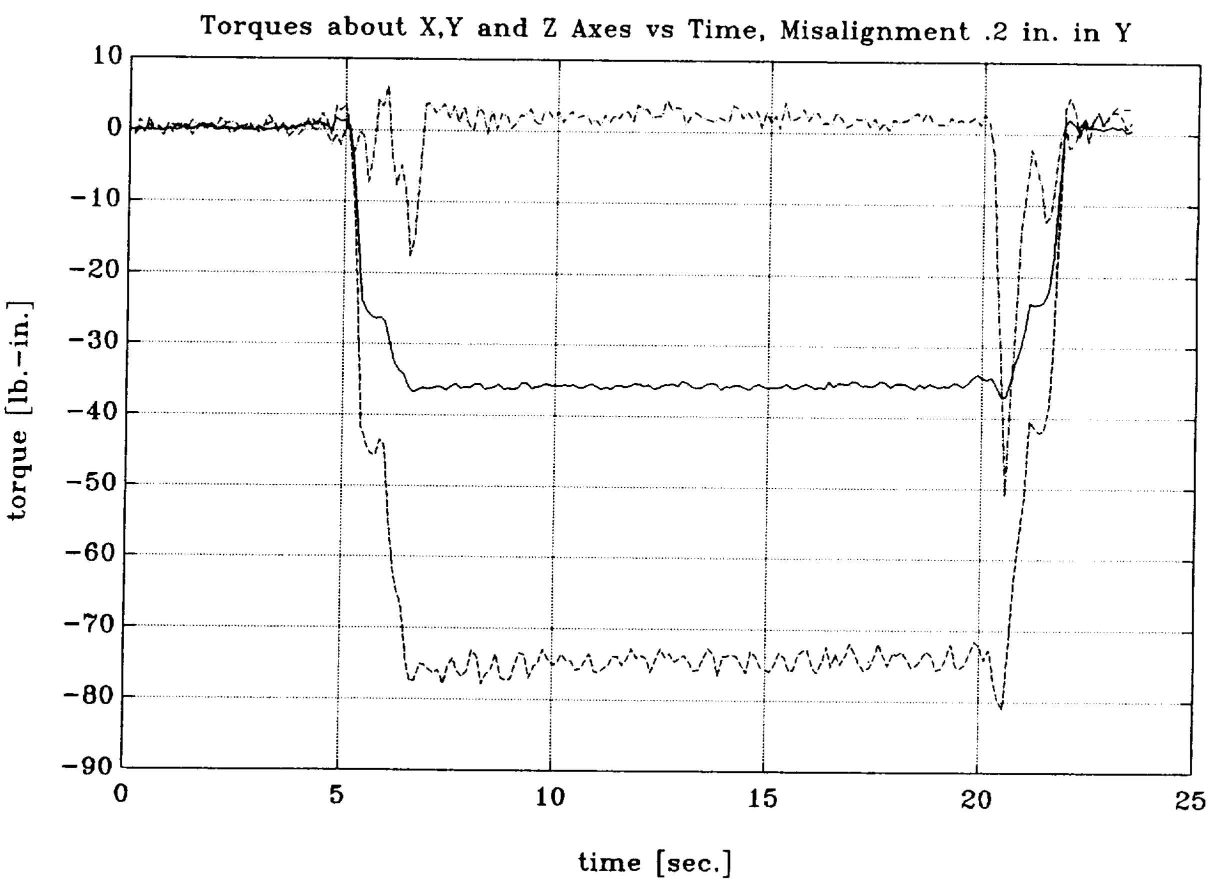

Figure HRACK11 Time histories of forces under 0.25 in. misalignment
dashed: F_x; dashed-dotted: F_y; solid: F_z

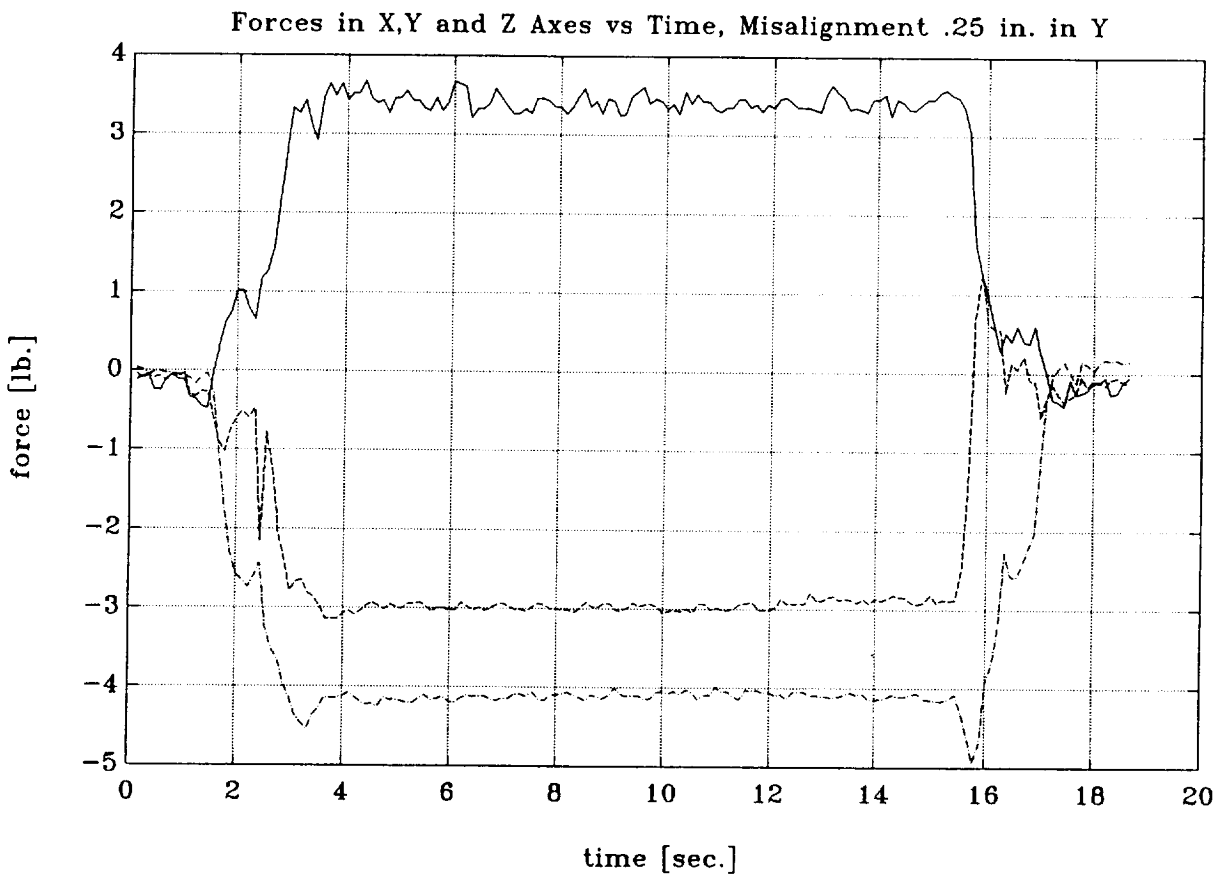

Figure HRACK12 Time histories of torques under 0.25 in. misalignment
dashed: T_x; *dashed-dotted:* T_y; *solid:* T_z

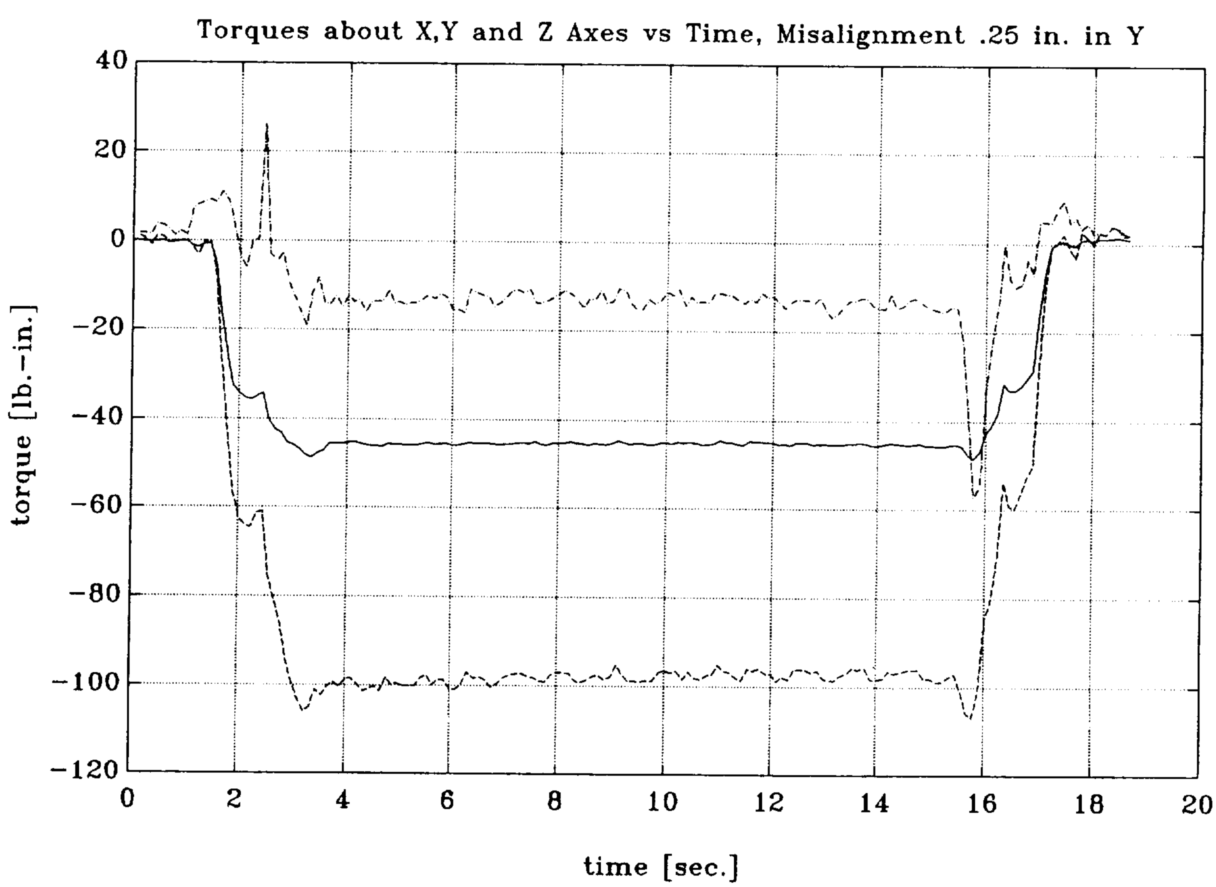

Figure HRACK13 Time histories of forces under 0.30 in. misalignment
dashed: F_x; *dashed-dotted:* F_y; *solid:* F_z

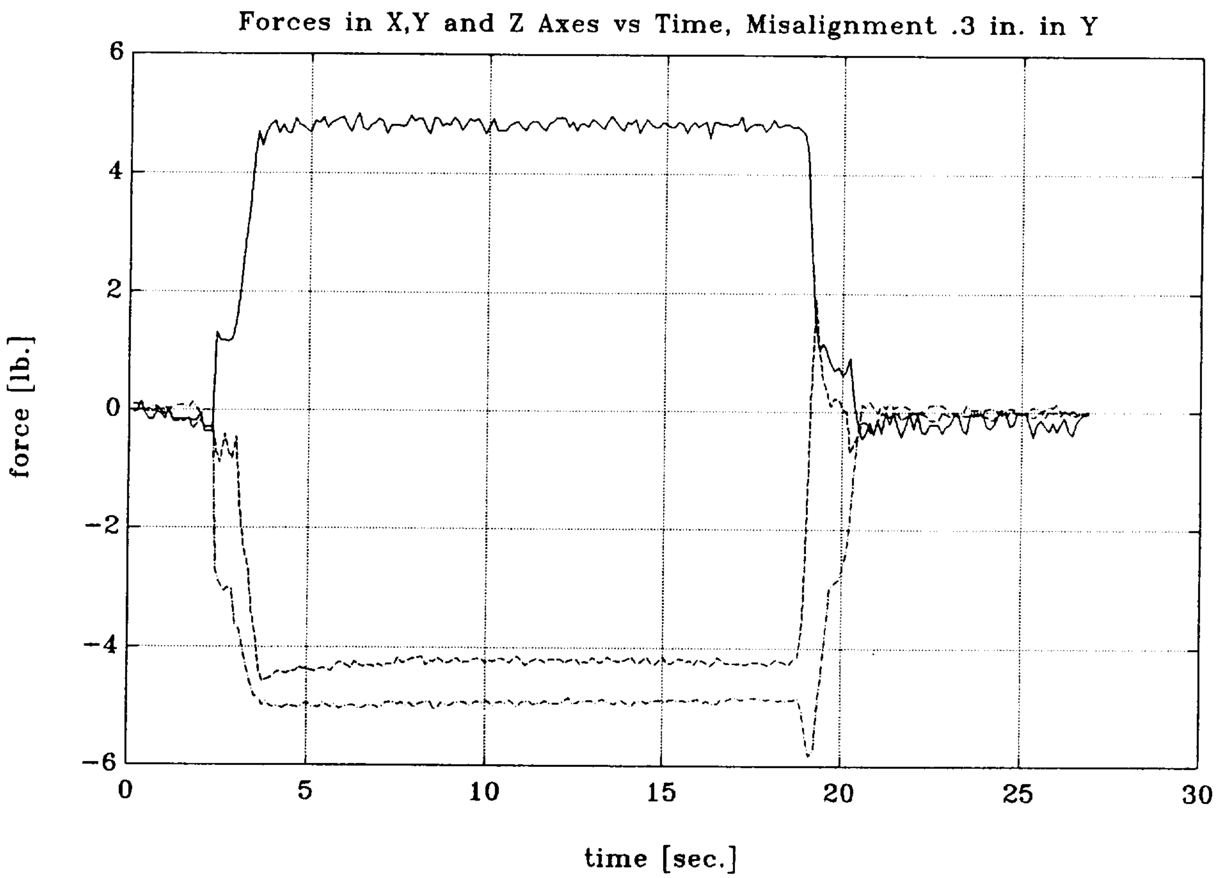

Figure HRACK14 Time histories of torques under 0.30 in. misalignment
dashed: T_x; *dashed-dotted:* T_y; *solid:* T_z

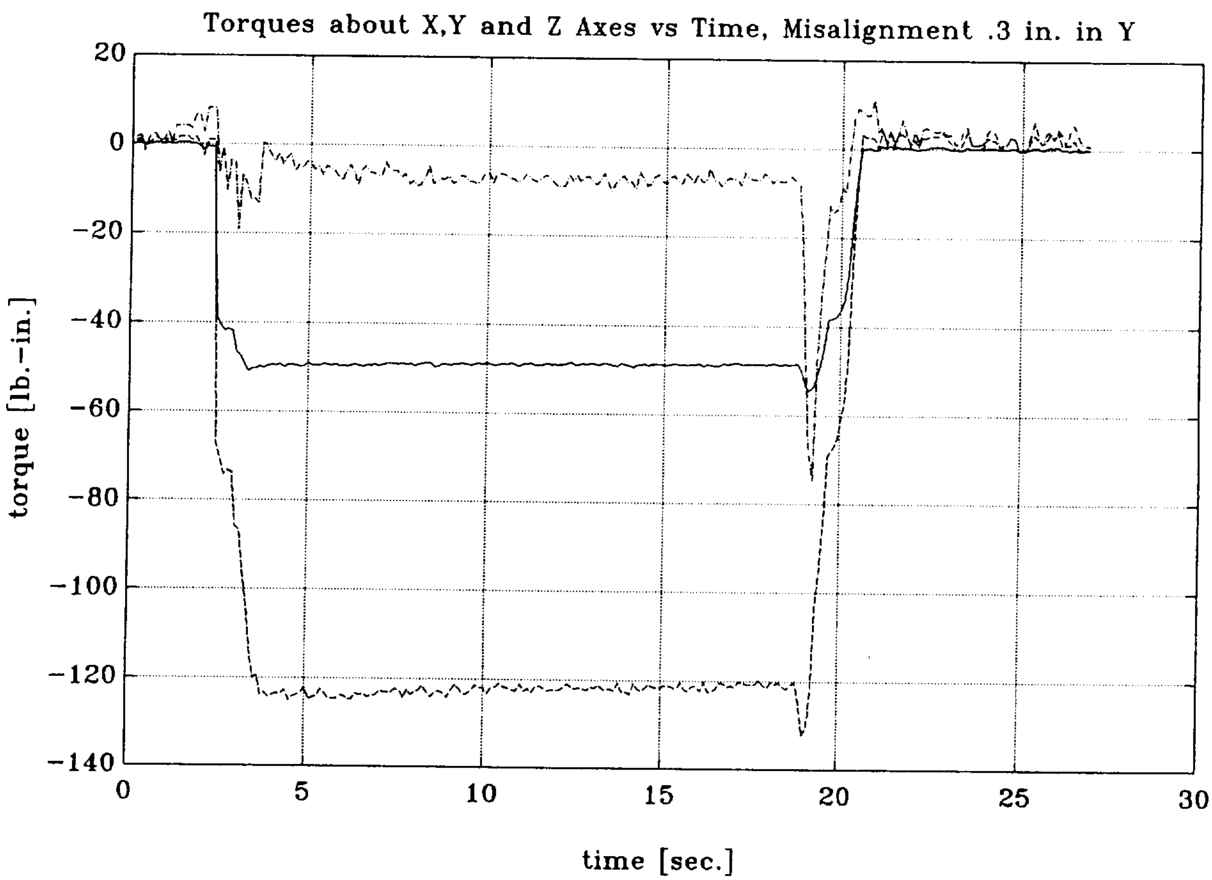

Figure HRACK15 Time histories of forces under -0.05 in. misalignment
dashed: F_x; *dashed-dotted:* F_y; *solid:* F_z

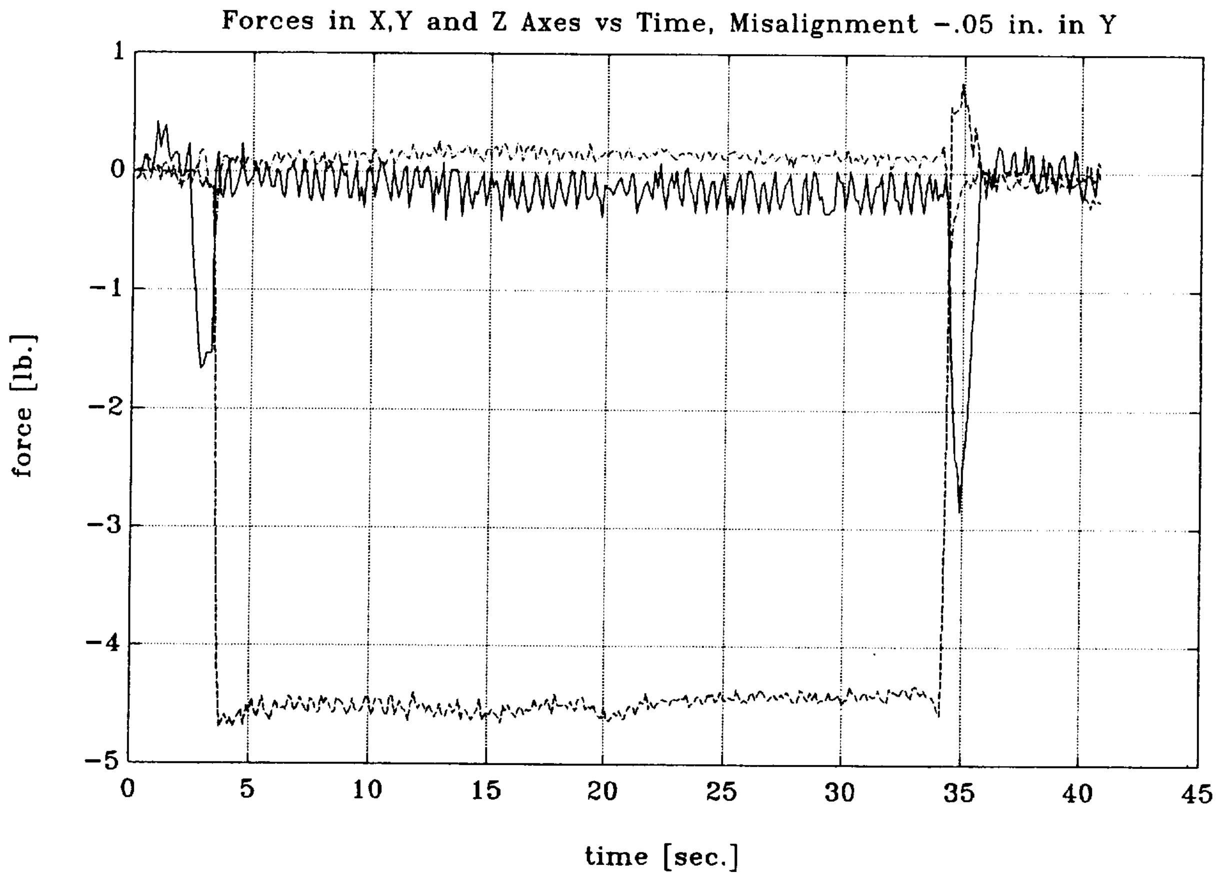

Figure HRACK16 Time histories of torques under -0.05 in. misalignment
dashed: T_x*; dashed-dotted:* T_y*; solid:* T_z

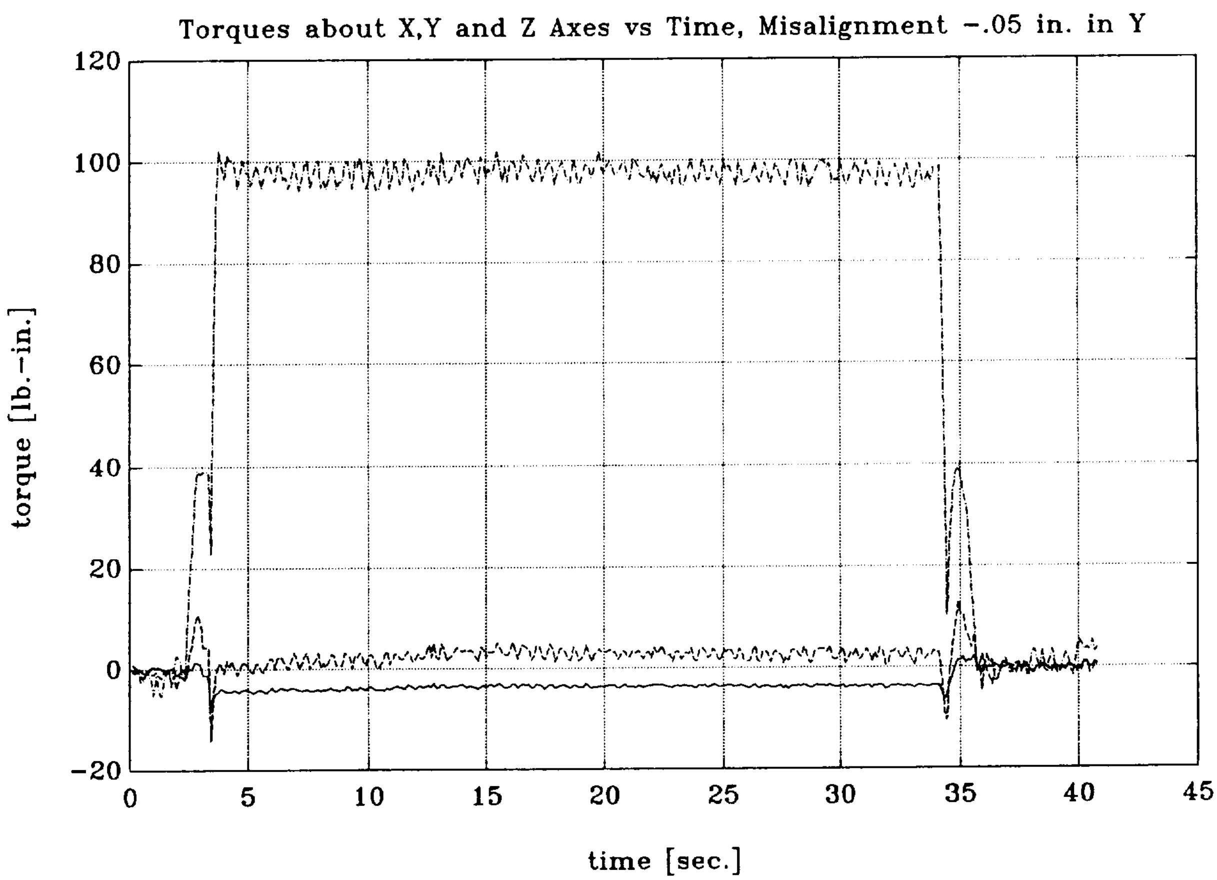

Figure HRACK17 Time histories of forces under -0.1 in. misalignment
dashed: F_x; *dashed-dotted:* F_y; *solid:* F_z

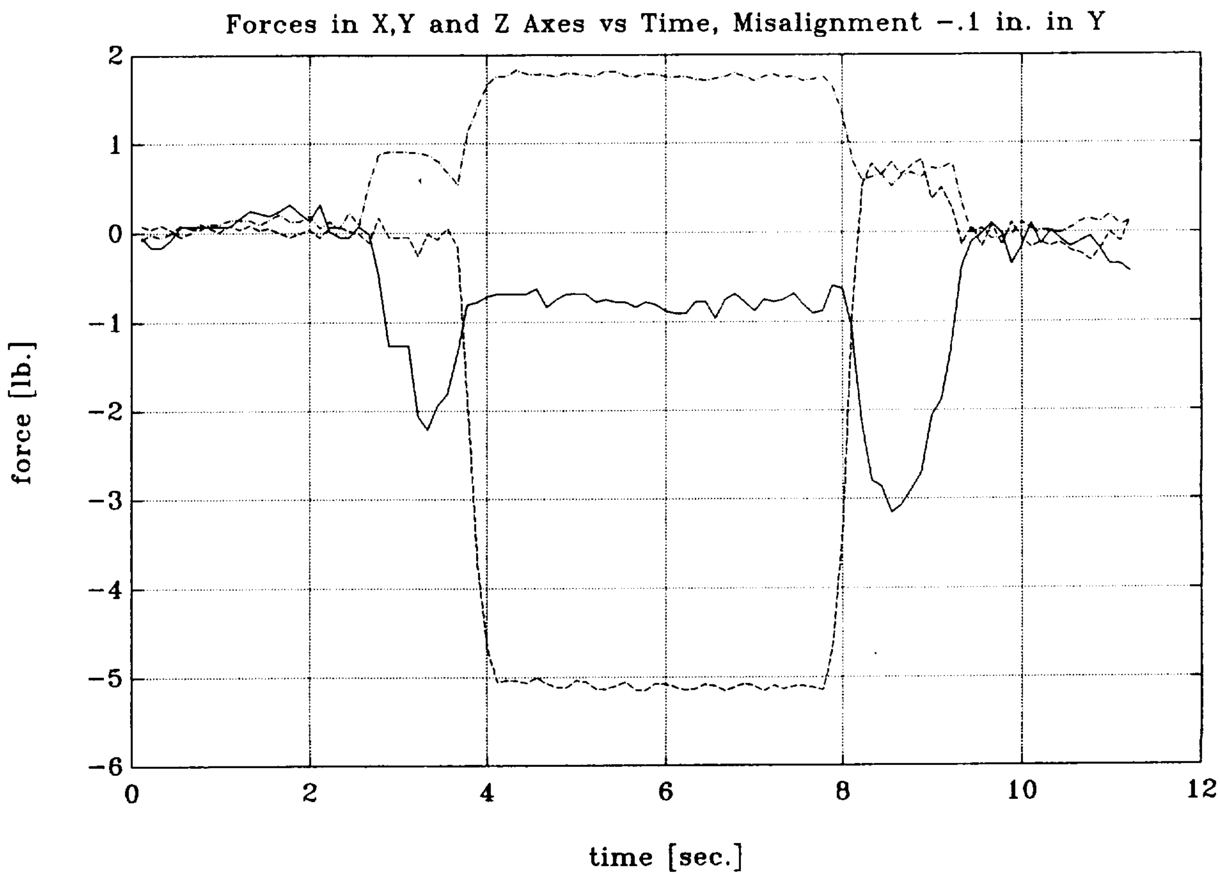

Figure HRACK18 Time histories of torques under -0.1 in. misalignment
dashed: T_x; *dashed-dotted:* T_y; *solid:* T_z

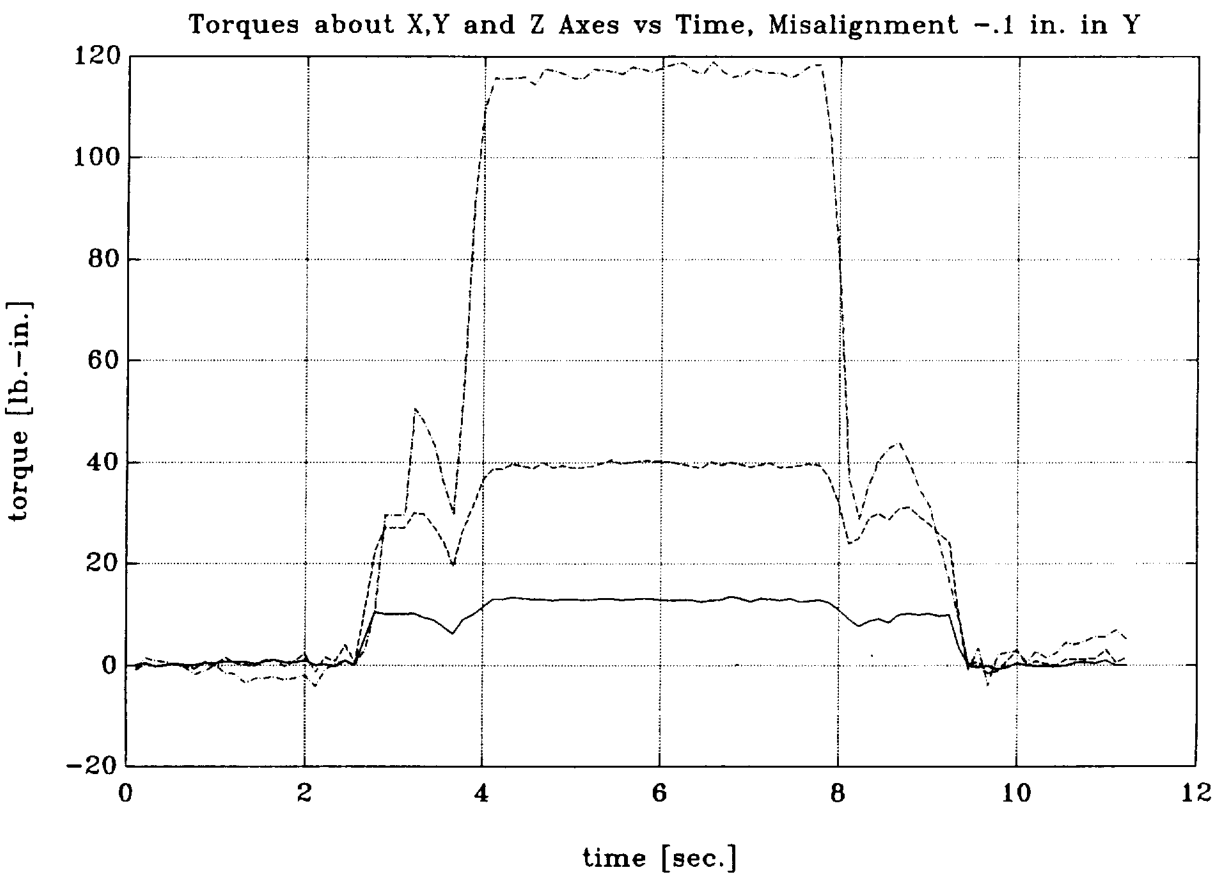

Figure HRACK19 Time histories of forces under -0.15 in. misalignment
dashed: F_x; *dashed-dotted:* F_y; *solid:* F_z

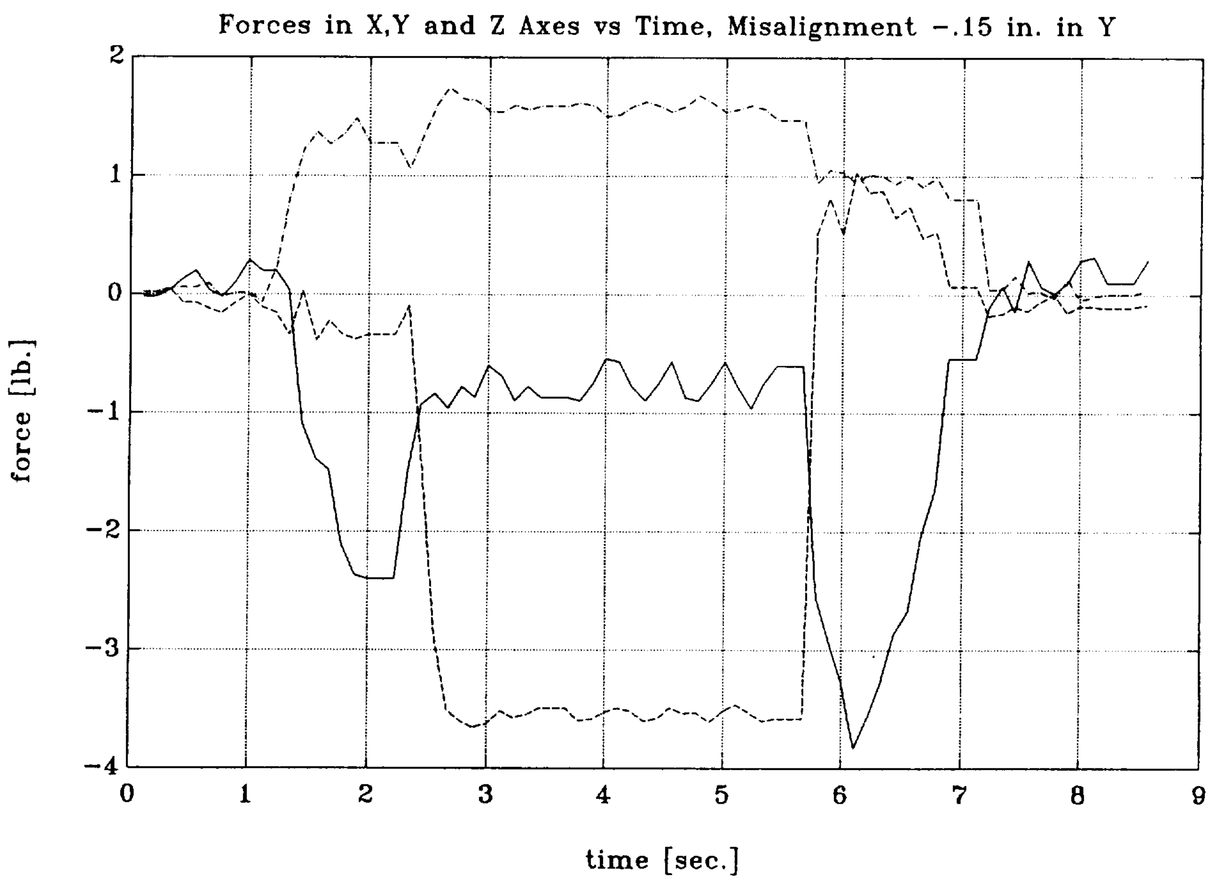

Figure HRACK20 Time histories of torques under -0.15 in. misalignment
dashed: T_x; dashed-dotted: T_y; solid: T_z

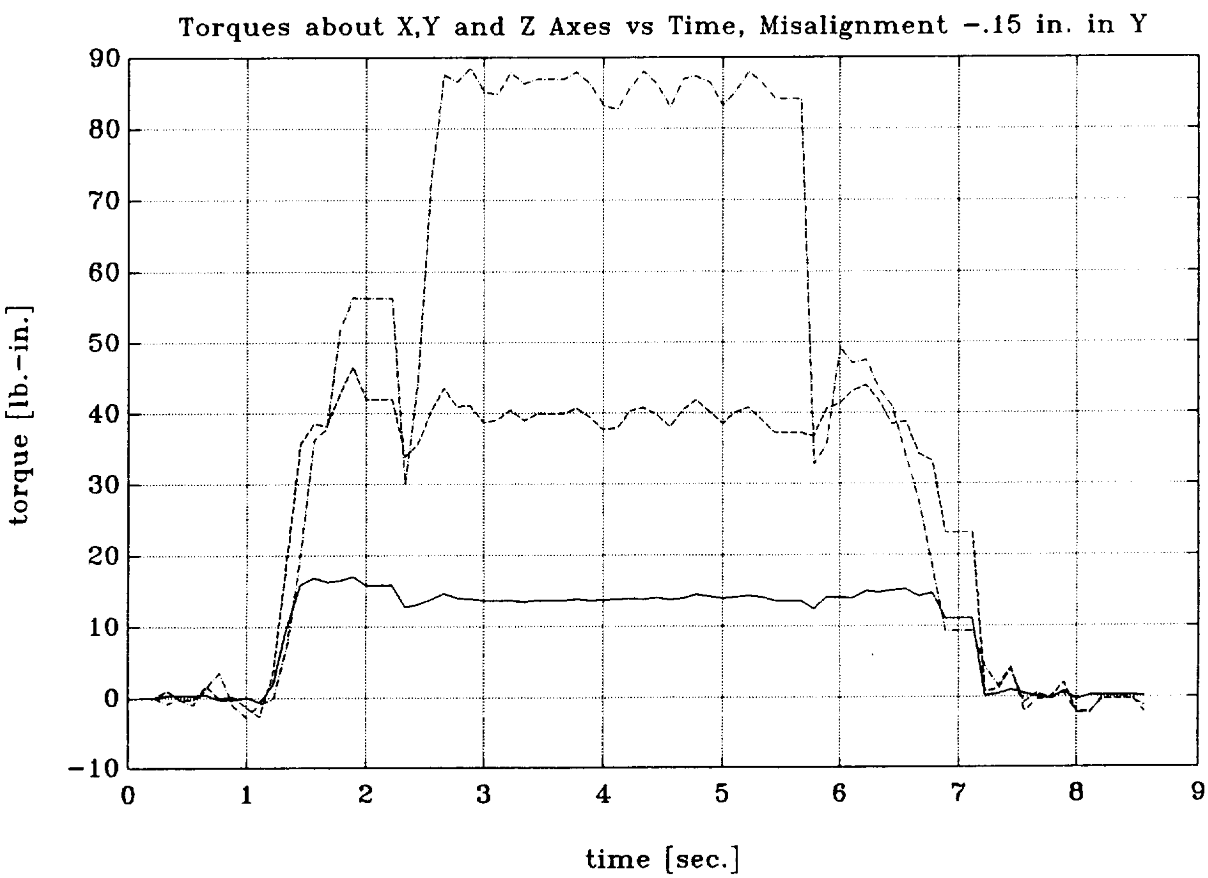

Figure HRACK21 Time histories of forces under -0.20 in. misalignment
dashed: F_x*; dashed-dotted:* F_y*; solid:* F_z

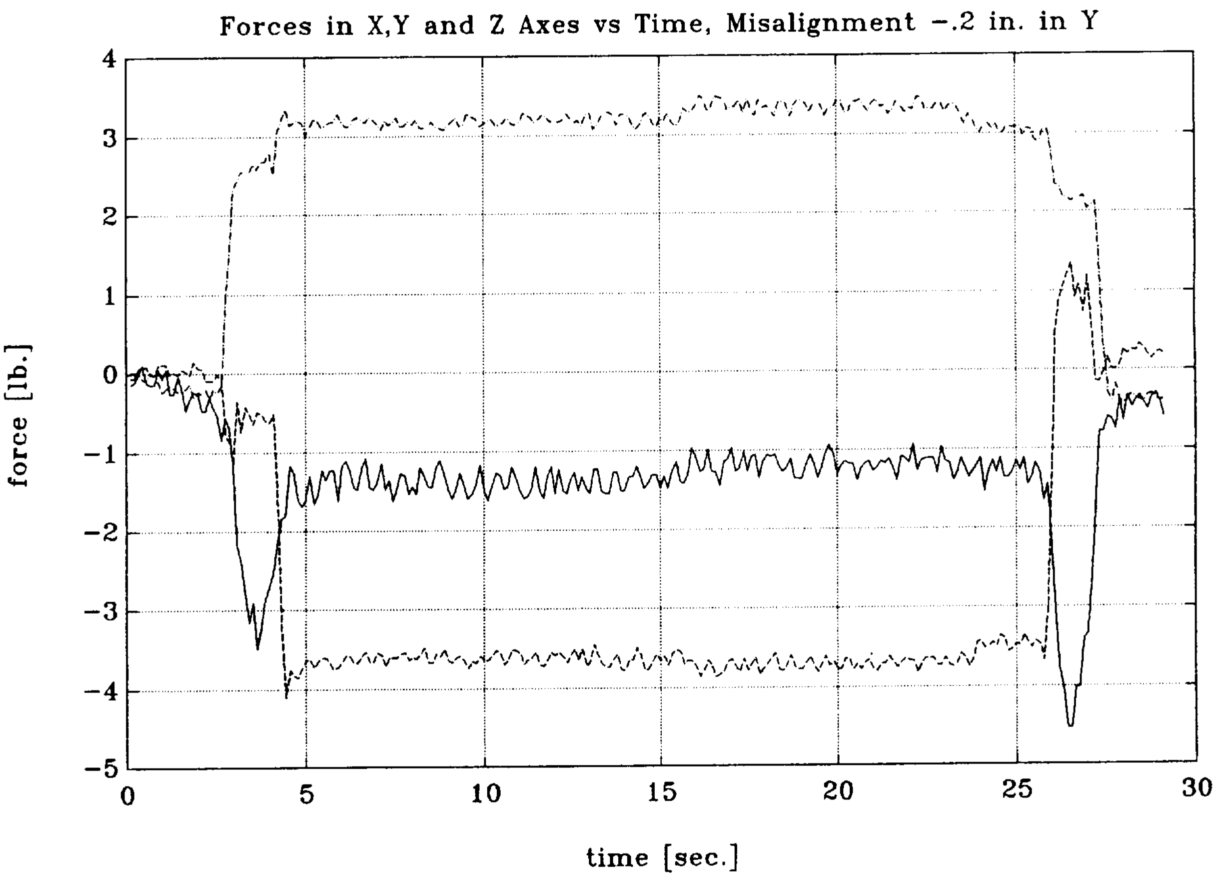

Figure HRACK22 Time histories of torques under -0.20 in. misalignment
dashed: T_x; *dashed-dotted:* T_y; *solid:* T_z

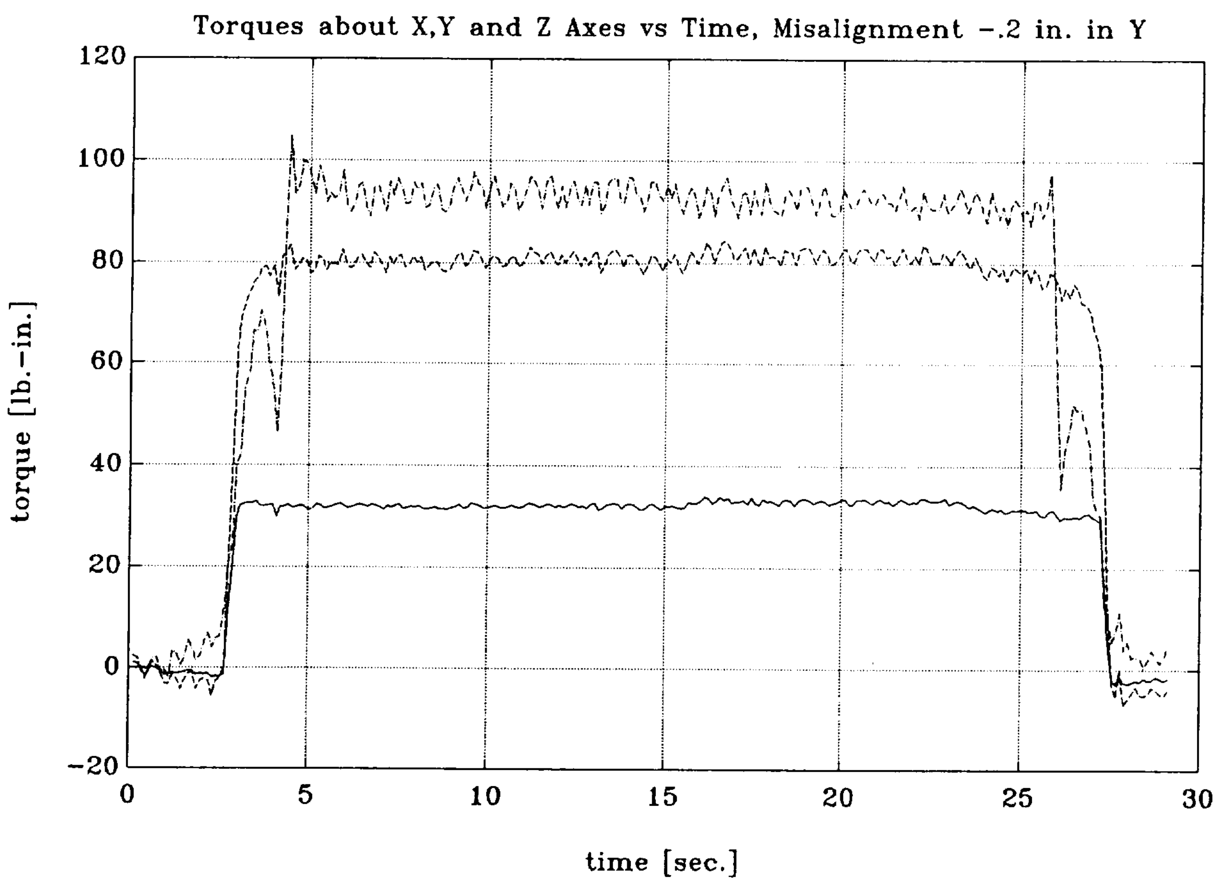

Figure HRACK23 Time histories of forces under -0.25 in. misalignment
dashed: F_x*; dashed-dotted:* F_y*; solid:* F_z

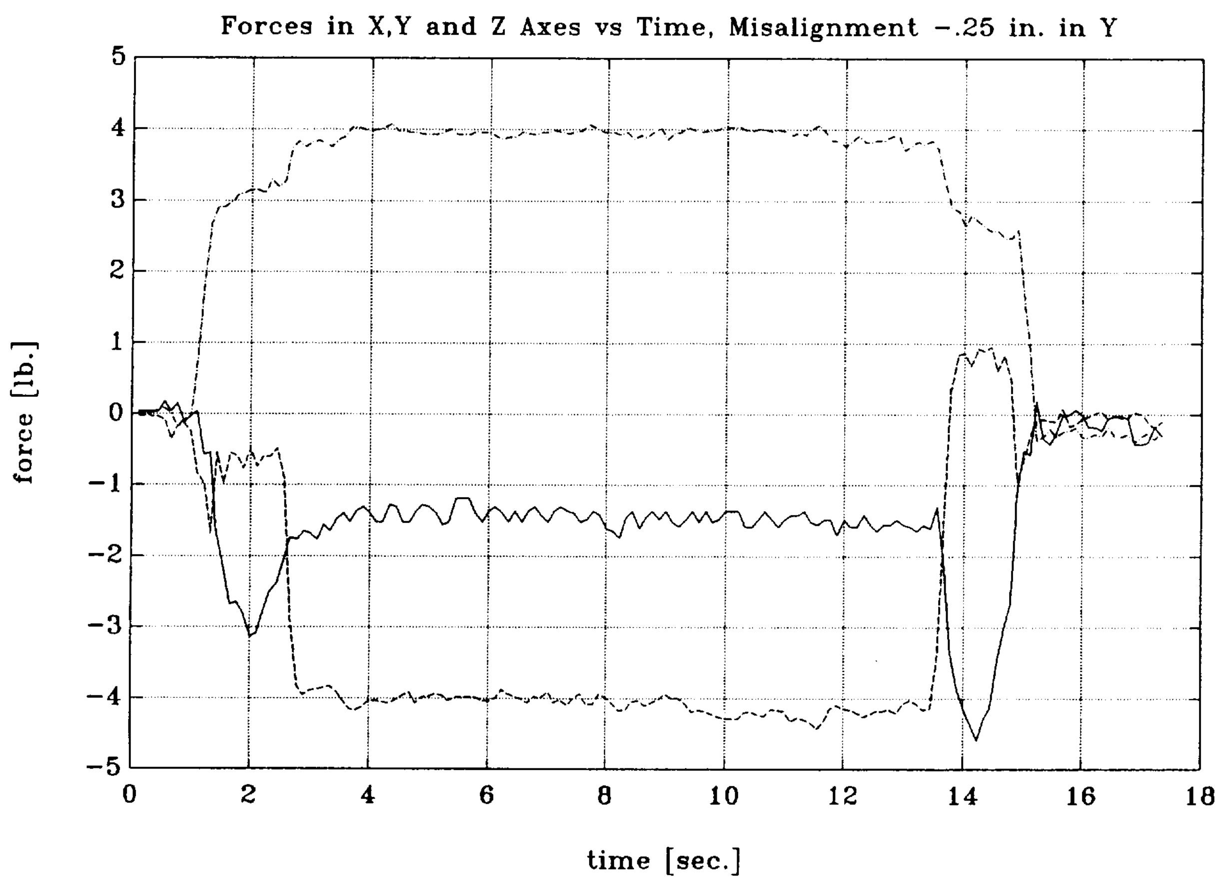

Figure HRACK24 Time histories of torques under -0.25 in. misalignment
dashed: T_x; *dashed-dotted:* T_y; *solid:* T_z

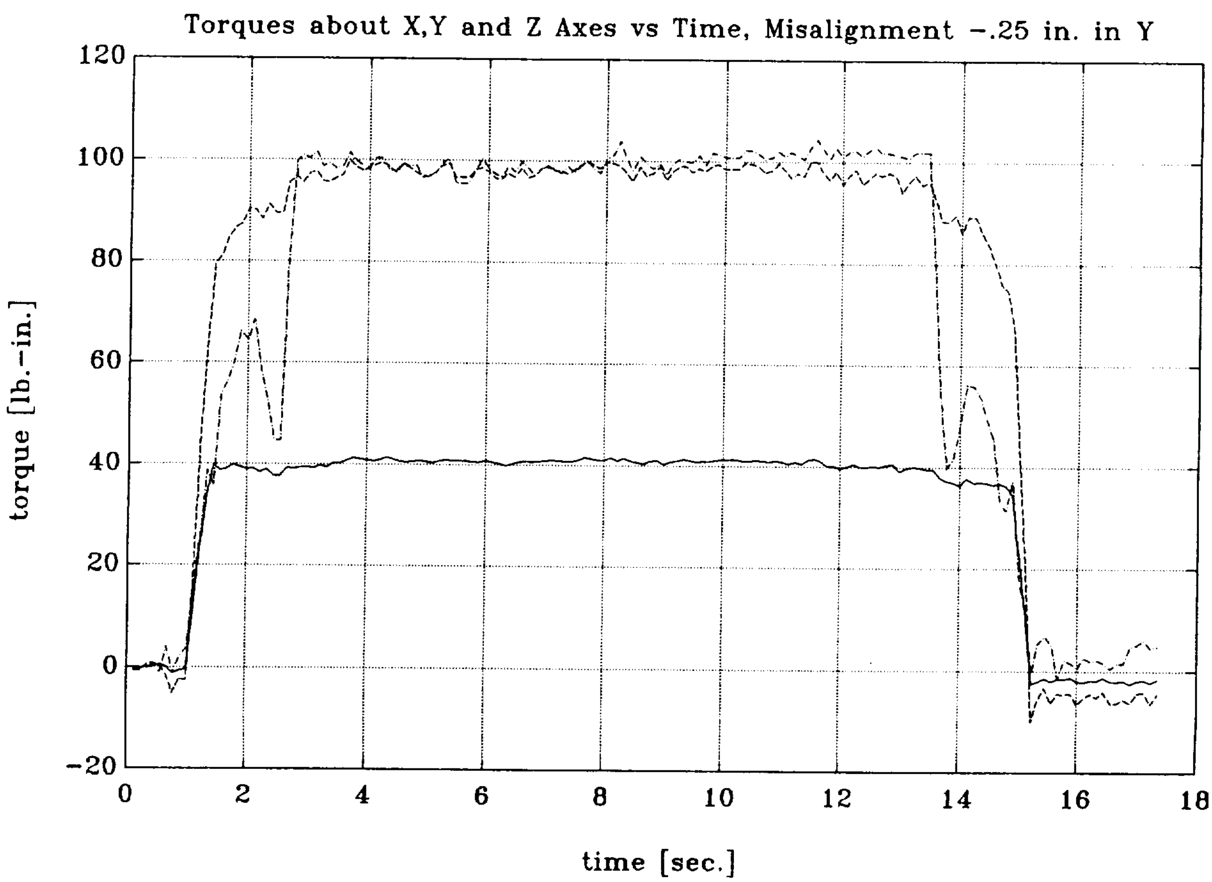

Figure HRACK25 Time histories of forces under -0.30 in. misalignment
dashed: F_x; *dashed-dotted:* F_y; *solid:* F_z

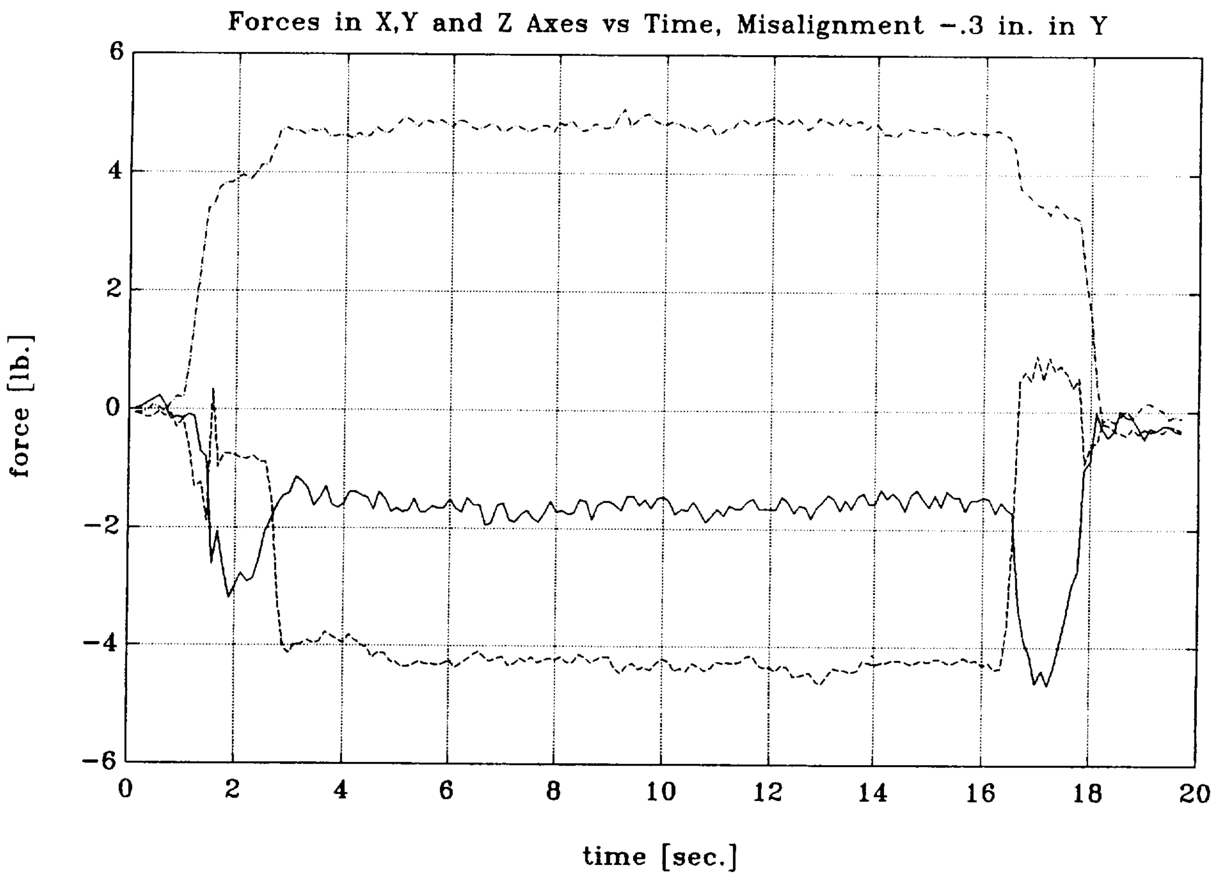

Figure HRACK26 Time histories of torques under -0.30 in. misalignment
dashed: T_x; *dashed-dotted:* T_y; *solid:* T_z